

Stabilization of dendritic spines in an Alzheimer mouse model

Inaugural-Dissertation

zur Erlangung des Doktorgrades
der Mathematisch-Naturwissenschaftlichen Fakultät
der Heinrich-Heine-Universität Düsseldorf

vorgelegt von

Georgia-Ioanna Kartalou
aus Cholargos, Attica, Griechenland

Düsseldorf, Mai 2020

aus dem Institut für Neuro- und Sinnesphysiologie
der Heinrich-Heine-Universität Düsseldorf

Gedruckt mit der Genehmigung der
Mathematisch-Naturwissenschaftlichen Fakultät der
Heinrich-Heine-Universität Düsseldorf

Referent: Prof. Dr. rer. nat. Kurt Gottmann
Korreferent: Prof. Dr. rer. nat. Christine Rose
Tag der mündlichen Prüfung: 25.06.2020

Dedicated to my parents, Mihalis and Eleni

δόξαν ἀληθῆ μετὰ λόγου ἐπιστήμην εἶναι¹
Πλάτων, *Θεαίτητος*, 202c.

¹ “[T]rue opinion accompanied by reason is knowledge.” Plato, *Theaetetus*, 202c, trans. H. N. Fowler.

Table of Contents

Summary	ix
Zusammenfassung	xi
Abbreviations	xiii
1. Introduction	1
1.1 Alzheimer's Disease (AD)	1
1.1.1 Historical perspective of AD	1
1.1.2 Epidemiology and etiology of AD	3
1.1.3 Neuropathological hallmarks of AD	5
1.1.4 The amyloid pathology of AD	7
1.1.5 Neuroinflammation in AD	10
1.1.6 Therapeutic approaches for the treatment of AD	12
1.2 The mammalian hippocampus.....	12
1.2.1 The hippocampal formation	12
1.2.2 The laminar organization of the hippocampus	14
1.2.3 CA1 pyramidal neurons	14
1.3 Dendritic spines.....	15
1.3.1 The structure and function of dendritic spines	15
1.3.2 Brain-derived neurotrophic factor (BDNF) and its role in dendritic spines.....	17
1.4 Fingolimod (FTY720).....	17
1.4.1 Sphingosine-1-phosphate (SP1)	17
1.4.2 Structure, biochemistry and activity of FTY720.....	18
1.5 Synaptic cell adhesion molecules (CAMs)	18
1.5.1 N-cadherin (Ncad).....	19
1.5.2 Neuroligins (NLGs) and neurexins (NRXs).....	20
1.6 Aims of the study	20

2. Materials and Methods	23
2.1 Materials and equipment	23
2.1.1 Materials (chemicals, reagents, media and antibodies).....	23
2.1.2 Equipment (microscopes, devices and objects).....	25
2.1.3 Composition of buffers and solutions	25
2.2 Animals	26
2.3 Therapeutic interventions for AD tested in APP/PS1 mice	27
2.3.1 Voluntary running (VR).....	28
2.3.2 Chronic FTY720 administration	28
2.4 Composition and preparation of Golgi-Cox solution.....	28
2.5 Brain tissue collection and preparation for Golgi-Cox staining.....	29
2.6 Dendritic spine analysis in Golgi-Cox stained neurons	29
2.7 Combined Golgi-Cox staining with florescent labeling of amyloid plaques	31
2.8 Image processing and spine density analysis in Golgi-Cox impregnated neurons close to fluorescent stained amyloid plaques	31
2.9 Brain tissue collection and preparation of slices for immunohistochemistry	32
2.10 Immunofluorescence staining for Iba1	32
2.11 Immunofluorescence staining for GFAP.....	33
2.12 Thioflavine S staining	33
2.13 Immunofluorescence staining for total amyloid beta (A β)	33
2.14 Image analysis and quantitation of fluorescence stainings	34
2.15 Preparation of primary neuronal cultures	35
2.16 Pharmacological inhibition of γ -secretase in primary neuronal cultures and protein extraction.....	36
2.17 Protein extraction from post-mortem brain tissue.....	36
2.18 Western blot analysis from primary cultured mouse neurons and post-mortem human brains	37
2.19 Statistics	38

3. Results	39
3.1 Spine density analysis in Golgi-Cox impregnated mouse hippocampal neurons	39
3.1.1 Deficits in spine density in apical secondary dendrites in Golgi-Cox stained CA1 pyramidal neurons in aged APP/PS1 mice.....	39
3.1.2 Spine density deficits in hippocampal CA1 pyramidal neurons in 6- to 7-month-old BDNF ^{+/-} and APP/PS1/BDNF ^{+/-} transgenic mice.....	40
3.2 Spine density analysis in the vicinity of amyloid plaques in Golgi-Cox impregnated hippocampal neurons.....	41
3.2.1 Combination of fluorescent labeling of amyloid plaques with Golgi-Cox staining of CA1 pyramidal neurons in the hippocampus of APP/PS1 mice	41
3.2.2 Reduced spine density in Golgi-Cox impregnated CA1 pyramidal neurons in the vicinity of amyloid plaques in 6- to 7-month-old APP/PS1 mice.....	42
3.3 Effects of voluntary running (VR) on spine density in mouse hippocampal neurons ...	44
3.3.1 VR rescues spine density deficits in the hippocampus of APP/PS1 mice	44
3.4 Effects of chronic treatment with fingolimod (FTY720) in WT and APP/PS1 transgenic mice	46
3.4.1 Chronic treatment with FTY720 rescued dendritic spine deficits in hippocampal neurons of APP/PS1 mice	46
3.4.2 Chronic treatment with FTY720 reduced microgliosis in the hippocampus and neocortex of APP/PS1 mice	49
3.4.3 Chronic treatment with FTY720 reduced astrogliosis in the hippocampus and neocortex of APP/PS1 mice	51
3.4.4 Chronic treatment with FTY720 reduced amyloid plaque load in the hippocampus and neocortex of APP/PS1 mice	53
3.4.5 Chronic treatment with FTY720 reduced the accumulation of A β in the hippocampus and neocortex of APP/PS1 mice.....	55
3.5 Expression of C-terminal fragment 1 (CTF1) of N-cadherin (Ncad), neuroligin 1 (NLG1) and neurexin (NRX) in sporadic AD.....	57
3.5.1 Pharmacological inhibition of γ -secretase activity increased Ncad CTF1, NLG1 CTF1 and NRX CTF1 levels in primary neuronal cultures	57

3.5.2 Ncad CTF1, NLG1 CTF1 and NRX CTF1 expression levels in post-mortem brains from patients with sporadic AD	58
4. Discussion	61
4.1 Reduced spine density in the CA1 area of the hippocampus in a mouse model of AD. 61	
4.1.1 Dendritic spine loss in the hippocampus of 13-month-old APP/PS1 mice and in 6 to 7-month-old APP/PS1/BDNF ^{+/-} animals	61
4.1.2 Dendritic spine deficits near amyloid plaques in the hippocampus of 6- to 7-month-old APP/PS1 mice	62
4.2 Potential therapeutic interventions for rescuing spine pathology in APP/PS1 mice.....	63
4.2.1 Voluntary running (VR) rescues spine deficits in APP/PS1 mice	64
4.2.2 FTY720 rescues spine deficits and reduces neuroinflammation along with amyloid pathology in APP/PS1 mice	65
4.3 Analysis of the expression of selected γ -secretase substrates in sporadic AD.....	68
5. References	71
Acknowledgements	91
Curriculum vitae.....	93
List of publications.....	94
List of poster presentations in conferences	95
Declaration	96
Eidesstattliche Erklärung.....	97

Summary

Alzheimer's disease (AD) is a chronic neurodegenerative disorder, characterized by a progressive decline in memory. Synaptic failure and cognitive dysfunction have been described as early events in AD pathogenesis. The function of the hippocampus plays a pivotal role in memory formation and consolidation and the mechanisms underlying this process involve synaptic plasticity. Moreover, dendritic spines are postsynaptic sites of excitatory synapses in the brain constituting the most critical players in synaptic plasticity. Their loss directly affects synaptic function, and has also been correlated with learning and memory impairments in AD. In addition, pathological changes in brain-derived neurotrophic factor (BDNF) availability and signaling have also been reported in AD. Despite the current scientific advances, there are no effective therapeutic approaches for the prevention and curing of AD yet. It is clear therefore, that one of the most challenging topics in AD research is the identification of therapeutic strategies, which could potentially target the presumed pathogenic mechanisms that underlie this disorder.

Aiming at finding possible options able to slowdown the pathogenesis of AD, this research study focused on the development of novel therapeutic interventions possible to counteract the AD-like spine pathology observed in the hippocampus of APP/PS1 transgenic mice (an animal model of AD). For this reason, this research used therapeutic approaches, which have been suggested to increase BDNF levels in the brain, such as voluntary running (VR) or chronic fingolimod (FTY720) administration. FTY720 is a modulator of sphingosine-1 phosphate (S1P) receptors, which is thought to have neuroprotective effects and to regulate inflammatory responses. In this work, significant dendritic spine deficits were observed in the hippocampus of both APP/PS1 and APP/PS1/ BDNF^{+/-} (AD mice with reduced BDNF levels) animals after Golgi-Cox brain impregnations. Furthermore, a more detailed spine analysis in correlation to amyloid plaques was performed, after establishing an innovative combination of the Golgi-Cox staining of neurons with the fluorescent labeling of amyloid plaques. The use of this novel method revealed a significant spine loss near and also distant from the amyloid plaques in the hippocampus of APP/PS1 mice. As expected, a stronger spine pathology was detected in the vicinity of the plaques. Most interestingly, this study showed that both VR and FTY720 treatment (in a high dose of 1 mg/kg/2ndday as well as in a lower dose of 0.2 mg/kg/2ndday) completely rescued spine pathology distant from the plaque border, and significantly ameliorated spine loss near the plaques. Moreover, this work revealed that

FTY720 (1 mg/kg/2ndday) reduced the observed robust microgliosis and astrogliosis along with the amyloid beta deposition and accumulation in the hippocampus and cortex of APP/PS1 mice. Overall, these findings suggest a beneficial role of VR and FTY720 in preventing progression of the disease in this AD mouse model.

This work also investigated potential γ -secretase activity impairments in sporadic AD in relation to the metabolism of N-cadherin (Ncad), neuroligin-1 (NLG1) and neurexin (NRX). These synaptic cell adhesion molecules (CAMs) are well known to be expressed at pre- or postsynaptic sites of neuronal synapses. These molecules are proteolytically cleaved similar to amyloid precursor protein (APP) and are important substrates of γ -secretase. There is strong evidence that misprocessing by γ -secretase [without carrying a mutation in the presenilin-1 (PS1)] can occur in sporadic AD. This work revealed that the level of the C-terminal fragment 1 (CTF1) of Ncad was significantly elevated, whereas the NLG1 CTF1 levels were significantly reduced in post-mortem brains of patients with sporadic AD. Furthermore, the level of NRX CTF1 was not different between AD patients and non-demented controls. These findings showed that potential γ -secretase functional impairments in sporadic AD may result in specific changes in proteolytic cleavage for different substrates.

In summary, the major outcomes of this dissertation are the beneficial effect of VR on spine pathology in AD, and the use of FTY720 as a potential treatment for rescuing spine impairments in AD based on the drug's anti-neuroinflammatory actions on microglia and astrocytes. Furthermore, this work also suggests that potential γ -secretase dysfunction in sporadic AD may lead to altered proteolytic cleavage of specific substrates.

Zusammenfassung

Morbus Alzheimer (AD) ist eine durch fortschreitenden Rückgang des Gedächtnisses gekennzeichnete chronische neurodegenerative Erkrankung. Die Fehlfunktionen von Synapsen und die kognitive Dysfunktion sind frühere Anzeichen der AD-Pathogenese. Die Funktion des Hippocampus spielt eine zentrale Rolle bei der Gedächtnisbildung und -konsolidierung, und die zugrundeliegenden Mechanismen umfassen die synaptische Plastizität. Die dendritischen Spines bilden die postsynaptischen Anteile exzitatorischer Synapsen im Gehirn und sie stellen damit den Hauptort der synaptischen Plastizität dar. Ihr Verlust wirkt sich direkt auf die synaptische Funktion aus und ist dadurch mit Lern- und Gedächtnisstörungen bei AD korreliert. Außerdem sind pathologische Veränderungen bei der Verfügbarkeit und Signalüberleitung des Wachstumsfaktors BDNF (von eng.: „Brain-derived neurotrophic factor“) in AD berichtet worden. Trotz der wissenschaftlichen Fortschritte existieren aktuell keine effektiven therapeutischen Ansätze zur Prävention und Heilung der AD. Daher stellt die Identifikation von der Krankheitspathogenese zugrundeliegenden pathophysiologischen Mechanismen einen zentralen Meilenstein therapeutischer Strategien dar.

Mit dem Ziel, mögliche Therapieoptionen zu finden, die die Pathogenese von AD verlangsamen könnten, konzentrierte sich diese Forschungsstudie auf die Entwicklung neuartiger therapeutischer Interventionen, die der im Hippocampus von transgenen APP/PS1-Mäusen (ein Tiermodell für AD) beobachteten AD-ähnlichen dendritischen Spine-Pathologie entgegenwirken können. Aus diesem Grund wurden in dieser Studie therapeutische Ansätze verwendet, die möglicherweise den BDNF-Spiegel im Gehirn erhöhen, z. B. die Verabreichung von „voluntary running“ (VR) oder chronischem Fingolimod (FTY720). Fingolimod ist ein Modulator von Sphingosin-1-Phosphat (S1P)-Rezeptoren, von dem angenommen wird, dass er neuroprotektive Wirkungen hat und Entzündungsreaktionen reguliert. In dieser Arbeit wurden signifikante dendritische Spine-Defizite im Hippocampus sowohl von APP/PS1- als auch von APP/PS1/BDNF+/- (AK-Mäuse mit reduzierten BDNF-Spiegeln) Tieren nach Golgi-Cox-Hirnimprägnierungen beobachtet. Darüber hinaus wurde eine detailliertere Analyse der dendritischen Spines im Zusammenhang mit Amyloid-Plaques durchgeführt, nachdem eine innovative Kombination der Golgi-Cox-Färbung von Neuronen mit der Fluoreszenzmarkierung von Amyloid-Plaques etabliert worden war. Die Verwendung dieser Methode ergab einen signifikanten Verlust der dendritischen Spines in der Nähe und

weit entfernt von den Amyloid-Plaques im Hippocampus von APP/PS1-Mäusen, wobei eine stärkere Pathologie der dendritischen Spines bevorzugt in der Nähe der Plaques festgestellt wurde. Interessanterweise zeigte diese Studie, dass sowohl die VR- als auch die FTY720-Behandlung (in einer hohen Dosis von 1 mg/kg jeden 2. Tag sowie in einer niedrigeren Dosis von 0,1 mg/kg jeden 2. Tag) die Pathologie der dendritischen Spines weit entfernt von der Plaquegrenze vollständig rettete und den Verlust dendritischer Spines in der Nähe der Plaques signifikant verbesserte. Darüber hinaus ergab diese Untersuchung, dass FTY720 (1 mg/kg jeden 2. Tag) die robuste Mikroglie und Astroglie zusammen mit der Amyloid-Beta-Ablagerung und -Akkumulation im Hippocampus und Cortex von APP/PS1-Mäusen reduzierte. Insgesamt deuten diese Ergebnisse auf eine vorteilhafte Rolle von VR und FTY720 bei der Verhinderung des Fortschreitens der Krankheit in diesem AD-Mausmodell hin.

Diese Forschungsstudie untersuchte auch mögliche Beeinträchtigungen der γ -Sekretaseaktivität bei sporadischer AD in Bezug auf den Metabolismus von synaptischen Zelladhäsionsmolekülen (CAMs) von N-Cadherin (Ncad), Neuroligin-1 (NLG1) und Neurexin (NRX). Diese Proteine sind an den prä- oder postsynaptischen Strukturen von Neuronen exprimiert. Diese Moleküle werden proteolytisch ähnlich wie das APP-Protein gespalten und sind wichtige Substrate der γ -Sekretase, sodass sie in AD eine Rolle spielen könnten. Es gibt starke Hinweise darauf, dass bei sporadischer AD eine Fehlfunktion der γ -Sekretase ohne Mutation im Presinilin-1 (PS1) auftreten kann. Diese Arbeit beschreibt, dass die Expression des C-terminalen Fragments (CTF1) von Ncad signifikant erhöht waren, während die Expression von NLG1 CTF1 in post-mortem Gehirnen von Patienten mit sporadischer AD signifikant verringert waren. Die NRX CTF1-Expression zwischen AD-Patienten und nicht dementen Kontrollpersonen war nicht unterschiedlich. Diese Befunde legen nahe, dass γ -Sekretase-Funktionsstörungen bei sporadischer AD zu spezifischen Veränderungen der proteolytischen Spaltung verschiedener Substrate führen können.

Zusammenfassend sind die wichtigsten Ergebnisse dieser Dissertation die vorteilhafte Wirkung von VR auf die Pathologie der dendritischen Spine bei AD und die Verwendung von FTY720 als potenzielle Behandlung zur Verbesserung von Störungen der dendritischen Spines bei AD durch antineuroinflammatorische Wirkungen des Arzneimittels auf Mikroglia und Astrozyten. Diese Arbeit legt auch nahe, dass eine mögliche γ -Sekretase-Dysfunktion bei sporadischer AD zu einer veränderten proteolytischen Spaltung spezifischer Substrate führen kann.

Abbreviations

A β	Amyloid beta
ACh	Acetylcholine
AD	Alzheimer's Disease
ADAM10	A Disintegrin And Metalloproteinase 10
APOE	Apolipoprotein E
APP	Amyloid Precursor Protein
ASC	Adapter protein apoptosis-associated Speck-like protein containing a Caspase recruitment domain
BACE1	Beta-site Amyloid precursor protein Cleaving Enzyme 1 (Beta-secretase)
BBB	Blood-Brain Barrier
BDNF	Brain-Derived Neurotrophic Factor
BME	Basal Medium Eagle
BSA	Bovine Serum Albumin
CA	Cornu Ammonis
CAA	Cerebral Amyloid Angiopathy
CAMs	Cell Adhesion Molecules
CASK	Catenins, calcium/calmodulin-dependent Serine protein Kinase
CNS	Central Nervous System
CTF1	C-Terminal Fragment 1
CTF2	C-Terminal Fragment 2
DG	Dentate Gyrus
DMSO	Dimethyl Sulfoxide
DNA	Deoxyribonucleic Acid
EE	Enriched Environment
EOFAD	Early-Onset Familial Alzheimer's Disease
FCS	Fetal Calf Serum
FDA	Food and Drug Administration
FTY720	Fingolimod
FTY720-P	Fingolimod-Phosphate
GDNF	Glial-Derived Neurotrophic Factor
GFAP	Glial Fibrillary Acidic Protein

GPCR	G Protein-Coupled Receptor
HD	Huntington's Disease
Iba1	Ionized calcium binding adaptor molecule 1
IL-6	Interleukin 6
IL-1 β	Interleukin 1 β
LOAD	Late-Onset Alzheimer's Disease
MPBS ^(+/+)	Modified Phosphate Buffered Saline (+/+)
MPBS ^(-/-)	Modified Phosphate Buffered Saline (-/-)
MS	Multiple Sclerosis
NB	Neurobasal medium
Ncad	N-cadherin
NFTs	Neurofibrillary Tangles
NGS	Normal Goat Serum
NLG	Neuroigin
NMDA	N-Methyl-D-Aspartate
NO	Nitric Oxide
NRX	Neurexin
NTF	N-Terminal Fragment
PB	Phosphate Buffer
PBS	Phosphate Buffered Saline
PCR	Polymerase Chain Reaction
PDZ	Postsynaptic Density Protein 95 (PSD-95), Discs large (Dlg) and Zona occludens-1(ZO-1)
PFA	Paraformaldehyde
PSD95	Postsynaptic Density protein 95
PS1	Presinilin-1
PS2	Presinilin-2
PVDF	Polyvinylidene Difluoride
ROS	Radical Oxygen Species
SDS	Sodium Dodecyl Sulfate
SEM	Standard Error of the Mean
SH	Standard Housing
SLM	Stratum Lacunosum-Moleculare
SO	Stratum Oriens

SP	Stratum Pyramidale
SPHK1	Sphingosine Kinase 1
SPHK2	Sphingosine Kinase 2
SP1	Sphingosine-1-Phosphate
SP1R	SP1 Receptors
SR	Stratum Radiatum
TBS	Tris-Buffered Saline
TNF- α	Tumor Necrosis Factor- α
TREM2	Triggering Receptor Expressed on Myeloid cells 2
TrKB	Tropomyosin-related Kinase B
VR	Voluntary Running

1. Introduction

1.1 Alzheimer's Disease (AD)

Alzheimer's disease (AD) is a devastating age-related neurodegenerative disorder which is characterized by progressive memory loss and irreversible cognitive decline (Blennow et al., 2006). It is the most common form of dementia and there is evidence that patients develop the disease much earlier (20 years or more) before symptoms begin (Blennow et al. 2006; Rajan et al., 2015; Reiman et al., 2012). It has been estimated that 13.8 million patients of all ages will suffer from AD in the United States of America in 2050 (Hebert et al., 2013). Most AD patients have the sporadic form of the disease, developing a late onset (older than 80 years), whereas less than 1% of the AD patients have the familial form of the disease and they develop AD at a younger age (at about 45 years) (Blennow et al., 2006; Masters et al., 2015). The etiology as well as the progression of AD are still not completely elucidated but they have been correlated to amyloid plaques and neurofibrillary tangles (NFTs) which are detected in AD brains along with dystrophic neurites, reactive glial cells and several neurophysiological disruptions (Blennow et al., 2006; Masters et al., 2015; Lane et al., 2015). Although the research in the field of AD is extensive and innovative, there is still no effective treatment to cure this disorder; a fact that crucially highlights the importance of continuous discoveries towards new therapeutic interventions (Weinstein, 2018).

1.1.1 Historical perspective of AD

AD was first described by Alois Alzheimer, a German psychiatrist and neuropathologist, about a hundred years ago (Maurer et al., 1997). In 1901, Alzheimer reported the clinical symptoms of a 51-year-old woman, known as Auguste D, who was his patient at the Frankfurt Hospital and suffering from progressive memory loss, confusion, delusions, aphasia and psychosocial disability (Maurer et al., 1997; Möller and Graeber, 1998). Following Auguste D's death in 1906, Alzheimer proceeded with a brain autopsy, where he observed diffuse brain atrophy and unusual microscopic histopathological alterations in brain structures and cells which are known today as amyloid plaques and NFTs (Möller and Graeber, 1998; Selkoe, 2001). Alzheimer presented his discovery at a meeting in Munich in the end of 1906 and published it later in 1907 (Selkoe, 2001; Alzheimer et al., 1995). It was not until 1968,

and immediately after the published work of G. Blessed, B.E. Tomlinson and M. Roth, that AD was formally recognized as the most common form of dementia in the elderly population (Selkoe et al., 2012; Blessed et al., 1968).

Continuous research on causes of AD has been carried out since Alois Alzheimer's years with great progress made nowadays. Over the last decades, several theories about the etiology and pathogenesis of AD have been proposed but they are all still under examination and considered as complementary to each other.

In the mid-1970s, the 'cholinergic hypothesis' was the first theory reported, suggesting that AD is caused by reduced synthesis of the neurotransmitter acetylcholine (ACh) which in normal levels contributes significantly to learning and memory processes (Selkoe, 2001; Glenner and Wong, 1984; Hasselmo, 2006). Several pharmaceutical treatments based on this theory remain in common use today, such as the administration of cholinesterase inhibitors which limit the degradation of ACh in the brain of AD patients (Francis et al., 1999; Ferreira-Vieira et al., 2016).

In 1987 the amyloid beta ($A\beta$) protein was identified as the main component of senile plaques (Tanzi et al., 1987), and in 1991 it was reported that mutations in amyloid precursor protein (APP) gene could be responsible for causing some cases of AD (Goate et al., 1991). This theory was well linked by the earlier discovery of the location of the APP gene on the chromosome 21, along with the observation that patients with AD and Down Syndrome (trisomy 21) developed the disease by the age of 40 years (Lott and Head, 2005). In 1992, J. A. Hardy and A. Higgins proposed for the first time the 'amyloid cascade hypothesis,' suggesting that the extracellular deposition of $A\beta$ protein in the brain is the main cause of AD; followed by the formation of NFTs, neuronal loss and eventually memory dysfunction, as direct effects of the excessive $A\beta$ accumulation (Hardy and Higgins, 1992).

During the past years, the role of tau (a microtubule-associated protein) abnormalities, which lead to the formation of NFTs in the AD brains, has been extensively studied, and the 'tau hypothesis' has been proposed as an alternative approach to identify the cause of AD. This theory suggests that the main cause of AD is associated with tau (Chen and Mobley, 2019; Iqbal et al., 2005). It has been proposed that tau aggregations damage the axons of the brain cells and lead to neurodegeneration. Hyperphosphorylated tau starts to form paired helical filaments, leading the insoluble twisted fibers inside the neurons that cause biochemical disruption, which is then followed by the death of the neuronal cells (Goedert et al., 1991; W. Chun and Johnson, 2007; Chen and Mobley, 2019).

In the past few years, additional theories, such as the ‘inflammation hypothesis,’ shed new light on what causes AD as well as the disease’s progression and severity (Heneka et al., 2015). It has been discovered that reactive glia cells surround amyloid plaques and release pro-inflammatory cytokines (Kinney et al., 2018; Heneka et al., 2015). This process has been suggested to be one of the major contributors of neuronal loss and cognitive impairments in AD (Fakhoury, 2018; Kinney et al., 2018). It is believed that new insights in the mechanisms underlying microglia dysfunction and association with synaptic failure could bring advantages in the diagnosis and therapy of AD (Salter and Stevens, 2017; McGeer and McGeer, 2015; Jevtic et al., 2017).

Over the last decades, research on AD has made substantial progress in understanding the basis of the disease (Masters et al., 2015; Lane et al., 2018; Yiannopoulou and Papageorgiou, 2013). With a view to design beneficial targeted therapeutic approaches which could eliminate AD and improve patients’ lives, scientists throughout the world are mainly focusing on the two major neuropathological lesions observed in AD patients’ brains; the amyloid plaques and NFTs, which cause great and irreversible damage in the brain cells (Yiannopoulou and Papageorgiou, 2013; Cummings et al., 2019).

1.1.2 Epidemiology and etiology of AD

AD is a life-threatening disease and a big global health problem with an enormous impact in individuals’ lives and societal relations (Prince et al., 2014). It is the most usual type of dementia in the western nations, representing 50-60% of all dementia cases (Blennow et al., 2006; Hebert et al., 2013). According to recent estimates, 5.8 million people of all ages have AD in the United States of America today, while approximately 44 million people live with dementia worldwide. Interestingly, current predictions reveal that this number will be more than three times up by 2050 (Prince et al., 2014; Hebert et al., 2013). AD studies have also shown that the prevalence of the disease is increasing during the seventh and eighth decades of life, with a more than 10 times rise in patients in the age range 60-85 (Mayeux and Stern, 2012; Rizzi et al., 2014).

It is still very hard to estimate the incidence of the disease because of the difficulties in identifying the onset of AD as well as the disease-free individuals. The inherited early-onset familial Alzheimer’s disease (EOFAD) is an autosomal dominant case that is developed from mutations occurring in the genes of APP, presenilin-1 (PS1) and presenilin-2 (PS2), and it is associated with 1% of the AD cases (Masters et al., 2015; Qiu et al., 2009). The symptoms of

the EOFAD begin between 30-50 years of age (Qiu et al., 2009; Prince et al., 2014). However, most of the AD cases are related to the sporadic late-onset Alzheimer's disease (LOAD), which presents an heterogeneity in the associated disease risk factors as well as in the neuropathological features (Isik, 2010; Qiu et al., 2009). The symptoms of LOAD are usually developed after the age of 65, and determined by genetic and environmental factors (Isik, 2010).

The major genetic risk factor for LOAD is the $\epsilon 4$ allele of the apolipoprotein E (APOE) gene which is located on the chromosome 19q133 (Tanzi, 2012). $\epsilon 2$, $\epsilon 3$ and $\epsilon 4$ are variants of *APOE*, and it is known that the APOE $\epsilon 4$ increases the risk of AD approximately 4 times in $\epsilon 4$ heterozygotes and more than 10 times in $\epsilon 4$ homozygotes (Verghese et al., 2011; Tanzi, 2012). On the other hand, there is evidence that the APOE $\epsilon 2$ allele has a protective role against AD (Tanzi, 2012). Moreover, recent genome-wide association studies revealed 25 new genes that are related to AD, and are the following: *UNCSC*, *PLD*, *CASS4*, *CELF1*, *FERMT2*, *HLA-DRB5*, *INPP5D*, *MEF2C*, *NME8*, *PTK2B*, *SORL1*, *ZCWPW1*, *SIC24A4*, *CLU*, *PICALM*, *CRI*, *BINI*, *MS4A*, *ABCA7*, *EPHA1*, *CD2AP*, *CD33*, *EPHA1*, *DSG2* and *RIN3* (Lambert et al., 2013; Karch and Goate, 2015). These genes, when identified independently, demonstrate a low risk profile for developing AD; whereas when combined, the risk increases almost to double (Lambert et al., 2013; Karch and Goate, 2015). Notably, mutations in the gene which is encoding the triggering receptor expressed on myeloid cells 2 (TREM2) have been associated with the development of AD, while it has also been reported that TREM2 in microglia is related to the pathogenesis of the disease (Fig. 1) (Schlepckow et al., 2017; Jonsson et al., 2013; Karch and Goate, 2015). There is also strong evidence showing that the missense mutations in the A Disintegrin And Metalloprotease 10 (ADAM10) gene, which lead to the reduction of the enzyme's activity, are strongly related to the development of LOAD (Kim et al., 2009; Suh et al., 2013). ADAM10 possess α -secretase activity and is implicated in APP and several synaptic cell adhesion molecules (CAMs) metabolism in the brain (Kuhn et al., 2016; Uemura et al., 2006; Borcel et al., 2016; K. Suzuki et al., 2012). Reduction of ADAM10 activity affects A β production, due to the increased cleavage of APP by β -secretase (beta-secretase 1; BACE1), and might disrupt synaptic plasticity because of the alternative cleavage of synaptic CAMs (Vassar, 2013; Brummer et al., 2019; Suzuki et al., 2012).

Moreover, it is thought that other environmental risk factors, as well as hypertension, obesity or diabetes and the underlying mechanisms associated with these disorders, increase

the risk of AD; whereas physical activity, exercise and a good educational level may have a beneficial role against AD (Xu et al., 2015; Qizilbash et al., 2015; Chen et al., 2017).

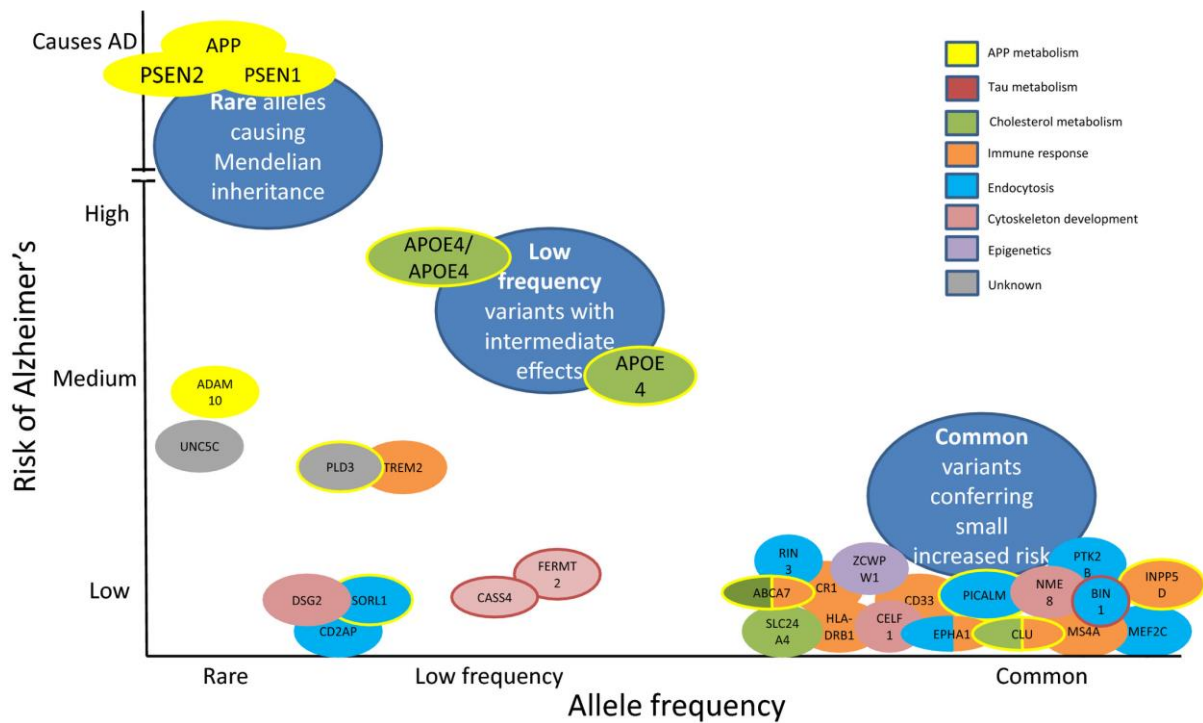


Figure 1: Genetic variants associated with the development of AD. The genes are illustrated according to the risk level. The colors indicate the biological function and pathways that the genes are implicated to. Some genetic variants are associated with more than one (double coloring). The figure is adapted from Lane et al., 2018 (Lane et al., 2018).

1.1.3 Neuropathological hallmarks of AD

AD is characterized by a progressive loss of neurons and synapses in the cerebral cortex and in some subcortical regions (McCloskey, 2017). The pathological alterations of the disease include both macroscopic and microscopic features (Serrano-Pozo et al., 2011). Macroscopic examinations of AD brains revealed a generalized brain atrophy, including a severe neurodegeneration in the hippocampus and cerebral cortex as well as enlarged ventricles (Fig. 2) (Serrano-Pozo et al., 2011; McCloskey, 2017). These observations are usually accompanied by cortical microinfarcts and lacunar infarcts in the basal ganglia as well as by white matter lesions, such as demyelination in the periventricular region (Braak and Del Tredici, 2011). There is also evidence that, in older patients, AD pathology coexists with Lewy body pathology (Schneider et al., 2009).

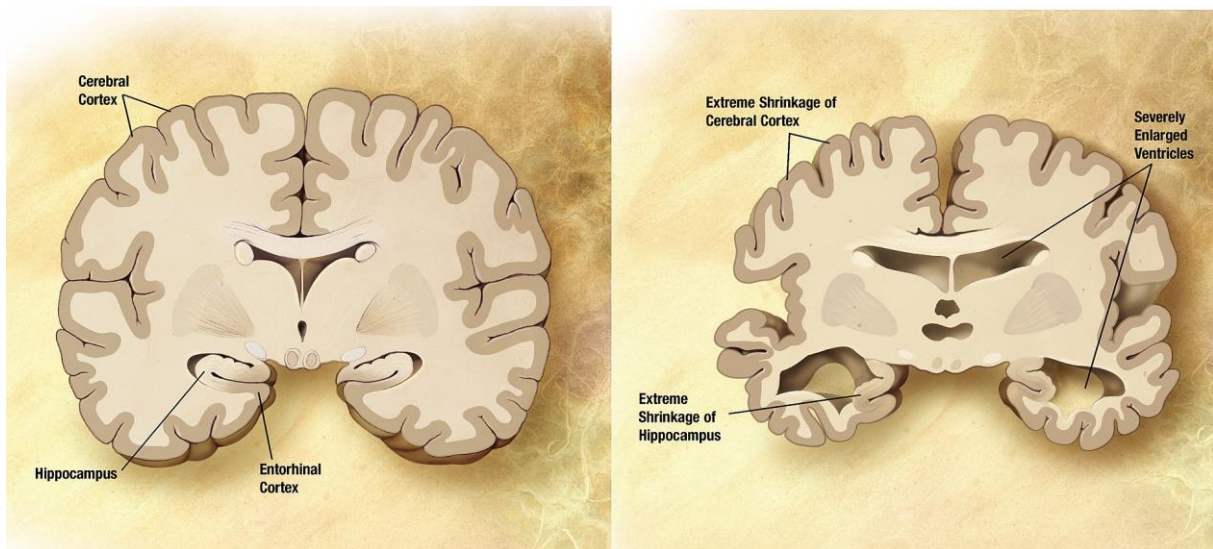


Figure 2: Representation of brain atrophy of the human brain in AD (on the right) compared to normal (on the left). During the stages from moderate to advanced AD, shrinkage of the cerebral cortex and hippocampus is evident, accompanied by an enlargement of the lateral ventricles due to the loss of neuronal cells. The figure is adapted from McCloskey, 2017 (McCloskey, 2017).

The major microscopic features of AD are amyloid plaques and NFTs (Fig. 3) (Serrano-Pozo et al., 2011; Selkoe, 2001). Additionally, activation of glial cells around plaques, loss of neuronal cells and synapses along with cerebral amyloid angiopathy (CAA) also constitute some of the main pathological characteristics of AD (Serrano-Pozo et al., 2011; Love et al., 2014).

Amyloid plaques are extracellular accumulations of A β fibrils, organized as beta-sheets (Chen et al., 2017). They are deposited between neurons as well as within blood vessels in the brains of AD patients (Serrano-Pozo et al., 2011). Amyloid plaques are mainly composed of misfolded A β with 40 or 42 amino acids in combination with several other proteins and other A β forms (Blennow et al., 2006; Serrano-Pozo et al., 2011). A β 42 is more insoluble, with higher levels of fibrillization compared to A β 40; therefore, amyloid plaques' composition is abundant in A β 42 peptides (Serrano-Pozo et al., 2011). Amyloid accumulation starts developing in the neocortex and progressively spreads to the subcortical areas (Braak and Braak, 1991; Serrano-Pozo et al., 2011).

Studies have shown that the loss of neurons, in combination with the severity of AD, correlates with the development of NFTs levels in the brains of patients (Ingelsson et al., 2004). Tau pathology in AD starts in the entorhinal cortex and hippocampus and it is later observed in the neocortex (Ingelsson et al., 2004).

Moreover, there is evidence that the A β peptide is also deposited on blood vessel walls in the brains of AD patients (Serrano-Pozo et al., 2011; Love et al., 2014). This is known as

CAA, and it is usually the A β 40 which is accumulated in the vascular wall of this angiopathy (Qi and Ma, 2017). CAA can be detected in post-mortem brain tissue, and it is estimated that 80% of AD cases are associated with CAA (Serrano-Pozo et al., 2011; Qi and Ma, 2017).

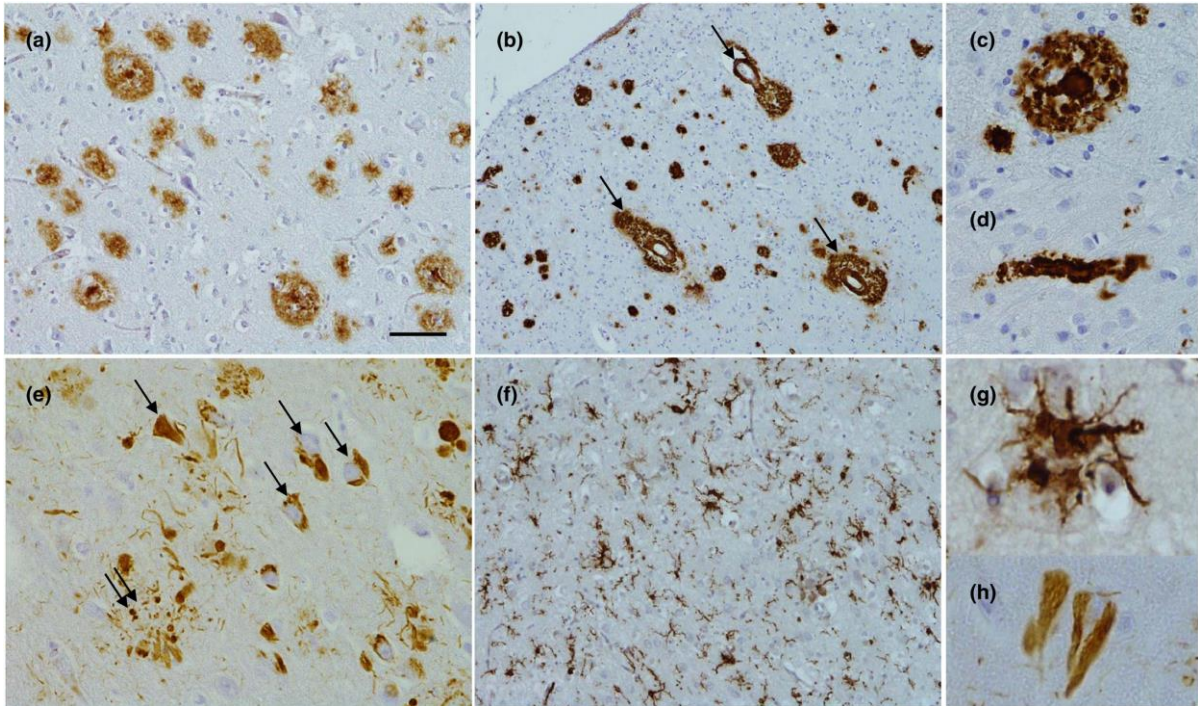


Figure 3: Pathological hallmarks of AD. Amyloid plaques in the frontal cortex after immunohistological detection of A β (a) and an example of cerebral amyloid angiopathy (CAA); the arrows are indicating the A β deposits on the blood vessel walls (b). High magnification of an amyloid plaque (c) highlighting a dense core of A β , accompanied by A β depositions in small blood vessels (d). Detection of neurofibrillary tangles after immunohistochemistry in (e, arrows) and an amyloid plaque (e, double arrow). Activated microglia after immunohistological detection in AD brain tissue (f), high magnifications of reactive microglia in (g); and, neurofibrillary tangles in (h). The figure has been made by Dr. Tammarny Lashley, Queen Square Brain Bank and it is adapted from Lane et al., 2018. (Lane et al., 2018)

1.1.4 The amyloid pathology of AD

The amyloid hypothesis is hitherto the most supported theory of AD, suggesting that excessive deposition of neurotoxic A β incites the pathological cascade of AD (Selkoe and Hardy, 2016). A β peptides are produced through the amyloidogenic proteolytic pathway after sequential processing of APP by β -secretase (BACE1) and γ -secretase (Fig. 4) (Hampel et al., 2020; Ishiura et al., 2000). APP is also metabolized via a non-amyloidogenic pathway by α -secretase (ADAM10) and γ -secretase activity, where α -secretase cleaves APP within the A β domain (Chen et al., 2017; Ishiura et al., 2000). Imbalance between A β generation and A β clearance leads to the progressive aggregation and accumulation of A β peptides in the brain

of patients with AD (Chen et al., 2017; Ishiura et al., 2000). Furthermore, it has been recently discovered that APP cleavage by η -secretase is an alternative processing pathway, which occurs after BACE1 inhibition, resulting in an increased accumulation of $A\eta$ - α peptide which has been shown to be associated with rescued neuronal activity in the hippocampus (Fig. 4) (Willem et al., 2015; Barao et al., 2016; Hampel et al., 2020)

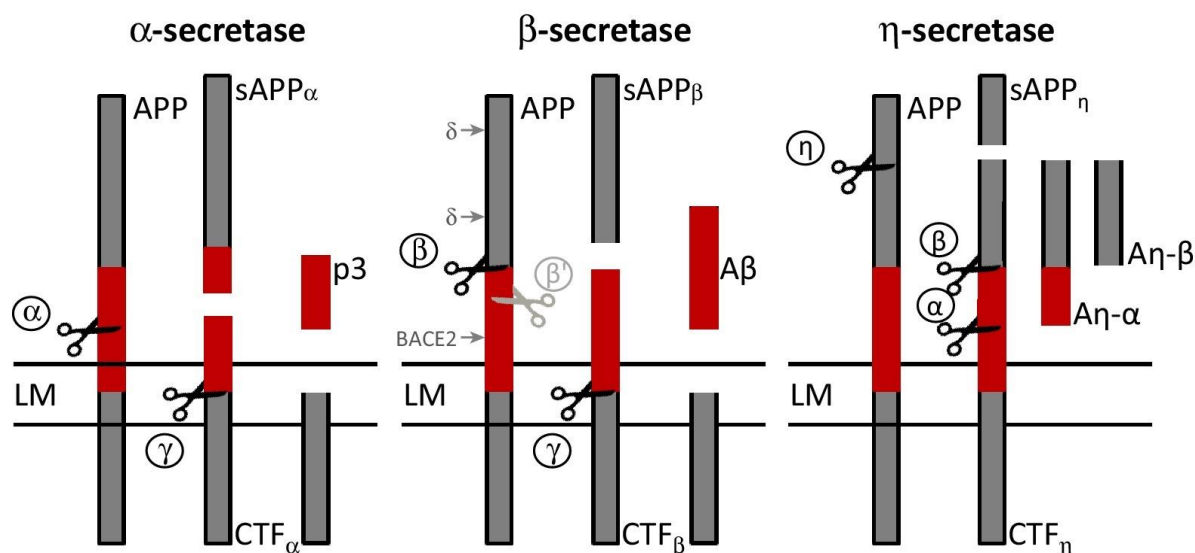


Figure 4: APP proteolytic pathways. The non-amyloidogenic processing of APP (α -secretase pathway) is carried out by sequential cleavages by α - and γ -secretases (to the left). α -secretase cuts within the $A\beta$ domain to generate the membrane-tethered C-terminal fragment α ($CTF\alpha$) and the N-terminal fragment (NTF) $sAPP\alpha$. The $CTF\alpha$ is further cleaved by γ -secretase activity to generate the extracellular p3. The amyloidogenic pathway of APP processing (β -secretase pathway) involves sequential cleavages by β - and γ -secretases (in the middle). β -secretase cuts APP to generate a N terminus of $A\beta$ ($sAPP\beta$) and a membrane-tethered C-terminal fragment β ($CTF\beta$). The $CTF\beta$ is subsequently cleaved by γ -secretase activity to release $A\beta$. The η -secretase pathway is occurred by sequential cleavages by α - and γ -secretases (to right). η -secretase cuts APP to generate the membrane-tethered C-terminal fragment η ($CTF\eta$) and the NTF $sAPP\eta$. The $CTF\eta$ is further processed by α - and β -secretases to release the long $A\eta$ - α and short $A\eta$ - β peptides (LM is the abbreviation of the lipid membrane). The figure is adapted from Hampel et al., 2020 (Hampel et al., 2020).

Until recently, it has been thought that the fibrillar $A\beta$ within the amyloid plaques was the most critical player contributing to the pathogenesis of AD (Hardy and Selkoe, 2002). Later research revealed that soluble $A\beta$ oligomers are the most neurotoxic forms and can be spread throughout the brain causing irreversible impairments in dendritic spines, synapses and lead to neuronal loss (Forloni et al., 2016). Studies have shown that $A\beta$ oligomers can prompt tau hyperphosphorylation and stimulate the development of NFTs in AD brains (Jin et al., 2011).

The amyloid cascade hypothesis has been highly supported by the discovery showing that all familial AD mutations in the APP, PS1 and PS2 genes are associated with the

generation and increased levels of the pathological A β forms (Hardy and Selkoe, 2002; Selkoe and Hardy, 2016). Moreover, in sporadic AD, genetic variants in *APOE*, or other genes that have been described as risk factors, are also implicated in A β clearance. This fact indicates that A β accumulation in the brain is a central event in the pathogenesis of AD (Hardy and Selkoe, 2002; Selkoe and Hardy, 2016). In both cases, A β oligomerization and deposition lead to synaptic disruption, gliosis, formation of NTFs as well as to the death of neuronal cells and, therefore, to neurotransmitter deficits that eventually result in dementia (Fig. 5) (Selkoe and Hardy, 2016). Nowadays, several therapeutic strategies against AD are based on the amyloid hypothesis targeting A β (Hardy and Selkoe, 2002).

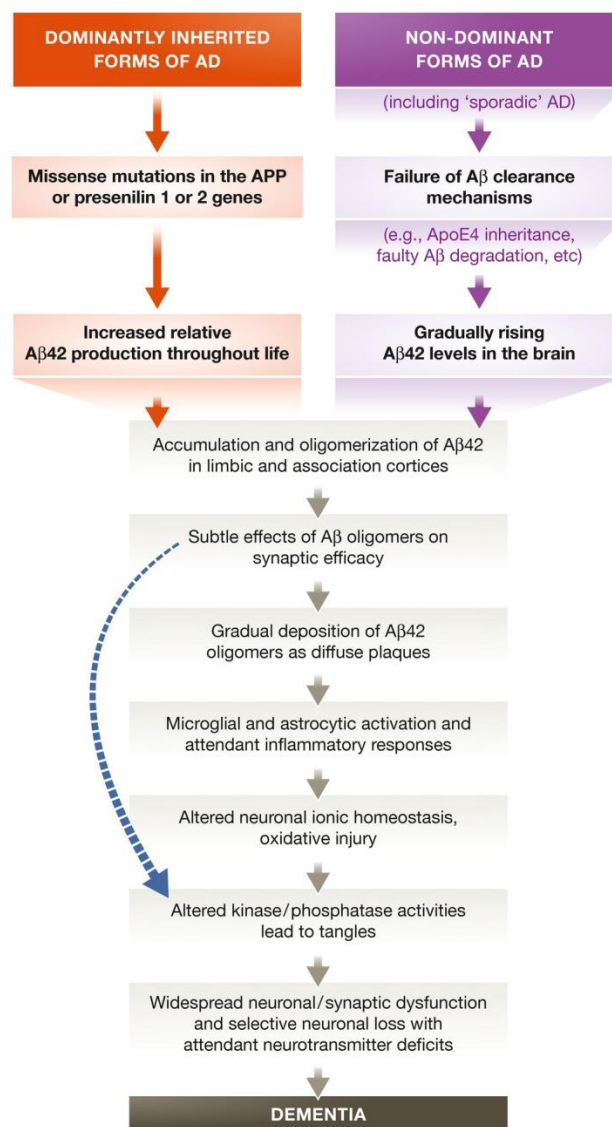


Figure 5: Schematic representation of the amyloid cascade hypothesis, showing the steps leading to AD. The blue dashed arrow on the left points out that A β oligomers may directly damage synapses and promote hyperphosphorylation of tau, leading to the formation of neurofibrillary tangles in addition to gliosis. The figure is adapted from Selkoe and Hardy, 2016 (Selkoe and Hardy, 2016).

1.1.5 Neuroinflammation in AD

Brain inflammation has a fundamental role in the pathogenesis of AD (Heneka and O'Banion, 2007). Chronically activated glial cells, such as microglia and astrocytes, are the main players of this process; by secreting pro-inflammatory mediators in the most affected brain areas they contribute to neuronal dystrophy and, eventually, to neuronal death (Rubio-Perez and Morillas-Ruiz, 2012; Tuppo and Arias, 2005). Numerous evidence suggests the accumulation of A β as the most prominent factor that leads to neuroinflammatory responses in AD (Kinney et al., 2018). Reactive microglia and astrocytes have been detected clustering around amyloid plaques and mediating A β clearance (Fig. 6) (Heneka et al., 2015).

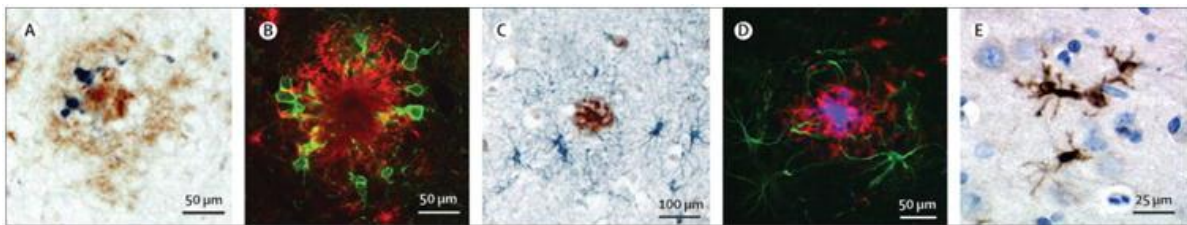


Figure 6: Microglial and astrocytic accumulation around amyloid plaques in AD in human brain tissue and mouse brain tissue (APP/PS1 mice) respectively. (A) CD11b-positive microglia (in blue color) around A β deposits (in brown color) in the parietal cortex of a post-mortem human brain section from a patient with AD. (B) Iba1-positive microglia (in green color) around an amyloid plaque (in red color) in a brain section of an APP/PS1 mouse. (C) GFAP-positive astrocytes (blue) surround A β depositions (brown) in the parietal cortex of a post-mortem human brain section from a patient with AD. (D) GFAP-positive astrocytes (green) around an amyloid plaque (red) in a brain section of an APP/PS1 mouse. (E) Interleukin-1 β (IL-1 β)-positive microglia (brown) in the frontal cortex of a post-mortem human brain section from a patient with AD. The figure is adapted from Heneka et al., 2015 (Heneka et al., 2015).

Microglia, brain-innate immune cells constitute approximately the 10% of all brain cells, and have a dual role in AD; either detrimental or beneficial (Cappellano et al., 2013; Sierra-Filardi et al., 2011; Schafer and Stevens, 2015). In 2002, the scientific work of Matthew R. Chapman and colleagues revealed that several known bacteria unexpectedly present A β sheets on their surfaces (Chapman et al., 2002). For a long time before this identification, these bacteria were used to be stained by the Congo red dye, an organic compound that is today commonly used for staining amyloid plaques in brain tissues from patients with AD (Chapman et al., 2002). Microglial cells have the ability to sense with their surface receptors the A β sheets in the same manner they detect a pathogen invasion (Heneka et al., 2015; Bamberger et al., 2003; Paresce et al., 1996). Microglia, have been equipped with danger-associated molecular pattern receptors to recognize molecules on pathogen surfaces; likewise

they recognize the deposited A β (Stewart et al., 2010; Liu et al., 2005; Yamanaka et al., 2012). Therefore, they mount a very strong inflammatory reaction because they act as defenders of the brain (Ardura-Fabregat et al., 2017; Heneka and O'Banion, 2007). Once activated, microglia can contribute to the phagocytosis and degradation of A β , thus reducing the load of amyloid plaques in AD brains (Lee and Landreth, 2010). Moreover, it has been proposed that microglia can release soluble factors beneficial for neuronal survival, such as the glial-derived neurotrophic factor (GDNF) or brain-derived neurotrophic factor (BDNF), where the later one is known to be implicated in memory formation processes (Gomes et al., 2013). On the other hand, current evidence has shown that A β and other pathological events in AD brains trigger microglia towards initiating an inflammatory response (a pro-inflammatory type of acute reaction) which releases complement, pro-inflammatory cytokines; such as interleukin 6 (IL-6), interleukin 1 β (IL-1 β) and tumor necrosis factor- α (TNF- α), chemokines, nitric oxide (NO) and radical oxygen species (ROS) which cause a severe brain inflammation (Wyss-Coray and Rogers, 2012). The transition of microglia from its pro-inflammatory detrimental phenotype (M1) to its beneficial anti-inflammatory phenotype (M2) might be accomplished by modulation of pro-inflammatory signaling pathways, such as the NLRP3 inflammasome (Heneka et al., 2013; Heneka et al., 2015; Heneka et al., 2019). It has been reported that A β recognition by microglia in AD is associated with NLRP3 inflammasome activation. It is thought that the activation of inflammasome is related with A β spread in the brain of AD patients (Heneka et al. 2019). Recent evidence revealed that adapter protein apoptosis-associated speck-like protein, containing a caspase recruitment domain (ASC) specks released by microglia, bind to A β and accelerate the A β aggregation and oligomerization, seeding A β pathology in the brain (Lu et al., 2014; Venegas et al., 2017; Heneka et al., 2019).

Furthermore, astrocytes are important brain cells for modulation of neuronal functions, being also well-known for their contribution to the maintenance of the blood-brain barrier (BBB). Astrocytes play a crucial role in synaptic transmission in the brain (Sofroniew and Vinters, 2010). It has been demonstrated that changes in astroglia morphology in animal models of AD are associated with disrupted synaptic connectivity, resulting in the development of cognitive impairments (Olabarria et al., 2010). Similar to microglia, astrocytes detect accumulated A β in AD brains and initiate inflammatory responses around amyloid plaques. Reactive astrocytes release several cytokines and chemokines that increase the inflammation levels in the brain and consequently lead to neuronal impairments (Heneka et al., 2015; Wyss-Coray and Rogers, 2012).

1.1.6 Therapeutic approaches for the treatment of AD

Until now, there is no treatment to cure AD (Weinstein, 2018). Although several drugs have been approved by the Food and Drug Administration (FDA) for AD patients, they have all been produced with a view to improving the symptoms of the disease, rather than curing it (Chen et al., 2017). These drugs have been described to be acting through two different mechanisms. Cholinesterase inhibitors block the hydrolysis of ACh, aiming to slowdown the progression of the disease. They belong to the first known drug category, with substances such as donepezil (Aricept; approved in 1996) (Rogers and Friedhoff, 1996; Bryson and Benfield, 1997), rivastigmine (Exelon; approved in 2000) (Rogers and Friedhoff, 1996; Bryson and Benfield, 1997) and galantamine (Razadyne; approved in 2001) (Woodruff-Pak et al., 2007). Memantine (Namenda approved in 2003), which acts as a blocker of the N-methyl-D-aspartate (NMDA) receptors, belongs to the second drug category of the FDA approved medications for AD (Riepe et al., 2006). This drug targets the glutamatergic system and improves the cognitive functions, behavior and mood of patients with moderate to severe AD. In 2014, a drug with stronger effects against AD symptoms, combining donepezil and memantine (Namzaric), was also approved by FDA for the treatment of AD in order to restore both ACh and glutamate levels in the patients' brains (Chen et al., 2017). In recent years, despite the critical failures in developing inhibitors of A β production and aggregation, several A β antibodies and new vaccines are undergoing clinical trials (Chen et al., 2017).

1.2 The mammalian hippocampus

The hippocampus is one of the most studied structures in the mammalian brain that belongs to the limbic system. It plays a crucial role in learning, memory formation and consolidation as well as in spatial navigation (Scoville and Milner, 1957; Lavenex and Amaral, 2000). Over the years, hippocampal function has been extensively investigated with the use of structural, molecular, electrophysiological and behavioural technology (Bird and Burgess, 2008; Witter et al., 1988; Neves et al., 2008).

1.2.1 The hippocampal formation

The hippocampus is located in the medial temporal lobe reciprocally connected with the entorhinal cortex, and it is subdivided into 3 *Cornu Ammonis* (CA) hippocampal subfields;

CA1, C2 and CA3 (Witter, 1993; Golgi et al., 2001). According to anatomists, the hippocampal formation consists of the dentate gyrus (DG), the subicular complex (parasubiculum, presubiculum and subiculum) and the entorhinal area (lateral and medial entorhinal cortices) which plays an important role in memory formation and spatial navigation (Andersen et al., 2007). A detailed description of the so-called trisynaptic loop of the EC connectivity with the hippocampal subfield is provided in (Fig. 7) (Neves et al., 2008).

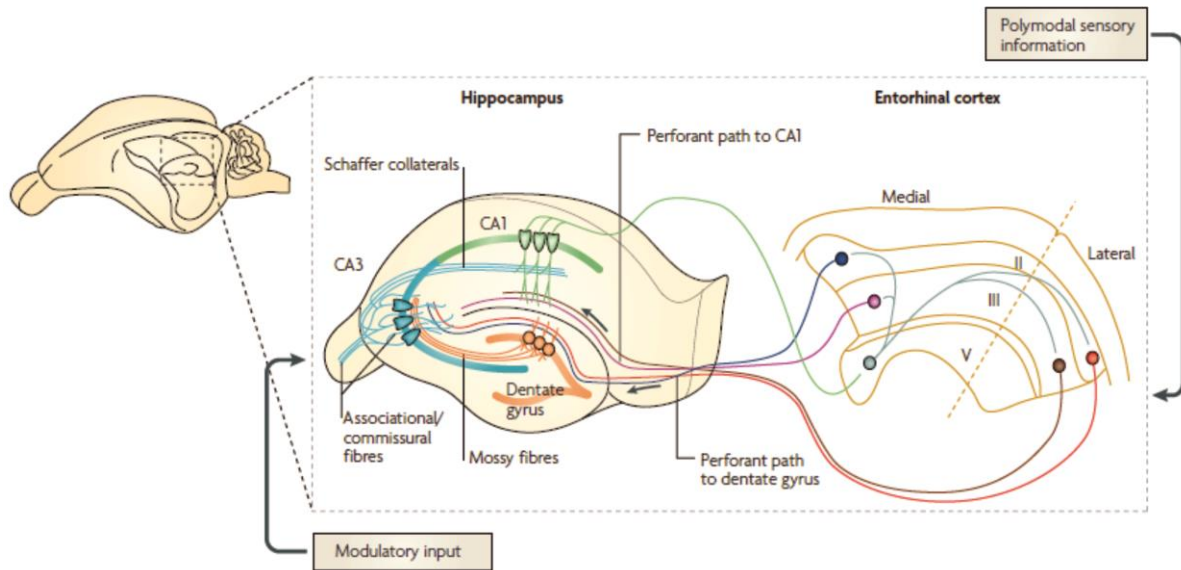


Figure 7: The basic hippocampal trisynaptic circuit. The outer and middle third of the dendritic tree of granular cells in the dentate gyrus receive inputs carrying polymodal sensory information from neurons located at the layer II of the lateral and medial entorhinal cortices via the perforant pathway respectively. Granule cells located in dentate gyrus contact the proximal apical dendrites of CA3 pyramidal neurons through mossy fibres which project to ipsilateral CA1 pyramidal neurons via Schaffer collaterals and to contralateral CA3 and CA1 pyramidal neurons through commissural fibres. In the same area there is also an associative network interconnecting CA3 pyramidal neurons. Moreover, the distal apical dendrites of CA1 pyramidal neurons are innervated by direct inputs from neurons located at the layer III of the lateral and medial entorhinal cortices. A modulatory input is carried by afferent fibres of cell bodies of neurons from the 3 hippocampal subfields (packed in an interlocking C-shaped arrangement) that make synaptic contacts with selective regions of the dendritic tree. The figure is adapted from Neves et al., 2008. (Neves et al., 2008)

A major hippocampal event, closely associated with cognition in the mammalian brain, is the glutamatergic neurotransmission (Sofroniew and Vinters, 2010; Lu et al., 2014). Astrocytes, as the principal elements of the physiological maintenance of the balance between glutamate uptake and release, have an important role in this process (Olabarria et al., 2011). Astrocytes express glutamate receptors on their surfaces, and therefore, they contribute to the initiation of intracellular signaling pathways. Moreover, astrocytes have high-affinity glutamate transporters that bind glutamate; a process that results in the balanced regulation of

glutamate release from the neuronal presynaptic buttons (Rose et al., 2017). This process increases the levels of the extracellular glutamate, and therefore, modifies the activation of the glutamate receptors which are expressed on the postsynaptic sites of nearby neurons (Rose et al., 2017). There is evidence that glutamate homeostatic system is disrupted in the late stages of AD, affecting the glutamatergic neurotransmission (Olabarria et al., 2011; Danysz and Parsons, 2012). It is also thought, that reduced levels of the glutamine synthetase, which is expressed in the astrocytes as well as in changes in the glutamine synthetase-immunoreactivity, are strongly associated with cognitive deficits in animal models of AD disease (Olabarria et al., 2011).

1.2.2 The laminar organization of the hippocampus

The laminar organization of the hippocampus is similar to all its CA subfields (Andersen et al., 2007; Witter, 1993; Golgi et al., 2001). Stratum pyramidale (SP) is the principal cell layer that contains the cell somata of all pyramidal neurons (Andersen et al., 2007). Stratum oriens (SO) is located deep to the pyramidal cell layer and contains the basal dendrites of the pyramidal neurons and some interneurons (Andersen et al., 2007). Stratum radiatum (SR) is above the SP and contains the apical dendrites of the pyramidal neurons. Commissural and Schaffer collateral fibres are also located in the SR layer along with some interneurons (Andersen et al. 2007). Stratum lacunosum-moleculare (SLM) is the most superficial layer of the hippocampus, and contains the apical tufts of the pyramidal cells and fibres from entorhinal cortex terminate as well as several interneurons (Andersen et al., 2007).

1.2.3 CA1 pyramidal neurons

The pyramidal neurons in the CA1 hippocampal subfield display homogenous dendritic trees with the similar total dendritic length and configuration (Fig. 8) (Spruston, 2008; Andersen et al., 2007). The diameter of the neuronal somata of the CA1 pyramidal neurons is approximately 15 μm ; some of these cells have one main apical dendrite, whereas others have two (Ishizuka et al., 1995). It has been observed that the CA1 pyramidal cells with one main apical dendrite have larger basal dendritic trees than those with two (Andersen et al., 2007; Pyapali et al., 1998). Despite the overall homogeneity of the hippocampal pyramidal neurons in the CA1 region, the cells can receive different inputs along the different hippocampal layers (Pyapali et al., 1998).

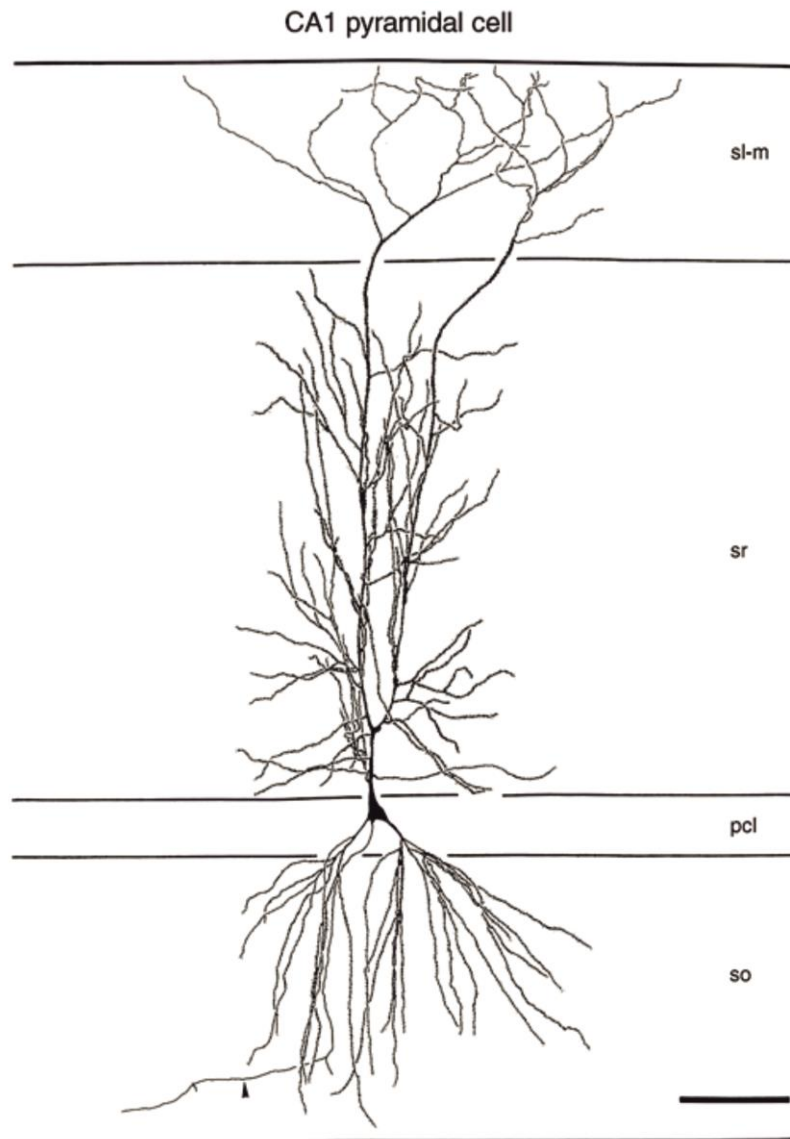


Figure 8: Representation of a hippocampal CA1 pyramidal neuron. The basal dendrites are depicted in the stratum oriens (SO), the neuronal cell body is located in the stratum pyramidale (pyramidal cell layer; PCL), the main apical dendrites and all side branches that emerge by them are located in the stratum radiatum (SR) and the apical tufts are in the stratum lacunosum-moleculare (SLM). The neuronal axon is indicated by an arrowhead in the SO layer (at the bottom left). Scale bar: 100 μ m. The figure is adapted from Andersen et al., 2007 (Andersen et al., 2007).

1.3 Dendritic spines

1.3.1 The structure and function of dendritic spines

Dendritic spines are tiny protrusions that emerge from a neuron's dendrite (Harris and Kater, 1994; Chicurel and Harris, 1992). They represent the main postsynaptic sites for excitatory input, where neurons receive and integrate information (Dorostkar et al., 2015). Dendritic

spines are important compartments for the modulation of synaptic strength and transmission of electrical signals to the neuronal soma (Spires-Jones and Knafo, 2012).

It has been calculated that the dendritic spine density in mature neurons ranges from 1 to 10 spines per μm of dendritic length. Spines are heterogeneous in shape (spine head volumes have a range of 0.01 to 0.8 μm^3), size (0.5-2 μm in length) or activity, and they are classified by shape into several categories; such as filopodium, thin, stubby, mushroom-shaped and cup-shaped spines (Harris and Kater, 1994; Chicurel and Harris, 1992; Harris, 1999; Sorra and Harris, 2000). These structures are extremely dynamic, having the ability to suddenly change their size or shape within seconds, minutes, hours or days (Fig. 9) (Hering and Sheng, 2001).

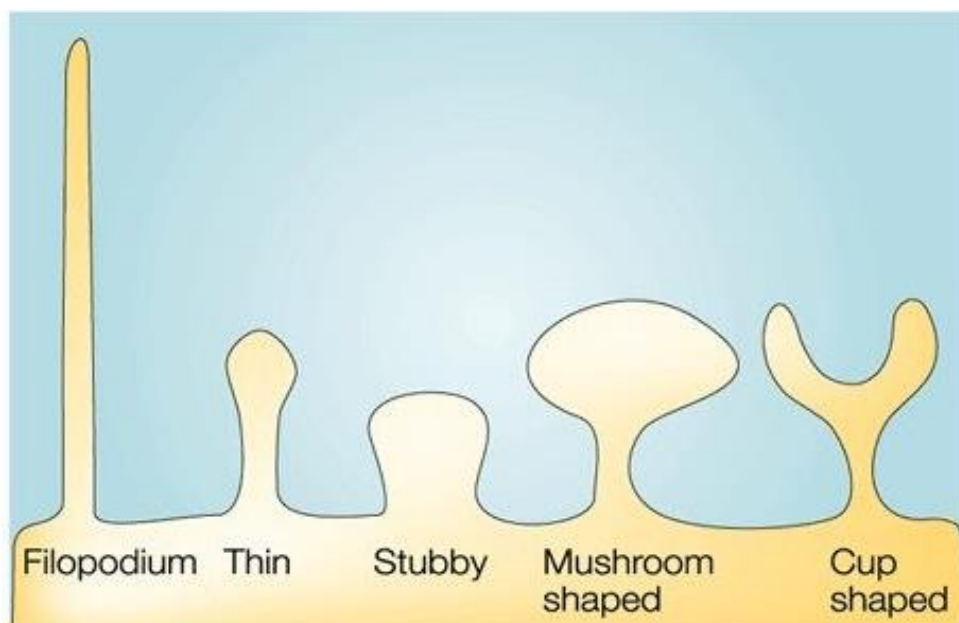


Figure 9: Dendritic spine classification based on their morphological characteristics. This figure represents the shape of filopodium, thin, stubby, mushroom-shaped and cup-shaped spines. Figure adapted from Hering and Sheng, 2001 (Hering and Sheng, 2001).

Dendritic spines constitute the most important players in synaptic plasticity which is mediated at hippocampal CA3-CA1 synapses mainly by trafficking of AMPA receptors to and away from their postsynaptic membrane (Dorostkar et al., 2015). These changes in synaptic strength are also accompanied by morphological alterations, such as changes in the dendritic spine density and shape, representing the so-called structural plasticity (Hering and Sheng, 2001). Dendritic spine plasticity has shown to be implicated in learning and memory processes. Impaired spine homeostasis (i.e. the loss of dendritic spine) is well known to accompany several neurodegenerative diseases such as AD (Herms and Dorostkar, 2016; Liebscher et al., 2014; Wei et al., 2009; Tsai et al., 2004).

1.3.2 Brain-derived neurotrophic factor (BDNF) and its role in dendritic spines

Brain-derived neurotrophic factor (BDNF) is a member of the neurotrophin family of growth factors, essential for neuronal development and function (Lessmann, 1998; Lessmann et al. 1994). BDNF is a crucial player in numerous processes of synaptic and structural plasticity, having effects on pre- and postsynaptic sites (Gottmann et al., 2009; Ohno-Shosaku and Kano, 2014). Activation of BDNF/tropomyosin-related kinase B (TrkB) signalling promotes the expression and trafficking of AMPA and NMDA receptors and increases synaptic transmission (Kang and Schuman, 1995; Lessmann et al., 1994).

Recent studies on primary hippocampal neuronal cultures have revealed that BDNF is also implicated in dendritic spine density and morphology of mature neurons (von Bohlen und Halbach and von Bohlen und Halbach, 2018; Ji et al., 2010). Mounting evidence has suggested BDNF as a key mediator for increasing spine density in neurons acting via TrkB or p75NGF receptors (Tyler and Pozzo-Miller, 2003). BDNF is required for the activity-dependent maintenance, maturation and stabilization of dendritic spines (Kellner et al., 2014).

1.4 Fingolimod (FTY720)

1.4.1 Sphingosine-1-phosphate (SP1)

Sphingolipids are the basic structural components of the plasma membrane lipid bilayer (Kraft, 2016). They are lipids, containing a set of aliphatic amino alcohols that include sphingosine, and they play an essential role in regulating cellular survival processes, such as cell growth and differentiation as well as apoptosis and autophagy (Pruett et al., 2008; Y. Li et al., 2014). Studies have shown that sphingolipids are highly expressed in the central nervous system (CNS), where it is also thought that they play a crucial role in several neuronal functions in the mammalian brain (Jesko et al., 2019; Olsen and Faergeman, 2017).

SP1 is produced after phosphorylation of sphingosine at the primary hydroxyl group by sphingosine kinase 1 (SPHK1) and sphingosine kinase 2 (SPHK2). SP1 molecule can bind to the five subtypes of SP1 receptors (SP1R₁, SP1R₂, SP1R₃, SP1R₄ and SP1R₅) (Chi, 2011). SP1R_{s(1-5)} are a class of G protein-coupled receptors (GPCRs), known to be highly expressed in neurons and glial cells in the brain (Chi, 2011; Jesko et al., 2019). Once SP1 binds SP1R_{s(1-5)} in cell surfaces, it is thought to be implicated in cell proliferation, apoptosis, and autophagy

processes or even in immune responses, depending on the cell type that it is bound to (Angelopoulou and Piperi, 2019).

1.4.2 Structure, biochemistry and activity of FTY720

FTY720 is a new oral drug, approved by the FDA, for the treatment of multiple sclerosis (MS) (J. Chun and Brinkmann, 2011). FTY720 is synthesized by myriocin (ISP-1); a metabolite derived from the fungus *Isaria sinclairii* (Adachi and Chiba, 2007). This synthetic substance is a structural analogue of sphingosine that can penetrate the BBB where it is phosphorylated by SPHK2 in the cytosol (Strader et al., 2011; Rothhammer et al., 2017). Once FTY720 is phosphorylated, it becomes a S1P analogue capable of binding to SP1Rs₍₁₋₅₎, exhibiting the highest affinity for SP1R₁ (Strader et al., 2011). Strong evidence has shown that activation of SP1Rs₍₁₋₅₎ by fingolimod-phosphate (FTY720-P) leads to receptor internalization effects and to the induction of expression mechanisms of genes that can modulate neuronal phenotype (Strader et al., 2011; Cruickshanks et al., 2015; Rothhammer et al., 2017).

Recent studies suggest that FTY720 treatment is implicated in the reduction of pro-inflammatory cytokines secreted by microglia, and that the drug is associated with increased BDNF levels providing neuroprotective effects (Fukumoto et al., 2014). Today, it is still unclear whether FTY720-P affects neurons or alters BDNF levels directly in the brain and which are the cell types that are involved in such processes (Doi et al., 2013; Fukumoto et al., 2014).

1.5 Synaptic cell adhesion molecules (CAMs)

Synaptic CAMs in the mammalian brain enable cell-to-cell interaction, and play an essential role in coordinating and triggering synapse formation as well as in regulating dendritic spine morphology in neurons (Li and Sheng, 2003; Gottmann, 2008).

Several synaptic CAM families have been identified to be located in the pre- or postsynaptic sites of mature synapses; such as cadherins, immunoglobulin-containing cell adhesion molecules (Ig-CAMs), neuroligins, neuroligins, ephrins, and Eph receptors (Fig. 10) (Bukalo and Dityatev, 2012). Each synaptic CAM of the different families bears specific characteristics in regards to its adhesion type or calcium sensitivity, and is thought to be implicated in different synaptic processes (i.e. synaptic differentiation, plasticity and stability) as well as functions (Li and Sheng, 2003; Bukalo and Dityatev, 2012). Several synaptic cell

adhesion molecules, such as N-cadherin (Ncad), neuroligin 1 (NLG1) and neurexin (NRX), undergo metabolism identical to the APP protein (Suzuki et al., 2012; Vassar, 2013; Brummer et al., 2019; Bot et al., 2011). The C-terminal fragment 1 (CTF1) of these proteins is an important substrate of γ -secretase and therefore, linked to AD (Andreyeva et al., 2012; Marambaud et al., 2002).

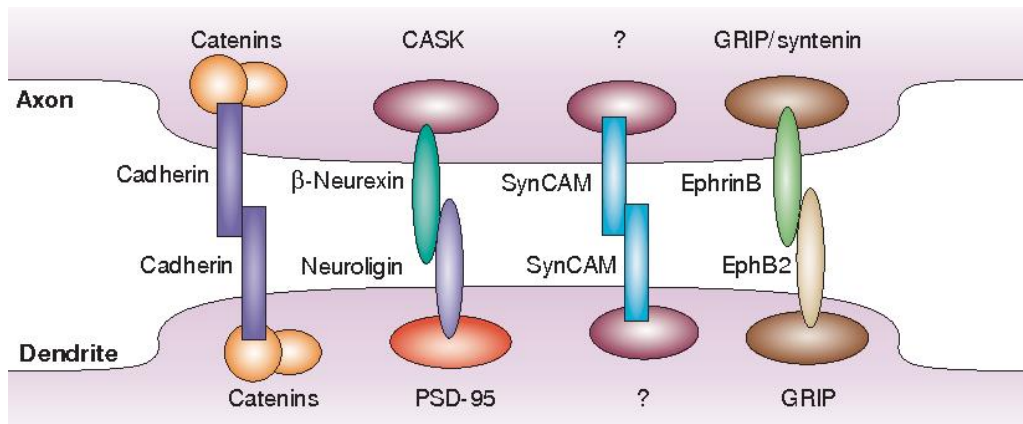


Figure 10: Interactions between synaptic cell adhesion molecules (CAMs). Homophilic interactions are represented by the same colour. β -neurexin, neuroligin, EphB2, ephrinB and SynCAM (synaptic cell-adhesion molecule) are shown to bind to specific PDZ [postsynaptic density protein 95 (PSD-95), discs large (Dlg) and zona occludens-1(ZO-1)]-domain-containing proteins. Catenins, calcium/calmodulin-dependent serine protein kinase (CASK) and GRIP/syntenin proteins associated with CAMs are also shown in the figure. The question marks indicate that SynCAM can bind numerous PDZ-domain-containing proteins, involving CASK but its exact partner is still not well known. The figure is adapted from Li and Sheng, 2003 (Li and Sheng, 2003).

1.5.1 N-cadherin (Ncad)

Ncad belongs to the cadherin family of synaptic CAMs and is expressed in neurons (Andreyeva et al., 2012; Gottmann, 2008). It is present in both presynaptic and postsynaptic sites of excitatory synapses (Bukalo and Dityatev, 2012). Strong evidence supports that Ncad is essentially implicated in morphological maturation of dendritic spines as well as in synapse integrity and plasticity processes. It is also thought that this molecule may play an important role in a synapse formation and growth (Gottmann, 2008; Li and Sheng, 2003; Bukalo and Dityatev, 2012).

Ncad is cleaved by α -secretase (ADAM10) activity, upon NMDA receptor stimulation, generating a truncated membrane CTF1 (Ncad CTF1) and liberating the NTF (Ncad NTF) (Andreyeva et al., 2012; Uemura et al., 2006). The subsequent intramembrane cut of Ncad CTF1 by γ -secretase produces another truncated cytoplasmic fragment, the so-called Ncad CTF2 (Ncad CTF2), which regulates gene expression (Uemura et al., 2006; Marambaud et al.,

2003). It has been suggested that Ncad proteolytic processes and products affect synapse function, and therefore, they are implicated in learning and memory physiology (Uemura et al., 2006).

1.5.2 Neuroligins (NLGs) and neurexins (NRXs)

NLGs and NRXs are two different families of synaptic CAMs which constitute a pair of specific transsynaptic binding partners in neurons (Gottmann, 2008). NLGs are expressed in the postsynaptic compartments of a synapse, whereas NRXs are presynaptic membrane proteins (Li and Sheng, 2003; Bukalo and Dityatev, 2012). It is known that NLG-NRX interactions are important for the formation of excitatory and inhibitory synapses and control them in an activity-dependent manner (Gottmann, 2008; Bukalo and Dityatev, 2012).

The proteolytic processing of NLRs and NRXs is similar. Both molecules are primarily cleaved by α -secretase, producing a membrane CTF1 (NLG CTF1 or NRX CTF1) and liberating a NTF (NLG NTF or NRX NTF) (Suzuki et al., 2012; Bot et al., 2011). Specifically, there is evidence that NLRs are cleaved by ADAM10, whereas NRXs are proteolytically processed by both ADAM10 and ADAM17 (Borcel et al., 2016; Peixoto et al., 2012). NLG CTF1 and NRX CTF1 are then further cleaved by γ -secretase activity to release the intracellular domains. Recent studies have shown that proteolytic events of these proteins are activity dependent and have a critical importance in synaptic function (Suzuki et al., 2012; Peixoto et al., 2012; Borcel et al., 2016).

1.6 Aims of the study

Dendritic spine dysfunction and synaptic alterations play an important role in the pathogenesis of AD (Dennis J Selkoe 2011). Dendritic spines are tiny protrusions emerging from neuronal dendritic branches in the mammalian brains (Alvarez and Sabatini, 2007). They constitute the postsynaptic neuronal compartment on which excitatory synapses are formed (Spires-Jones and Knafo, 2012). Impairments of dendritic spines, such as spine loss, lead to synaptic deficits, and therefore, are strongly associated with cognitive decline (Herms and Dorostkar, 2016). Dendritic spine pathology in AD is caused through direct or indirect effects that occur in AD (Dorostkar et al., 2015). The A β depositions (amyloid plaques) and soluble oligomeric A β are thought to be major factors in developing spine pathology in AD (Bittner et al., 2012; Liebscher et al., 2014; Tsai et al., 2004). Moreover, pro-inflammatory

mediators derived by activated glial cells, such as microglia and astrocytes, are also implicated in the disruption of spine physiology in AD (Dorostkar et al., 2015). Pathological changes in the availability and signaling pathways of several neurotrophins, such as BDNF, are thought to be involved in AD (Kellner et al., 2014). Potential pharmacological targeting of the alleviation of these disease-associated pathologies could represent an innovative treatment for dendritic spine pathology resulting in the slowdown of the progression of AD.

In the present study, the core of the interest lied in the development of novel therapeutic approaches for AD. The major aim of this research project, which is described in the first part of this thesis, was to investigate how voluntary running (VR) or application of FTY720, which are thought to enhance BDNF expression in the brain, lead to the reduction of dendritic spine pathology; thus rescuing dendritic spine loss in AD. FTY720, an immunosuppressant drug approved by the FDA for the treatment of multiple sclerosis (MS), was further used to test its potential in reducing both the observed robust microgliosis and astrogliosis, and the A β deposition and accumulation in AD.

This study was conducted *in vivo*, using APP/PS1 transgenic mice of AD, and all data were acquired and analyzed post-mortem. Golgi-Cox staining was used for identifying spine deficits in the hippocampus of APP/PS1 mice and of double transgenic APP/PS1 animals with a reduction in BDNF (APP/PS1/BDNF^{+/-}). Furthermore, a novel staining technique was established combining fluorescent labeling of amyloid plaques with the classical Golgi-Cox neuronal impregnation, in order to observe spine deficits in the vicinity of amyloid plaques in the hippocampus of APP/PS1 mice. The beneficial effects of VR and FTY720 (in a high dose of 1 mg/kg/2ndday and a lower dose of 0.2 mg/kg/2ndday) against AD spine pathology were investigated in the hippocampus of the APP/PS1 mice, while the potential positive effects of FTY720 (1 mg/kg/2ndday) were tested in the hippocampus and cortex of this animal model of AD.

The second part of this work focused on the investigation of potential γ -secretase dysfunction in sporadic AD. There is evidence that trans-synaptic interactions between synaptic CAMs at neuronal pre- and postsynaptic sites are essential for synapse stabilization (Li and Sheng, 2003). Ncad, NLG1 and NRX are synaptic CAMs which are known to be associated with synaptic processes; such as synaptic differentiation, synaptic plasticity and stability (Li and Sheng, 2003; Bukalo and Dityatev, 2012). As the proteolytic processing of these proteins is similar to the APP protein, they consist important substrates of γ -secretase, and therefore, they might be implicated in AD (Andreyeva et al., 2012; Marambaud et al., 2003; Bot et al., 2011; Suzuki et al., 2012). γ -secretase dysfunction due to loss-of-function

mutation in the presenilin-1 (PS1) gene has been reported in EOFAD, leading to alternative processing of APP and consequently to increased A β levels in AD brains (Veugelen et al., 2016; De Strooper et al., 2012). On the other hand, recent studies have also shown that increased levels of A β protein in the brains, due to γ -secretase misprocessing or alternative processing of APP, occur also in sporadic AD without mutations in PS1, indicating a potential γ -secretase dysfunction also in sporadic AD (Kim et al. 2009).

In this study, specific alterations in proteolytic processing of different substrates potentially caused by γ -secretase functional impairments in sporadic AD were identified by characterizing the CTF1 levels of Ncad, NLG1 and NRX in post-mortem brains from patients with sporadic AD.

2. Materials and Methods

2.1 Materials and equipment

2.1.1 Materials (chemicals, reagents, media and antibodies)

Ammonium hydroxide solution	Sigma-Aldrich
Antibody: anti-A β (IC16)	Prof. Claus Pietrzik (donation)
Antibody: donkey anti-rabbit Alexa Fluor 555 conjugated	Thermo Scientific
Antibody: goat anti-mouse Alexa Fluor 488 conjugated	Thermo Scientific
Antibody: goat anti-mouse IgG HRP-conjugated	Sigma
Antibody: goat anti-rabbit IgG HRP-conjugated	Sigma
Antibody: mouse anti-beta actin	Sigma
Antibody: mouse anti-GFAP (clone G-A-G; G 3893)	Sigma
Antibody: mouse anti-N-Cadherin	BD Transduction Laboratories
Antibody: rabbit anti-Iba1 antibody	Wako
Antibody: rabbit anti-Neuroigin 1	Synaptic Systems
Basal medium eagle (BME)	Gibco
BCA Protein Assay Kit	Thermo Scientific
Bovine serum albumin (BSA)	Serva and Sigma
B27 supplement	Tocris Bioscience
CaCl ₂	Sigma
DePex medium	Serva
Dimethyl sulfoxide (DMSO)	Sigma-Aldrich
DNase	Roche
Ethanol absolut	CHEMSOLUTE
Fetal calf serum (FCS)	Gibco
Fingolimod (FTY720)	Abcam
Glucose	Sigma
GlutaMAX	Invitrogen
Glycin	Sigma
HEPES, pH 7.4	Roth
ImmunoMount mounting medium	Thermo Scientific

Insulin	Sigma
KCl	Sigma
Ketamine hydrochloride/xylazine hydrochloride	Sigma-Aldrich
Laemmli buffer (4x)	BIO-RAD
Mercuric chloride	Merck
Methanol	J.T.Baker
Methoxy-X04	TOCRIS
MgCl ₂	Roth
Milk (nonfat)	Roth
MOPS (3-(N-morpholino) propanesulfonic acid)	Sigma
Neurobasal medium (NB)	Gibco
Normal goat serum (NGS)	Dianova
Paraformaldehyde (PFA)	Electron Microscopy Sciences
PBS ^(-/-) 1x	Gibco
Penicillin/Streptomycin	Gibco
Phenol red	Sigma
PMSF	EuroClone
Potassium chromate	Merck
Potassium dichromate	Merck
Protease inhibitor cocktail 25x	Roche
RIPA 10x	Cell Signaling
Rotiphorese 10x SDS-PAGE	Roth
SDS (sodium dodecyl sulfate)	Amersham Pharmacia Biotech
Sodium citrate	Merck
Sodium Pyruvate	Invitrogen
Sucrose	AppliChem
SuperSignal West Dura substrate	Thermo Scientific
Thioflavine S	Sigma-Aldrich
Tris, ultra pure	Biomol
Triton X-100	Sigma
Trypsin 2.5%	Gibco
Tween-20	Sigma
Xylol	Roth
β-mercaptoethanol	Sigma

γ -secretase inhibitor L-685,458

TOCRIS

2.1.2 Equipment (microscopes, devices and objects)

Centrifuge (420 R)	Hettich
Centrifuge (Mikro 200R)	Hettich
Confocal imaging system (LSM 780)	Zeiss
Cryostat CM 3050	Leica
Homogenizer (T 10 basic ULTRA-TURRAX)	IKA
LEITZ DM R microscope	Leica
Microscope slides (superfrost)	Thermo Scientific
PVDF (polyvinylidene difluoride) membrane	Roth
SDS-PAGE (12%)	BIO-RAD
Semi-dry blotter	Peqlab
Syringe (Omni fix-F)	Roth
Thermomixer	Eppendorf
Vibratome (Pelco Model 1000)	The Vibratome Company

2.1.3 Composition of buffers and solutions

MPBS ^(+/+) buffer (50ml), pH7.4		
Components	Volume	End concentration
MPBS ^(-/-) (table 2)	50 ml	
CaCl ₂ 2 M (Sigma)	25 μ l	1 mM
MgCl ₂ (Roth)	290 μ l	5.8 mM

Table 1: The composition of the modified phosphate buffered saline (+/+) [MPBS^(+/+)], pH 7.4.

MPBS ^(-/-) buffer (500 ml), pH 7.4			
Stock concentration	Components	Volume	End concentration
1x	1x PBS ^(-/-) (Gibco)	473.25 ml	
1 M	HEPES (Roth), pH 7.4	5 ml	10 mM
100 mM	Sodium Pyruvate (Invitrogen)	5 ml	1 mM
6 mg/ml	DNase (Roche)	500 μ l	6 μ g/ml
100 mg/ml	BSA (Serva)	5 ml	1 mg/ml
1 M	Glucose (Sigma)	5 ml	10 mM
100x	Penicillin/Streptomycin (Gibco)	1.25 ml	0.25x
200 mM	GlutaMAX (Invitrogen)	2.5 ml	1 mM
5 μ g/ml	Phenol red (Sigma)	500 μ l	1 mM

Table 2: The composition of the modified phosphate buffered saline (-/-) [MPBS^(-/-)], pH 7.4.

BME/10% FCS medium (500 ml)			
Stock concentration	Components	Volume	End concentration
	BME (Gibco)	438.50 ml	
200 mM (100x)	GlutaMAX (Invitrogen)	2.5 ml	1 mM
100%	FCS (Gibco)	50 ml	10%
100x	Penicillin/Streptomycin (Gibco)	1.25 ml	0.02x
10 mg/ml	Insulin (Sigma)	1.8 ml	0.036 mg/ml
1 M	Glucose (Sigma)	2.5 ml	5 mM
1 M	HEPES (Roth), pH 7.4	5 ml	10 mM

Table 3: The composition of the BME with 10% FCS (BME/10% FCS medium).

NB-B27 medium (500 ml)			
Stock concentration	Components	Volume	End concentration
	NB (Gibco)	483.75 ml	
200 mM (100x)	GlutaMAX (Invitrogen)	5 ml	2 mM
100x	Penicillin/Streptomycin (Gibco)	1.25 ml	0.25x
1x	B27 supplement (Tocris Bioscience)	10 ml	0.02x

Table 4: The composition of the NB with B27 supplement (NB-B27 medium).

Cell collecting buffer (5 ml)		
Components	Volume	
1x PBS ^(-/-) (Gibco)	5 ml	
Protease inhibitor cocktail (Stock 25x, Roche)	200 μ l	

Table 5: The composition of the cell collecting buffer.

Cell lysis buffer (1 ml)	
Components	Volume
1x RIPA [1:10 dilution in ddH ₂ O (10x RIPA; Cell Signaling)]	1 ml
Protease inhibitor cocktail (Stock 25x; Roche)	40 μ l
PMSF (stock 200 mM in 100% ethanol; EuroClone)	5 μ l

Table 6: The composition of the cell lysis buffer.

Hypotonic buffer (100 ml), pH 7.0	
Components	End concentration
ddH ₂ O	100 ml
MOPS (3-(N-morpholino) propanesulfonic acid; Sigma)	0.01 M
KCl (Sigma)	0.01 M

Table 7: The composition of cell the hypotonic buffer.

2.2 Animals

For this study, several lines of mice were used, such as APP/PS1 heterozygous mice (Radde et al., 2006) [6- to 7-month-old (male and female) and 13-month-old (male)], brain-derived neurotrophic factor (BDNF) heterozygous knockout mice (Korte et al., 1995) [BDNF^{+/-}; 6- to

7-month-old (male)] and APP/PS1/BDNF^{+/-} animals (Psotta et al., 2015) [BDNF^{+/-} mice crossbred with APP/PS1 mice; 6- to 7-month-old (male)] with their corresponding C57BL/6J wild-type (WT) littermates. APP/PS1 mice combine the ‘Swedish’ double mutation in the amyloid precursor protein (APP) gene (KM670/671NL) and a mutation in the Presenilin-1 (PS1) gene (Leu166Pro) under control of the Thy1 promoter (Radde et al., 2006). Both mutations are related to the early-onset familial Alzheimer’s disease (EOFAD) (Radde et al., 2006). APP/PS1 and BDNF^{+/-} mice were bred on the C57/BL/6J genetic background and constantly backcrossed with C57BL/6J mice.

The genotype of the animals was identified with polymerase chain reaction (PCR), using deoxyribonucleic acid (DNA) extracted from ear tissue biopsies obtained from three weeks old mice by an ear punch. All animals were housed in groups of 3 or 4 mice in standard cages supplied with nesting material. The animals had constant access to food and water and were maintained at the local conventional animal facility with a room temperature of 21 ± 0.3 °C and humidity of $55 \pm 10\%$ in a dark-light cycle of 12 hours (lights on at 7 a.m.).

The experimental work of the present study was conducted at the laboratory of Prof. Dr. Volkmar Lessmann at the Institute of Physiology in Magdeburg, in collaboration with Prof. Dr. Kurt Gottmann’s laboratory at the Institute of Neuro- and Sensory Physiology in Düsseldorf, in the context of a Neurodegenerative Disease Research (JPND) consortium [CircProt: Protection of Synaptic Circuits by BDNF/TrkB and Arc Signaling Pathways in Mouse Models of Alzheimer’s Disease (AD) and Huntington’s Disease (HD)]. All experiments were performed during the light phase of the cycle in accordance with the European Committee Council Directive (63/10 EU) on the protection and ethical guidelines for experimental animal methods, and were approved by the local animal care committee (Landesverwaltungsamt Sachsen-Anhalt).

2.3 Therapeutic interventions for AD tested in APP/PS1 mice

In the current study, APP/PS1 mice were used to investigate exercise (voluntary running) or chronic fingolimod (FTY720) administration as potential therapeutic strategies against dendritic spine pathology in AD. The assistance of Dr. Thomas Endres in providing animals, which were held under different housing conditions, was decisive for the progress of the project.

2.3.1 Voluntary running (VR)

Male APP/PS1 mice and WT littermates were held until the age of 4 to 5 months in standard housing (SH) conditions, and afterwards were distributed into treatment groups with different housing conditions and stayed there for 2 months until the age of 6 to 7 months. The testing group of voluntary running (VR) was made up of animals with all-time access to running wheels, while the control groups were consisted of mice held in cages under SH conditions (without running wheels) or mice kept in an enriched environment (EE) where they had access to blocked running wheels. All cages included the standard nesting materials.

2.3.2 Chronic FTY720 administration

Male APP/PS1 mice and WT littermates were treated with 1 mg/kg/2ndday FTY720 or with a lower dose of 0.2 mg/kg/2ndday at the age of 5 to 6 months. The drug, was dissolved in 3% DMSO (Sigma-Aldrich) in saline and was administered every second day for 1 month via intraperitoneal injections. Control APP/PS1 and their WT littermates were treated with vehicle solution.

2.4 Composition and preparation of Golgi-Cox solution

The Golgi-Cox solution was composed of 5% potassium dichromate (Merck), 5% mercuric chloride (Merck) and 5% potassium chromate (Merck) (Das et al., 2013). Stock solutions were prepared by dissolving 5 g of each chemical in 100 ml of warm, hot and cold distilled water respectively. The preparation of the Golgi-Cox solution was performed in a glass bottle according to the protocol steps used by Bayram-Weston et al. which are as follows: 100 ml of the potassium dichromate stock solution was mixed with 100 ml of the mercuric chloride stock solution and 200 ml of distilled water were added to 80 ml of the potassium chromate stock solution. Finally, 200 ml of the mixture potassium dichromate and mercuric chloride solution were slowly poured into the glass bottle with the 280 ml diluted potassium chromate solution. The formed precipitate in the bottom of the bottle indicated a successful mixture of the solutions. The prepared Golgi-Cox solution was kept in the dark for at least 3 days, and was finally filtered and stored in the dark at room temperature (Bayram-Weston et al., 2016).

2.5 Brain tissue collection and preparation for Golgi-Cox staining

APP/PS1 mice and their WT littermates were anesthetized by intraperitoneal injection of ketamine hydrochloride/xylazine hydrochloride (Sigma-Aldrich), and transcardially perfused with 0.9 % saline followed by 4% PFA (Electron Microscopy Sciences) in 0.1 PB pH 7.4. The brains were removed from the skulls, and post-fixed in 4% PFA in 0.1 M phosphate buffer (PB) pH 7.4 at 4 °C overnight. They were then placed into 7 ml of Golgi-Cox solution for 14 days and kept in the dark at room temperature. The solution was refreshed only once after 7 days. At the last impregnation day, all brains were transferred into 25% sucrose (AppliChem) in phosphate buffered saline (PBS) and stored in the dark at 4 °C for at least 1 or 2 days. The sucrose solution was renewed daily; 100 µm coronal sections were taken using a vibratome (Pelco Model 1000, The Vibratome Company, St. Louis, USA). For the sectioning procedure, all brains were glued to the vibratome base perpendicular to the blade. The vibratome glass-base was then placed to the vibratome chamber which contained PBS. Afterwards, the sections were first transferred into PBS-filled 24-well-plates, and then mounted onto gelatin-coated slides. The excess liquid was absorbed by paper wipes, and the sections were let to dry.

The Golgi-Cox stained brain sections were washed with distilled water for 2 min and then placed into 20% ammonium hydroxide (Ammonium hydroxide solution, ACS reagent, 28.0 - 30.0% NH₃ basis, Sigma-Aldrich) in distilled water. They were then rinsed twice with distilled water for 2 min each and dehydrated, passing through ascending grades of ethanol 70%, 95% and 100% for 5 min each. The sections were finally cleaned in xylol (Roth) twice for 10 min each. They were coverslipped with DePex medium (Serva). All slides were stored in dark boxes at room temperature.

2.6 Dendritic spine analysis in Golgi-Cox stained neurons

The density of dendritic spines was quantified for apical main and secondary dendrites in stratum radiatum (SR) and for apical tufts in stratum lacunosum-moleculare (SLM) in hippocampal CA1 pyramidal neurons (Figs. 11 & 12). The analysis was conducted manually, and the spine density was calculated as the number of spines per dendritic length in µm. The length of the Golgi-Cox stained dendrites was estimated with NeuronJ (a plugin of the National Institutes of Health (NIH) ImageJ software; <https://imagej.nih.gov/ij/>) in 40x magnification bright-field images taken by a monochrome SPOT camera connected with a LEITZ DM R microscope (Leica). Dendritic segments (>20 µm long) were selected from

fully stained neurons. For apical main or secondary dendrites, spine density was calculated in branches located in the whole range of SR, and approximately 50 to 200 μm distance from the soma. A 100x magnification oil-immersion objective was used for counting the number of spines for 10 dendritic segments per animal from different neurons. The analysis was conducted blindly to the mouse genotype.

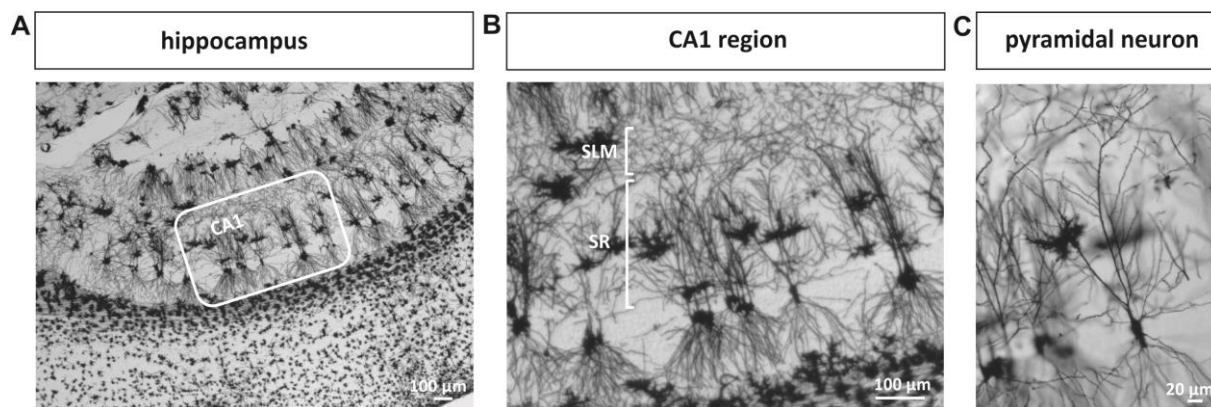


Figure 11: Representative images of Golgi-Cox impregnation in coronal mouse brain sections. (A) Golgi-Cox stained hippocampus (the white box shows the CA1 area). (B) Golgi-Cox impregnated pyramidal neurons in the CA1 area of the hippocampus. The layers of stratum radiatum (SR) and stratum-lacunosum moleculare (SLM) are indicated with white brackets. (C) A Golgi-Cox impregnated pyramidal neuron in the CA1 area of the hippocampus. Magnification: 5x (A, B) and 20x (C). Modified figure from Kartalou et al., under review.

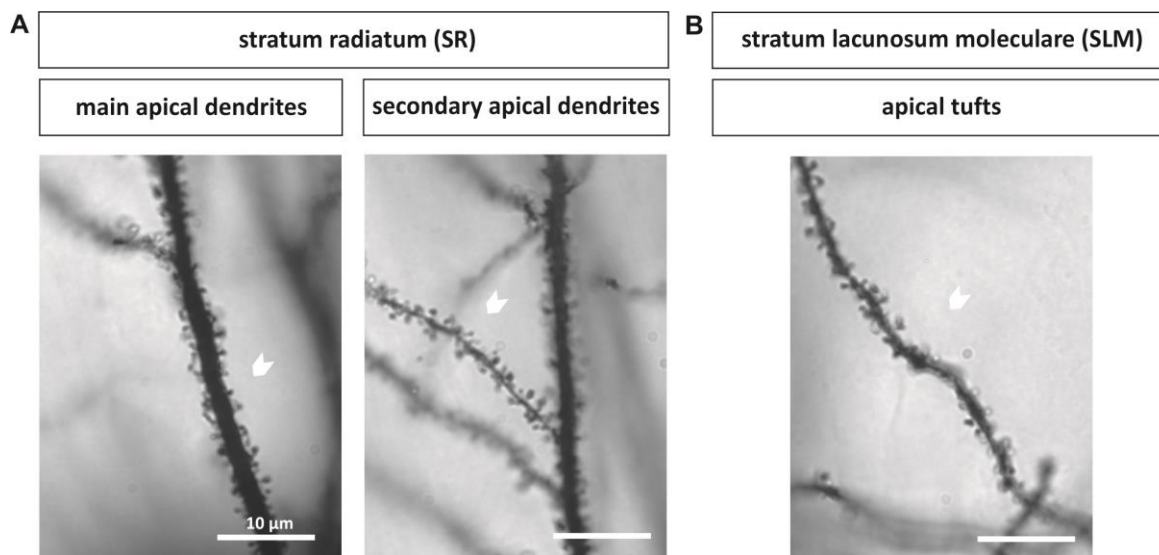


Figure 12: Visualization of dendritic spines in Golgi-Cox stained hippocampal CA1 pyramidal neurons in stratum radiatum (SR) and stratum-lacunosum moleculare (SLM). Representative images showing dendritic spines in apical main and secondary dendrites in SR (A) as well as in apical tufts in SLM (B) in coronal mouse brain sections. The arrowheads indicate the respective dendritic segments. Magnification: 100x (A, B). Modified figure from Kartalou et al., under review.

2.7 Combined Golgi-Cox staining with fluorescent labeling of amyloid plaques

Methoxy-X04 is a fluorescent dye which binds selectively to fibrillary β -sheet deposits, and it is used for the detection of amyloid plaques.

WT and APP/PS1 mice were intraperitoneally injected twice (24h interval) with 75 μ l of 10 mg/ml methoxy-X04 (TOCRIS) in DMSO (Sigma-Aldrich), according to the injection steps, as these have been described by Jährling et al. (Jährling et al., 2015). Two hours after the last injection, the animals were anesthetized and transcardially perfused with 0.9% saline followed by 4% PFA (Electron Microscopy Sciences) in 0.1 M PB pH 7.4. The brains were then post-fixed in 4% PFA overnight at 4 °C and placed into Golgi-Cox solution for 14 days. The solution was renewed after 7 days and the protocol was completed, following the final steps as mentioned in section 2.5 “Brain tissue collection and preparation for Golgi-Cox staining” of this chapter. In short, on day 14, the brains were transferred into 25% sucrose (AppliChem) in PBS and then, 100 μ m thick coronal sections attached on gelatin coated slides were rinsed, dehydrated, cleared with xylene and coverslipped with DePex medium (Serva).

2.8 Image processing and spine density analysis in Golgi-Cox impregnated neurons close to fluorescent stained amyloid plaques

Spine density analysis was performed in apical secondary dendritic segments in SR of hippocampal CA1 pyramidal neurons in 10 dendritic segments (>15 μ m long) per animal from different neurons, following the same criteria and tools as described in section 2.6 “Dendritic spine analysis in Golgi-Cox stained neurons” of this chapter. For APP/PS1 mice, spine density for 10 dendritic segments located at a distance more than 50 μ m from the plaque border (AD distant) and 10 dendritic segments within 50 μ m from the plaque border (AD near) was calculated per animal. Bright-field and fluorescent images for Golgi-Cox stained dendrites and methoxy-X04 stained amyloid plaques were captured respectively with a 40x magnification objective, using the same SPOT digital camera that was attached to a LEITZ DM R microscope (Leica), while the fluorescent imaging was performed with a filter cube (excitation filter: BP 360/40 nm, dichroic mirror: 400 nm, emission filter: LP 425; Leica). The distance of the dendritic branches to an amyloid plaque was defined as the average distance of the segment’s end- and middle-points to the plaque boarder in merged images using ImageJ

software. The number of spines was counted manually, and the analysis was conducted blindly to the treatments in WT and AD mice.

2.9 Brain tissue collection and preparation of slices for immunohistochemistry

APP/PS1 mice and WT littermates were anesthetized with intraperitoneal injection of ketamine hydrochloride/xylazine hydrochloride (Sigma-Aldrich), and transcardially perfused with ice-cold 0.9% saline. Immediately after opening the cranium, the brains were removed and cut along the sagittal midline. The right hemi-brains were post-fixed in 4% PFA (Electron Microscopy Sciences) in 0.1 M PB pH 7.4 for 24 hours at 4 °C, and then, they were cryoprotected in 25% sucrose (AppliChem) in PBS. The left hemi-brains were dissected at the anterior and posterior neocortex and hippocampus in ice-cold artificial cerebrospinal fluid solution, and afterwards they were snap-frozen and stored at -80 °C for future protein analysis. 40 µm thick coronal sections were taken by the fixed right hemispheres using a cryostat (Leica CM 3050). The technical assistance of Mrs Anja Reupsch was valuable for the brain sectioning. Three free-floating sections 240 µm apart from each other between Bregma levels -2.46 mm to -3.08 mm (Franklin and Paxinos atlas, 1996) containing the hippocampus and neocortex were selected per animal for every histological fluorescent staining. Finally, the stained sections were transferred to slides (Superfrost, Thermo Scientific), and coverslipped with ImmunoMount mounting medium (Thermo Scientific) for imaging purposes.

2.10 Immunofluorescence staining for Iba1

The ionized calcium binding adaptor molecule 1 (Iba1) is commonly used as a specific marker for microglia identification. In this study, free-floating coronal brain sections were treated with sodium citrate buffer (10 mM, pH 6.0) for 30 min at 80 °C to perform antigen retrieval, and they were then washed 3 times with PBS for 10 min each. The sections were blocked in 10% fetal bovine serum (FBS; Gibco) and 1% BSA (Sigma) in PBS with 0.3% Triton X-100 (Sigma) for 3 hours at room temperature. Afterwards, they were incubated with a rabbit anti-Iba1 antibody (1:500, Wako) in 1% FBS and 0.1% BSA in PBS with 0.3% Triton X-100 overnight at 4°C. The sections were washed with PBS 5 times for 10 min each, and incubated with a donkey anti-rabbit Alexa Fluor 555 labeled antibody (1:500, Thermo Scientific) in 1% FBS and 1% BSA in PBS with 0.3% Triton X-100 for 1 hour at room

temperature. The sections were finally washed 5 times with PBS for 10 min each. The slides were coverslipped and stored in the dark at 4 °C.

2.11 Immunofluorescence staining for GFAP

The glial fibrillary acidic protein (GFAP) is an often used marker for astrocyte detection. However, it has been reported that GFAP is also expressed in other cells, such as the radial glial progenitor cells (RGPs) in mice (Berg et al., 2018; Docampo-Seara et al., 2019; Shapiro et al., 2005). In this research, in order to study the activation level of the astrocytes, free-floating coronal brain sections were initially treated with sodium citrate buffer (10 mM, pH 6.0) for 30 min at 80 °C for performing antigen retrieval, and were then washed 3 times with Tris-buffered saline (TBS) for 5 min each. The sections were blocked in 5% NGS (Dianova) in TBS with 0.4% Triton X-100 (Sigma) for 1 hour at room temperature, and incubated with a mouse anti-GFAP antibody (1:500, clone G-A-G, Sigma: G 3893) in blocking solution overnight at 4°C. The sections were washed with TBS 5 times for 10 min each and developed with a goat anti-mouse Alexa Fluor 488 labeled secondary antibody (1:500, Thermo Scientific) in blocking solution for 1 hour at room temperature. The sections were finally washed 5 times with TBS for 10 min each. All slides were coverslipped and kept in the dark at 4 °C.

2.12 Thioflavine S staining

Thioflavine S is a fluorescent dye which binds to amyloid fibrils, and is widely used to stain amyloid plaques. In this study, free-floating coronal brain sections were incubated for 9 min in 1% thioflavine S (Sigma-Aldrich) aqueous solution. The sections were treated with 80% ethanol twice for 3 min each, and then, with 95% ethanol for 3 min. All sections were finally rinsed 3 times with distilled water. The slides were coverslipped and stored in the dark at 4 °C.

2.13 Immunofluorescence staining for total amyloid beta (A β)

Free-floating coronal brain sections were permeabilized with PBS with 0.1% Triton X-100 (Sigma) 3 times for 10 min each, followed by antigen retrieval with 98% formic acid for 5 min. The sections were washed 3 times with PBS for 5 min each and blocked in 20% NGS

(Dianova) in PBS with 0.1% Triton X-100 (Sigma) for 1 hour at room temperature. The sections were incubated with a mouse anti-A β 'IC16' antibody (1:400; kindly provided by Prof. Claus Pietrzik, Johannes-Gutenberg-University Mainz, Germany) in 10% NGS (Dianova) in PBS with 0.1% Triton X-100 (Sigma) overnight at 4 °C. They were then washed 5 times with PBS with 0.1% Triton X-100 for 10 min each, and incubated with a secondary goat anti-mouse Alexa Fluor 488 labeled antibody (1:500, Thermo Scientific) in 10% normal goat serum (Dianova) in PBS with 0.1% Triton X-100 0.1% for 90 min at room temperature. The sections were finally washed with PBS 3 times for 15 min each. All slides were coverslipped and kept in the dark at 4 °C.

2.14 Image analysis and quantitation of fluorescence stainings

Quantification of Iba1- or GFAP-positive staining in the total CA1 area of the hippocampus and in an identical cortical section for all section was performed in images captured with a 10x magnification objective, using a SPOT camera attached to a LEITZ DM R microscope (Leica) through the appropriate filter cube (excitation filter: BP 515-560 nm, dichroic mirror: 580 nm, emission filter: LP 590 nm, Leica). The National Institutes of Health (NIH) ImageJ software (<https://imagej.nih.gov/ij/>) was used for the analysis of both stainings. In hippocampus and neocortex, the load was expressed as the percentage area covered by GFAP- or Iba-positive staining, and the integrated intensity was expressed in pixels (the intensity was normalized to the CA1 area in the analysis of the hippocampus).

Quantification of thioflavine S- or A β -positive staining in total hippocampus and neocortex was performed in images captured by a ZEISS 2010 software in a confocal imaging system (LSM 780, Zeiss, Germany), using a 5x magnification objective. The green fluorescence was excited using 488 nm laser line from an Argon laser. 16-bit images were converted to 8-bit gray-scale images and thresholded within a linear range using the NIH ImageJ software. The load was expressed as the percentage area covered by thioflavine S- or A β -positive staining [Thio S plaque load (%), A β load (%)]. The 'Analyze Particles' tool of ImageJ software was used to quantify the plaque number and size (plaque area in μm^2) of Thioflavine S stained plaques.

Quantifications for all stainings were performed blind to the treatments for WT and APP/PS1 mice.

2.15 Preparation of primary neuronal cultures

Cultures of hippocampal neurons were prepared from 12 C57BL/6J (WT) mice at postnatal day 1 (P1). The mice were decapitated, and their brains were cut along the sagittal midline. The hemi-brains were transferred to a culture dish containing pre-cooled MPBS^(+/+) (Table 1). The hippocampi were removed from each hemisphere, cut and kept on ice in an eppendorf tube (3 hippocampi/tube) filled with 0.5 ml cold MPBS^(+/+). Subsequently, the buffer was slowly removed from each tube and replaced with 0.9 ml MPBS^(-/-) (Table 2) and 0.1 ml trypsin 2.5% (Gibco), resulting in a final 0.25% trypsin concentration. The tissues were incubated in a thermomixer (Eppendorf) at 800 rpm for 8 min at 37 °C, and they were then kept on ice for at least 3 min. The cell suspension from each tube was transferred into another tube (tube-A) filled with 3 ml of cold BME/10% FCS medium (Table 3). 1 ml of fresh MPBS^(-/-) was then added to each tissue sample and all of them were triturated approximately 12 to 15 times up and down. They were then kept on ice for at least 5 min, and the cell suspensions were finally transferred to the tube-A. All samples were triturated once again for 12 to 15 times, and finally added to the tube-A as well. The cells were centrifuged using a 420 R centrifuge (Hettich) at 1,100 for 10 min at 4 °C, and the pellet was resuspended in 2ml of fresh BME/10% FCS medium and filled up to 9 ml also with BME/10% FCS. The cell density was determined using a Neubauer counting chamber. 9.49×10^6 mixed cells were calculated and equally preplated on 6 cm culture dishes (3×10^6 /dish; 3 dishes) in 3 ml BME/10% FCS medium and incubated for 70 min at 37 °C with 5% CO₂. The supernatant containing the non-adherent neurons, was separated from the glial cells that were adherent to the bottom of the culture dish by slow transferring into a clean tube, and it was then centrifuged (420 R centrifuge; Hettich) at 1,100 rpm for 10 min at room temperature. The supernatant was then discarded, and the pellet which contained the neurons was resuspended in 9 ml fresh NB-B27 medium (Table 4). 10^6 neurons were equally plated on 3.5 cm culture dishes in NB-B27 medium (896 µl of cell suspension and 1,100 µl NB-B27 medium/dish; 9 dishes) and incubated for 12 days at 37 °C with 5% CO₂. The technical support of Mrs Sabine Eichler for the preparation of the primary neuronal cultures was priceless.

2.16 Pharmacological inhibition of γ -secretase in primary neuronal cultures and protein extraction

Cultures of mouse hippocampal neurons (10^6 cells/3.5 cm culture dish; 3 dishes) were treated with 10 μ l of γ -secretase inhibitor L-685,458 (5 μ M) (stock solution in DMSO: 1mM; TOCRIS) in 2 ml NB-B27 medium (Table 4) at 8 days *in vitro*. Cultures containing only 0.5% DMSO (10 μ l DMSO in 2 ml NB-B27 medium; 10^6 cells/3.5 cm culture dish; 3 dishes) and native cultures (containing only 2 ml NB-B27 medium; 10^6 cells/3.5 cm culture dish; 3 dishes) were used as controls.

At 12 days *in vitro*, the cells were washed twice with 1 ml cold PBS^(-/-) (Gibco) and scraped into 400 μ l of cell collecting buffer (Table 5). The same procedure was followed for all culture dishes. Cells from each treatment group were pooled in one tube and centrifuged (Mikro 200R centrifuge; Hettich) at 3,000 rpm for 5 min at 4 °C. The pellets were suspended in 150 μ l of cell lysis buffer (Table 6), and gently triturated 10 times up and down with a G26 needle (Roth) attached to a 1 ml syringe (Omnifix-F, Roth). Each homogenate was kept on ice for 30 min (short vortex every 10 min), and centrifuged (Mikro 200R centrifuge; Hettich) at 10,000 rpm for 8 min at 4 °C. The supernatants, which contained the neuronal proteins (cell lysate), were slowly transferred into clean tubes and stored at -80 °C for future protein analysis. 30 μ l of the cell lysates were stored at -20 °C for immediate protein determination. Protein concentration was determined by bicinchoninic acid (BCA) Protein Assay Kit (Thermo Scientific), and cell lysates were later analyzed by western blot technique. The technical support of Mrs Sabine Eichler was valuable for treating the primary neuronal cultures and performing protein extraction from the cells.

2.17 Protein extraction from post-mortem brain tissue

Post-mortem brain tissue samples (superior frontal gyrus) from 6 female patients with late onset AD (age range: 80-87 years; Braak stages V-VI) and 5 female non-demented individuals (age range: 83-87 years; Braak stages I-II), provided by the Netherlands Brain Bank (Amsterdam, the Netherlands), were used for this experiment. The study on human brain samples was approved by the ethics committee of the Universtätsklinikum Düsseldorf/Heinrich-Heine-University Düsseldorf.

Small frozen pieces, from AD or control brain tissues, were cut and homogenized in a sterile Class II Biosafety Cabinet (Werkbank Sicherheitsklasse II) using an T 10 basic

ULTRA-TURRAX homogenizer (IKA) in 500 μ l hypotonic buffer (Table 7), approximately 12 to 15 times up and down (one brain tissue sample at a time). The homogenates were kept on ice, diluted 1:10 (50 μ l sample and 450 μ l 50 mM Tris-HCL, pH 7.5), and slowly triturated with the use of a pipette. Immediately after this step, the specimens remained on ice and diluted 1:10 in 5 times (40 μ l sample and 160 μ l 50 mM Tris-HCL, pH 7.5), resulting in 1:50 samples which were only used for protein determination. All specimens (1:10 diluted samples and 1:50 diluted samples) were stored at -80 °C. Protein concentration was determined by bicinchoninic acid (BCA) Protein Assay Kit (Thermo Scientific). The 1:10 diluted homogenates were finally used for western blot analysis.

2.18 Western blot analysis from primary cultured mouse neurons and post-mortem human brains

Equal amounts of protein from mouse neuronal cell lysates (15 μ g) or human brain homogenates (50 μ g) were mixed with 4x Laemmli buffer (BIO-RAD) and β -mercaptoethanol (Sigma), incubated on a thermomixer (Eppendorf) for 5 min at 95 °C, and separated on 12% sodium dodecyl sulfate polyacrylamide gels electrophoresis (SDS-PAGE; BIO-RAD) with 1x running buffer (Rotiphorese 10x SDS-PAGE; Roth) at 70 V for 20 min, and then at 140 V for 70 min. Following this step, the gels were equilibrated in 1x transfer buffer, [25 mM Tris (Biomol), 192 mM Glycin (Sigma) 0.05% SDS (Amersham Pharmacia Biotech), 20% methanol (J.T.Baker)] for 5 min. In the same time, the membranes were equilibrated in methanol (J.T.Baker) for 15 sec, in ddH₂O for 2 min and finally, in 1x transfer buffer for 5 min. The proteins were then electroblotted, using a semi-dry blotter (Peqlab) onto a 0.45 μ m PVDF membrane (Roth) for 60 min at 140 mA. The membranes were washed 3 times for 5 min in TBS with Tween-20 (Sigma) 0.1%, followed by another wash for 1 min in TBS. They were blocked with 5% nonfat milk (Roth) in TBS with Tween-20 0.1% and incubated (overnight at 4 °C) with specific primary antibodies: mouse anti-N-Cadherin (1:400; BD Transduction Laboratories), rabbit anti-Neurologin 1 (1:1000; Synaptic Systems), rabbit anti-Neurexin 1/2/3 (1:1000; Synaptic Systems) or mouse anti-beta actin (1:10,000; Sigma). The membranes were then incubated with the corresponding HRP-conjugated secondary antibody in 5% nonfat milk in TBS with Tween-20 0.1% [goat anti-mouse IgG (Sigma) or goat anti-rabbit IgG (Sigma)] for 1 hour at 4 °C, and were then developed using enhanced chemiluminescence (SuperSignal West Dura substrate; Thermo Scientific). Quantification of western blot signals of C-terminal fragment 1 (CTF1) of N-cadherin (Ncad),

neuroigin 1 (NLG1), neurexin (NRX) and beta-actin protein was performed using the National Institutes of Health (NIH) ImageJ software. Densitometric units of Ncad CTF1, NLG1 CTF1 and NRX CTF1 were calculated after normalization with the corresponding beta-actin signals. The technical assistance of Mrs Margit Schmidt for the conduction of western blot application and the immunoblotting detection of the proteins was essential for this study.

2.19 Statistics

Statistical analysis was conducted with GraphPad Prism (GraphPad Software Inc., La Jolla CA, USA). The data acquired from Golgi-Cox experiments, thioflavine-S fluorescent staining of amyloid plaques and immunofluorescence staining for total A β as well as those from all immunoblotting detections were analyzed by unpaired, two-tailed t-tests. The spine densities from the experiments of the combined method of fluorescence labeling of amyloid plaques combined with Golgi-Cox staining were analyzed by one-way ANOVA or two-way ANOVA, while the immunofluorescence stainings for GFAP and Iba1 were analyzed by two-way ANOVA. Tukey's post hoc test was used in cases of multiple comparisons. All data were tested for normal distribution by Kolmogorov-Smirnov test, and were found normally distributed (except for the female WT group dendritic spine data). All values are expressed as mean \pm standard error of the mean (SEM). Statistical significance was defined as $p < 0.05$.

3. Results

3.1 Spine density analysis in Golgi-Cox impregnated mouse hippocampal neurons

3.1.1 Deficits in spine density in apical secondary dendrites in Golgi-Cox stained CA1 pyramidal neurons in aged APP/PS1 mice

With a view to demonstrate deficits in spine density in a mouse model of Alzheimer's disease (AD), Golgi-Cox staining was used to analyze spine densities in CA1 pyramidal neurons in the hippocampus of male APP/PS1 mice and WT littermates at the age of 13 months. Spine density was determined in apical main and secondary dendrites located in stratum radiatum (SR) and in apical tufts in stratum lacunosum-moleculare (SLM) (Fig. 13).

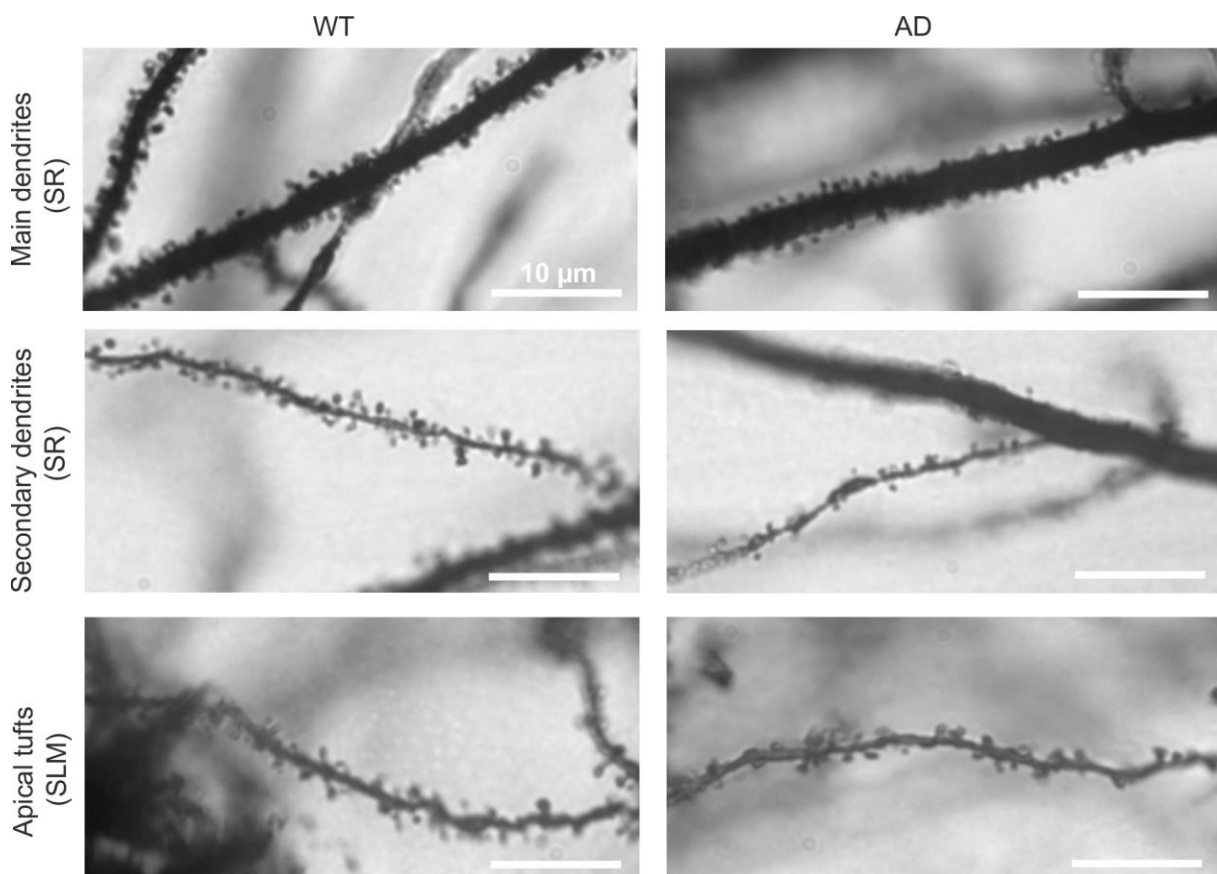


Figure 13: Representative images of dendritic spines in Golgi-Cox stained apical main and secondary dendrites in stratum radiatum (SR) as well as in apical tufts in stratum lacunosum moleculare (SLM) in coronal brain sections of male 13-month-old WT and APP/PS1 (AD) mice. Magnification: 100x. Modified figure from Kartalou et al., under review.

Quantification of spine densities showed that the number of spines was significantly reduced in apical secondary dendrites in SR in APP/PS1 mice compared to WT animals (APP/PS1: 1.08 ± 0.05 spines/ μm , WT: 1.59 ± 0.04 spines/ μm) (Fig. 14 B), while spine densities in apical main dendrites in SR and in apical tufts in SLM were not significantly different (Fig. 14 A, C). These results suggest a strong reduction of spine density in apical secondary dendrites of CA1 pyramidal neurons in APP/PS1 mice, which aligns with the strong amyloid pathology that is present in aged mice of this animal model of AD.

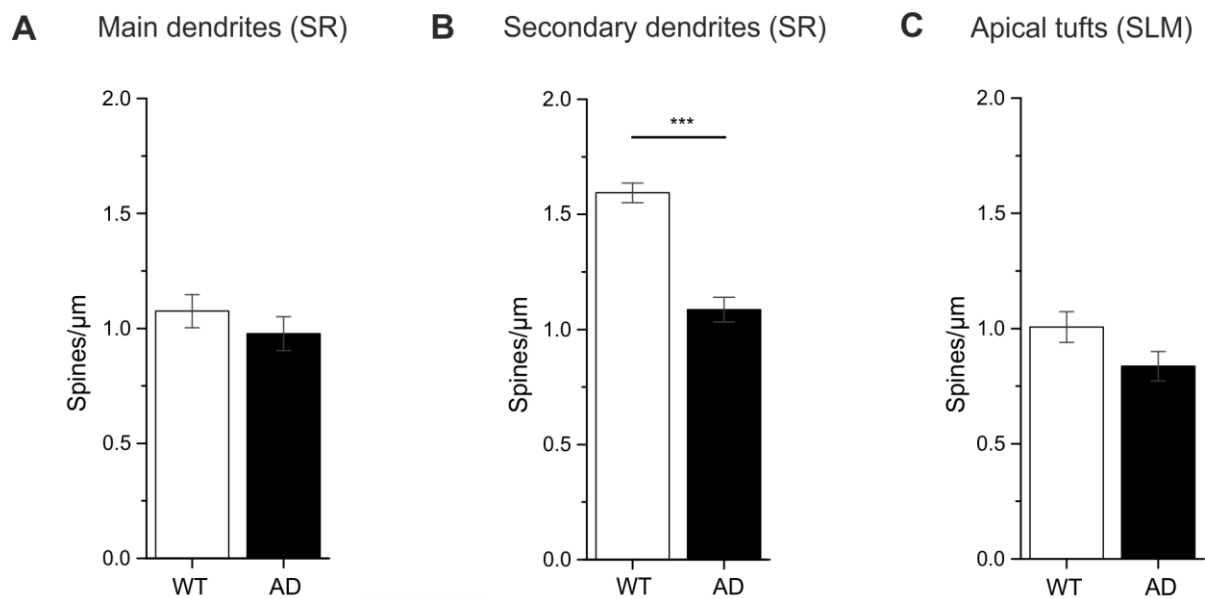


Figure 14: Quantification of spine density in secondary dendrites (B) shows a significant reduction of spine density in APP/PS1 (AD) mice, whereas spine densities in main dendrites (A) and apical tufts (C) exhibit only a slight reduction in hippocampal CA1 pyramidal neurons in 13-month-old AD mice compared to WT mice. Data are represented as mean \pm SEM; $n = 20$ dendrites from 2 mice per group. Statistical analysis was performed with unpaired Student's *t*-test and statistical significance was defined as $P < 0.05$. *** = $P < 0.0001$. Modified figure from Kartalou et al., under review.

3.1.2 Spine density deficits in hippocampal CA1 pyramidal neurons in 6- to 7-month-old BDNF^{+/-} and APP/PS1/BDNF^{+/-} transgenic mice

To further demonstrate alterations in spine density in brain-derived neurotrophic factor (BDNF) deficient transgenic mice, the number of spines was counted in apical secondary dendrites of Golgi-Cox impregnated CA1 pyramidal neurons in the hippocampus of 6- to 7-month-old male APP/PS1/BDNF^{+/-} transgenic mice, without knowing their location in regard to amyloid plaques, and was then compared with spine density in BDNF^{+/-}, APP/PS1 and WT littermates at the same age (Fig. 15 A).

Spine density analysis in 6-7 months APP/PS1 mice, independent of the location from the amyloid plaques, showed only a non-significant trend towards reduction as compared to WT littermates (Fig. 15 B). Spine densities were significantly reduced in APP/PS1/BDNF^{+/-} and BDNF^{+/-} mice compared to WT littermates (WT: 2.02 ± 0.04 spines/μm; BDNF^{+/-}: 1.73 ± 0.04 spines/μm; APP/PS1: 1.86 ± 0.03 spines/μm; APP/PS1/BDNF^{+/-}: 1.791 ± 0.05 spines/μm) (Fig. 15 B). These results suggest that low levels of endogenous BDNF production in young BDNF^{+/-} mice are associated with reduced spine density in hippocampal CA1 pyramidal neurons.

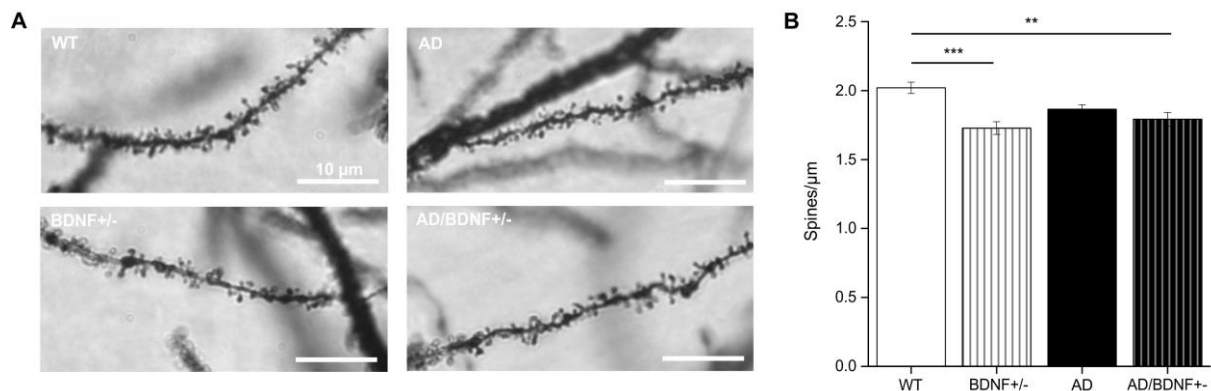


Figure 15: (A) Dendritic spines in apical secondary dendrites of Golgi-Cox stained hippocampal CA1 pyramidal neurons in coronal brain sections of 6- to 7-month-old male WT, BDNF^{+/-}, APP/PS1 (AD) and APP/PS1/BDNF^{+/-} (AD/BDNF^{+/-}) mice. Magnification: 100x. (B) Analysis of spine density in secondary dendrites of hippocampal CA1 pyramidal neurons reveals a trend of reduction in 6- to 7-month-old male AD mice and significant spine deficits in BDNF^{+/-} and AD/BDNF^{+/-} mice compared to WT littermates. Data are shown as mean ± SEM; n = 30 dendrites from 3 mice for BDNF^{+/-}, AD and AD/BDNF^{+/-} groups and n = 20 dendrites from 2 mice for WT group. Statistical analysis was performed with one-way ANOVA followed by Tukey's post hoc test, and statistical significance was defined as P < 0.05. ** = P < 0.01, *** = P < 0.001. Detailed information on one-way ANOVA: F(3, 106) = 6.878, P = 0.0003. The assistance of Ms Rieke Fritz in the spine density analysis was valuable for the brain sectioning.

3.2 Spine density analysis in the vicinity of amyloid plaques in Golgi-Cox impregnated hippocampal neurons

3.2.1 Combination of fluorescent labeling of amyloid plaques with Golgi-Cox staining of CA1 pyramidal neurons in the hippocampus of APP/PS1 mice

It has been described that spine pathology in young APP/PS1 mice that have a relatively low amyloid plaque load is developing mainly near the amyloid beta (Aβ) deposits (Spires-Jones et al., 2007; Liebscher et al., 2014; Bittner et al., 2012). To enable spine density analysis in relation to amyloid plaques, Golgi-Cox impregnation (Fig. 16 A) and fluorescent staining of

amyloid plaques (Fig. 16 B, C) were combined for spine density analysis in hippocampal CA1 pyramidal neurons close to amyloid plaques in 6- to 7-month-old APP/PS1 mice. In order to detect dendritic stretches close to plaques, the amyloid plaques were labeled by intraperitoneally injecting mice twice with the blue fluorescent dye methoxy-X04 24 hours (1st injection) and 2 hours (2nd injection) prior sacrificing the animals for Golgi-Cox impregnations. The Golgi-Cox and fluorescent methoxy-X04 stainings were successfully combined, allowing the detection of pyramidal neuron dendrites near amyloid plaques in merged images of the CA1 area of the hippocampus (Fig. 16 C).

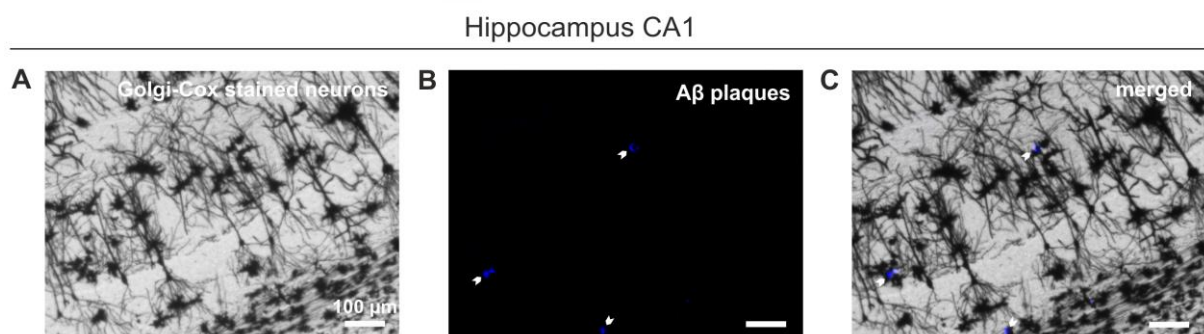


Figure 16: Representative images of Golgi-Cox impregnated pyramidal neurons (A) and methoxy-X04 blue fluorescent staining of amyloid plaques (B) in the CA1 area of the hippocampus in coronal brain sections of APP/PS1 (AD) mice. (C) A merged image of (A) and (B) displays methoxy-X04-positive amyloid plaques near Golgi-Cox stained CA1 pyramidal neurons (the arrowheads indicate the methoxy-X04-positive amyloid plaques). Magnification: 5x (A, B, C). Modified figure from Kartalou et al., under review.

3.2.2 Reduced spine density in Golgi-Cox impregnated CA1 pyramidal neurons in the vicinity of amyloid plaques in 6- to 7-month-old APP/PS1 mice

The technique of Golgi-Cox impregnation, combined with fluorescence staining of amyloid plaques (methoxy-X04), was used to determine spine density in apical secondary dendrites of hippocampal CA1 pyramidal neurons close to amyloid plaques in young 6- to 7-month-old male and female APP/PS1 mice. Male and female WT littermates were used as controls. For the APP/PS1 animals, spine analysis was conducted on dendritic branches which were located at a distance $<50 \mu\text{m}$ to the closest amyloid plaque (AD near; i.e. 2-40 μm) and at a distance $>50 \mu\text{m}$ from the plaque border (AD distant; i.e. 60-215 μm) (Figs. 17 A & 18 A).

Quantification of spine densities showed a significant reduction of the number of spines near amyloid plaques in male APP/PS1 mice (APP/PS1 near: 0.91 ± 0.05 spines/ μm ; WT: 1.65 ± 0.03 spines/ μm) as well as in female APP/PS1 mice (APP/PS near: 1.42 ± 0.02 spines/ μm ; WT: 1.88 ± 0.04 spines/ μm) compared to WT littermates (Figs. 17 B & 18 B).

The analysis also revealed significant spine deficits in dendritic segments distant to amyloid plaques selectively in male mice (APP/PS1 distant: 1.33 ± 0.04 spines/ μm ; WT: 1.65 ± 0.03 spines/ μm) (Fig. 17 B). This noticeable observation could indicate gender-specific differences in spine pathology in this mouse model of AD. These results suggest that spine deficits are more pronounced near amyloid plaques in CA1 pyramidal neurons in the hippocampus of APP/PS1 mice at this age (i.e. 6- to 7-month old).

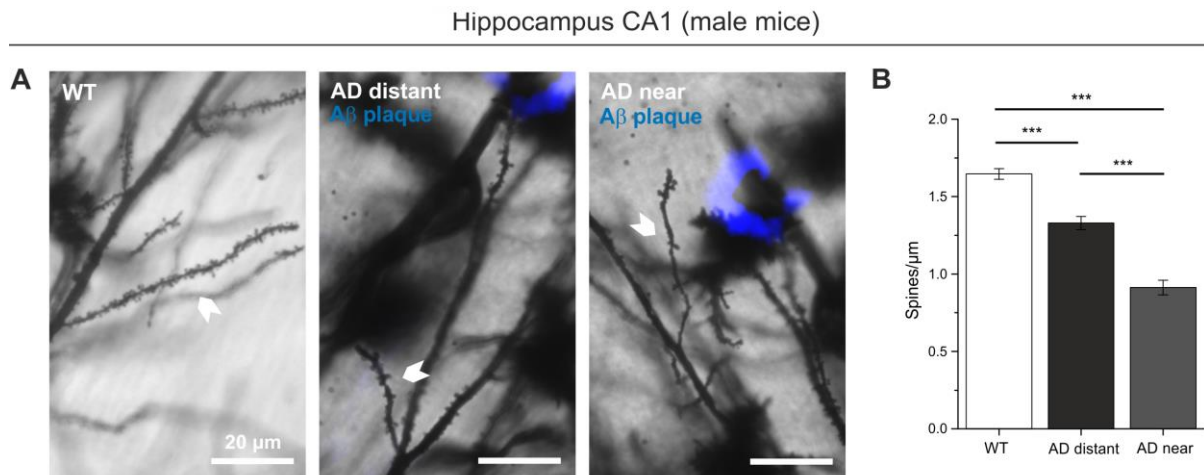


Figure 17: (A) Representative images of dendritic spines in apical secondary dendrites of Golgi-Cox stained hippocampal CA1 pyramidal neurons with methoxy-X04 fluorescent labeling of amyloid plaques in coronal brain sections in male APP/PS1 (AD) and WT mice at the age of 6 to 7 months. Dendrites $>50 \mu\text{m}$ away from the nearest plaque (AD distant) and $<50 \mu\text{m}$ away from the closest plaque (AD near) are shown (the arrowheads indicate the spines in the respective dendrites). Magnification: 40x. (B) Quantification of spine densities reveals a significant reduction distant from and near amyloid plaques in male AD mice compared to WT littermates. Data are represented as mean \pm SEM; $n = 30$ dendrites from 3 animals per group. Statistical analysis was performed with one-way ANOVA followed by Tukey's post hoc test, and statistical significance was defined as $P < 0.05$. *** = $P < 0.001$. Detailed information on one-way ANOVA: $F(2, 87) = 81.09$, $P < 0.0001$. Modified figure from Kartalou et al., under review.

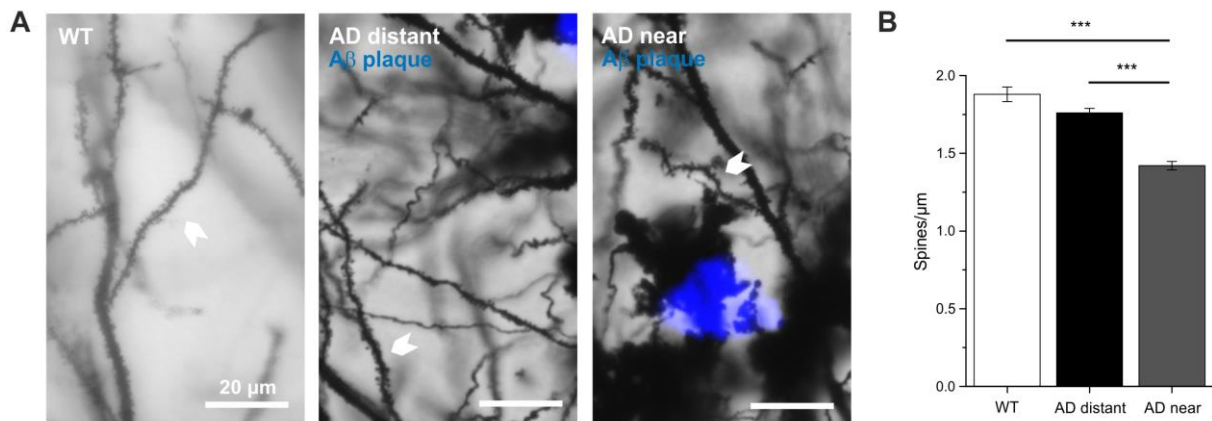


Figure 18: (A) Dendritic spines in apical secondary dendrites of Golgi-Cox impregnated hippocampal CA1 pyramidal neurons and methoxy-X04 fluorescent labeling of amyloid plaques in coronal brain sections in female 6- to 7-month-old APP/PS1 (AD) and WT mice. Dendrites $>50\ \mu\text{m}$ away from the nearest plaque (AD distant) and $<50\ \mu\text{m}$ away from the closest plaque (AD near) are shown for the AD animals (the arrowheads indicate the spines in the respective dendrites). Magnification: 40x. (B) Analysis of spine densities reveals a slight reduction distant to plaques, while spine density is significantly lower near plaques in female AD mice compared to WT littermates. Data are represented as mean \pm SEM; $n = 30$ dendrites from 3 animals per group. Statistical analysis was performed with one-way ANOVA followed by Tukey's post hoc test, and statistical significance was defined as $P < 0.05$. *** = $P < 0.001$. Detailed information on one-way ANOVA: $F(2, 87) = 44.96$, $P < 0.0001$. Normality test failed only for the WT group, because of a single outlier data point. Modified figure from Kartalou et al., under review.

3.3 Effects of voluntary running (VR) on spine density in mouse hippocampal neurons

3.3.1 VR rescues spine density deficits in the hippocampus of APP/PS1 mice

In order to study the effects of exercise (voluntary running) on spine pathology, Golgi-Cox staining combined with fluorescence labeling (methoxy-X04) of amyloid plaques was used to perform spine density analysis in apical secondary dendrites of hippocampal CA1 pyramidal neurons near amyloid plaques in 6- to 7-month-old APP/PS1 mice. Male mice were kept in groups under different housing conditions: standard housing (SH), enriched environment (EE), and voluntary running (VR). WT male littermates were used as controls for each housing environment. To relate spine density deficits to amyloid pathology, the analysis was performed in dendritic branches close to amyloid plaques, at a distance $<50\ \mu\text{m}$ from the closest amyloid plaque (AD near; i.e. 5-46 μm), and at a distance $>50\ \mu\text{m}$ from the plaque's border (AD distant; i.e. 55-264 μm) (Fig. 19).

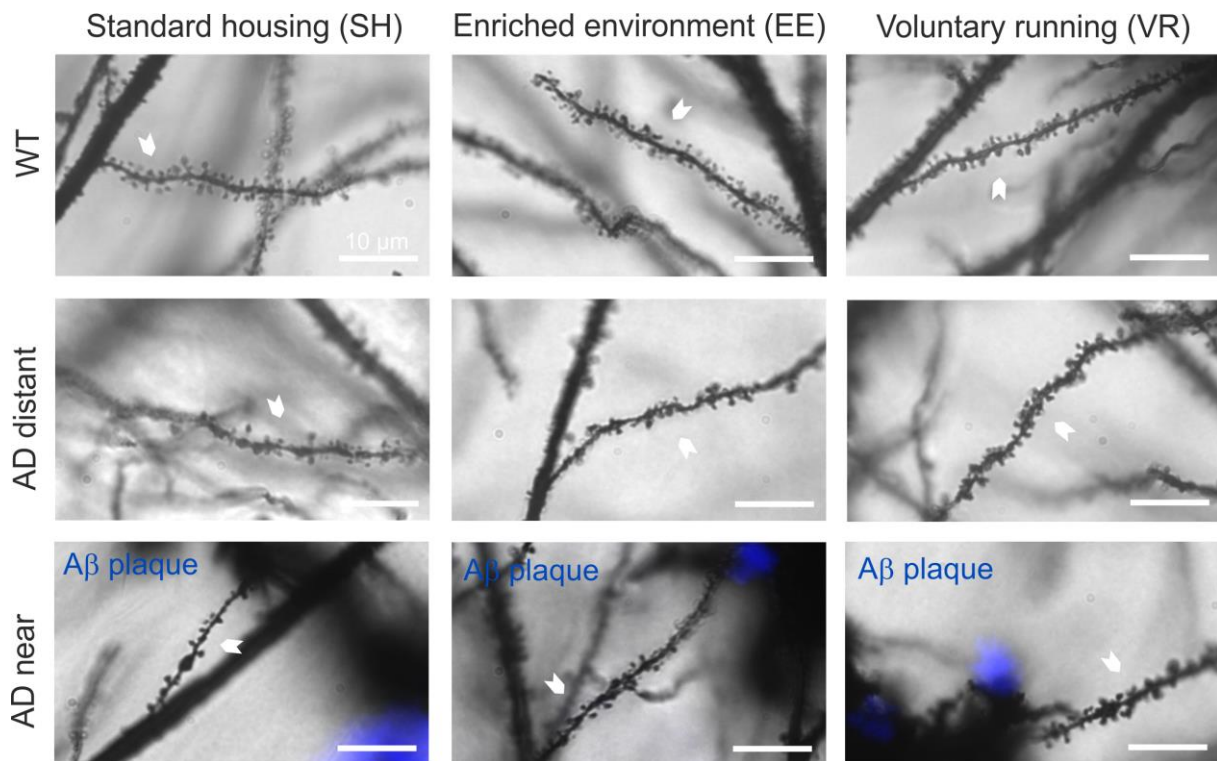


Figure 19: Dendritic spines in apical secondary dendrites of Golgi-Cox stained hippocampal CA1 pyramidal neurons and methoxy-X04 fluorescent labeling of amyloid plaques in coronal brain sections of 6- to 7-month-old male APP/PS1 (AD) and WT mice kept in different housing conditions such as standard housing (SH), enriched environment (EE) and voluntary running (VR). Dendrites $>50 \mu\text{m}$ away from the nearest plaque (AD distant) and $<50 \mu\text{m}$ away from the closest plaque's border (AD near) are depicted (the arrowheads indicate the spines in all of the respective dendrites). Magnification: 100x.

The spine density analysis for animals kept in SH conditions revealed spine deficits distant from amyloid plaques and an even stronger reduction of spine density near amyloid plaques in APP/PS1 mice compared to WT littermates (WT: 1.65 ± 0.03 spines/ μm ; APP/PS1 distant: 1.33 ± 0.04 spines/ μm ; APP/PS1 near: 0.91 ± 0.05 spines/ μm). VR for a two-month period, starting at the age of 4 to 5 months, rescued spine deficits in dendrites distant from amyloid plaques and significantly increased spine density near amyloid plaques in APP/PS1 mice; compared to SH- APP/PS1 and WT animals (APP/PS1 distant: 1.72 ± 0.04 spines/ μm ; APP/PS1 near: 1.42 ± 0.04 spines/ μm). Noticeably, EE housing condition improved spine deficits only in dendrites near amyloid plaques in APP/PS1 animals compared to SH- APP/PS1 and WT mice (APP/PS1 near: 1.28 ± 0.04 spines/ μm). Spine densities presented no changes in WT animals in VR or EE groups, compared to WT mice in SH conditions (Fig. 20). These results suggest that 2 months of VR regime, starting with the onset of AD symptoms, dramatically attenuates spine pathology in this animal model of AD.

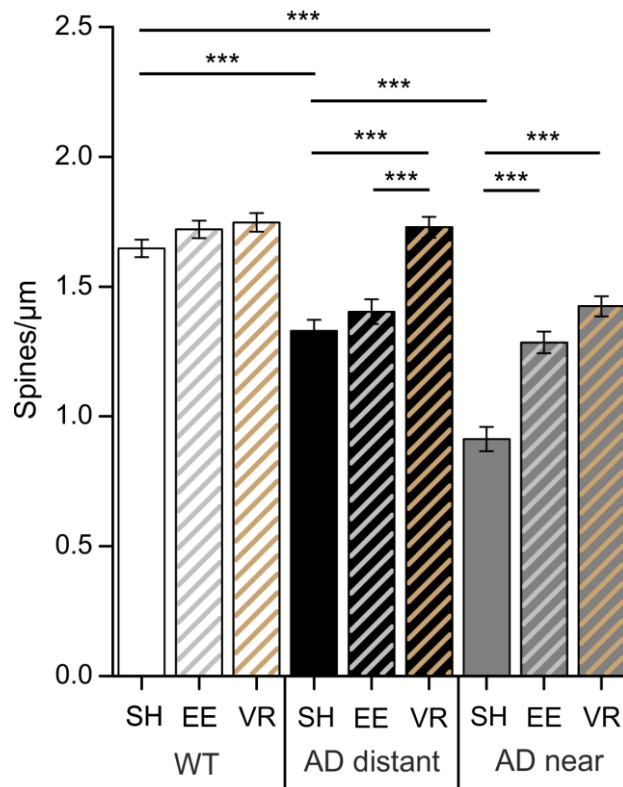


Figure 20: Spine density analysis in apical secondary dendrites of 6- to 7-month-old male WT and APP/PS1 (AD) mice held in standard housing (SH), enriched environment (EE) and voluntary running (VR) conditions. The quantification shows significant spine deficits distant and close to amyloid plaques in mice kept in SH conditions. VR completely rescues spine deficits in dendrites distant from amyloid plaques and significantly ameliorates spine loss in dendritic segments near amyloid plaques in AD mice, compared to AD and WT mice kept in SH conditions. EE significantly increases spine densities only in dendrites near amyloid plaques in AD mice compared to AD and WT mice held in SH conditions. Spine densities are not changed in WT mice which were kept in different housing conditions. The data for all animals kept in SH conditions are the same as already shown in Figure 17. Data are shown as mean \pm SEM; $n = 30$ dendrites from 3 animals per group. Statistical analysis was performed with two-way ANOVA followed by Tukey's post hoc test, and statistical significance was defined as $P < 0.05$. *** = $P < 0.001$. Detailed information on two-way ANOVA (genotype x treatment interaction): $F(4, 261) = 10.13$, $P < 0.0001$.

3.4 Effects of chronic treatment with fingolimod (FTY720) in WT and APP/PS1 transgenic mice

3.4.1 Chronic treatment with FTY720 rescued dendritic spine deficits in hippocampal neurons of APP/PS1 mice

With a view to study the potential of drug repurposing of the Food and Drug Administration (FDA)-approved drug FTY720 [for the treatment of multiple sclerosis (MS)], its effects on spine density deficits in APP/PS1 mice were tested. The method of Golgi-Cox brain impregnation combined with fluorescence staining of amyloid plaques (methoxy-X04) was

used to determine the extent of the amyloid plaque-associated spine loss in apical secondary dendrites of CA1 pyramidal neurons in 6- to 7-month-old untreated (vehicle) or treated (with FTY720) male APP/PS1 mice. Spine density in control untreated and treated WT littermates was analyzed as well. In APP/PS1 mice, the number of spines was counted in dendrites close to amyloid plaques at a distance $<50\ \mu\text{m}$ from the closest amyloid plaque (AD near; i.e. 3-44 μm), and in branches distant from the plaques at a distance $>50\ \mu\text{m}$ from the closest plaque's border (AD distant; i.e. 54-227 μm) (Fig. 21).

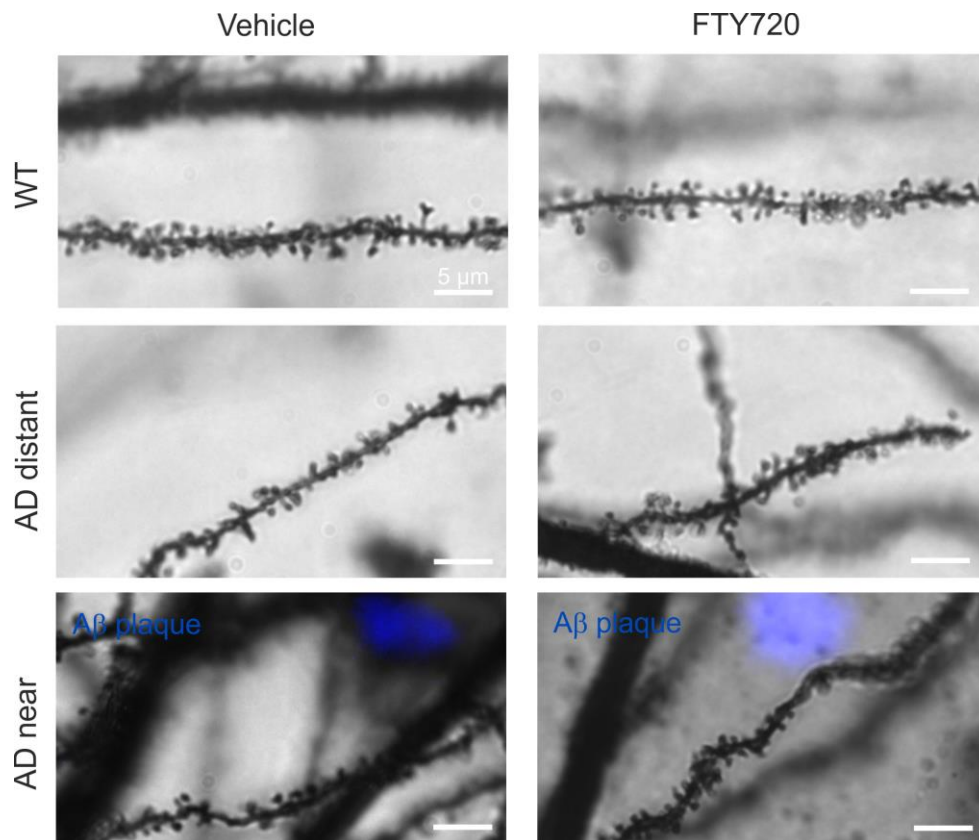


Figure 21: Representative images showing dendritic spines in apical secondary dendrites of Golgi-Cox impregnated hippocampal CA1 pyramidal neurons and methoxy-X04 fluorescent staining of amyloid plaques in coronal brain sections of 6- to 7-month-old vehicle- and FTY720-treated male APP/PS1 (AD) and WT mice. FTY720 was administered at a dose of 1 mg/kg/2ndday. Dendritic spines in dendrites $>50\ \mu\text{m}$ away from the nearest plaque (AD distant) and $<50\ \mu\text{m}$ away from the closest plaque's border (AD near) are depicted. Magnification: 100x. Modified figure from Kartalou et al., submitted; preprint available on bioRxiv (Kartalou et al. 2019).

Quantification of spine densities in hippocampal CA1 pyramidal neurons of untreated APP/PS1 mice exhibited decreased spine densities in dendritic segments, distant from- and near to-amyloid plaques, compared to WT littermates. Spine density analysis also indicated that high and low doses of FTY720, 1 mg/kg/2ndday (Fig. 22) and 0.2 mg/kg/2ndday (Fig. 23) respectively, completely rescued spine deficits in dendrites distant from the amyloid plaques,

and significantly ameliorated spine loss in dendritic segments close to the plaques in APP/PS1 mice, compared to untreated APP/PS1 mice [(‘1 mg/kg/2nd day dose’: WT-vehicle: 1.78 ± 0.02 spines/μm; WT-FTY720: 1.74 ± 0.01 spines/μm; APP/PS1-vehicle distant: 1.46 ± 0.03 spines/μm, APP/PS1-FTY720 distant: 1.71 ± 0.03 spines/μm; APP/PS1-vehicle near: 1.31 ± 0.03 spines/μm; APP/PS1-FTY720 near: 1.60 ± 0.03 spines/μm) and (‘0.2 mg/kg/2nd day dose’: WT-vehicle: 1.90 ± 0.04 spines/μm; WT-FTY720: 1.92 ± 0.02 spines/μm; APP/PS1-vehicle distant: 1.62 ± 0.03 spines/μm, APP/PS1-FTY720 distant: 1.79 ± 0.03 spines/μm; APP/PS1-vehicle near: 1.32 ± 0.03 spines/μm; APP/PS1-FTY720 near: 1.65 ± 0.03 spines/μm)]. Spine density was not changed in WT mice treated with FTY720 doses of 1 mg/kg/2nd day or 0.2 mg/kg/2nd day, compared to untreated WT littermates (Figs. 22 & 23). These results suggest that chronic FTY720 treatment in APP/PS1 mice, starting with the onset of AD symptoms, strongly ameliorates spine density deficits in this mouse model of AD.

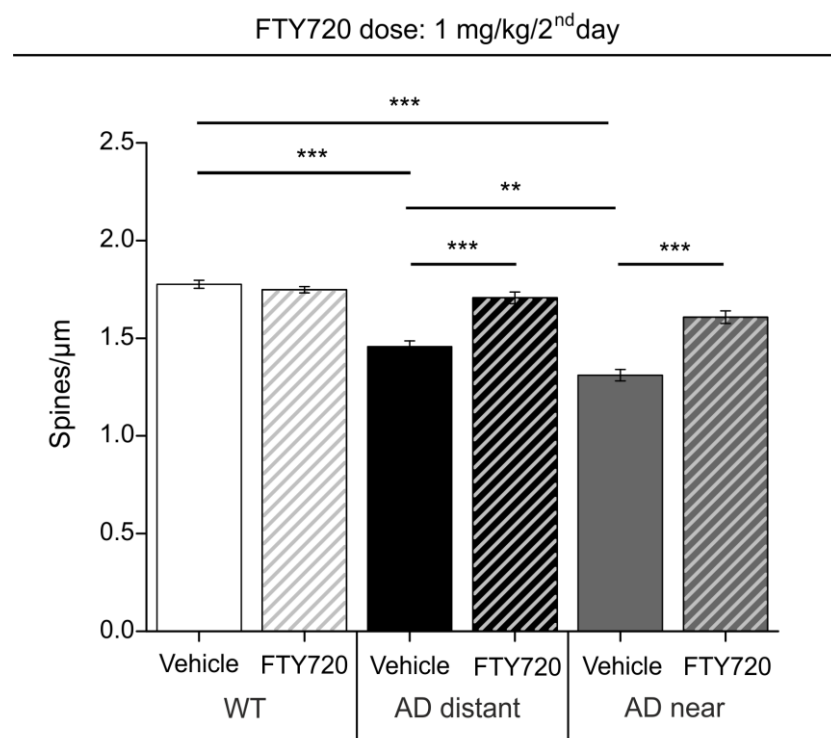


Figure 22: Quantification of spine densities in apical secondary dendrites in 6- to 7-month-old male WT and APP/PS1 (AD) mice upon vehicle and FTY720 treatment at a dose of 1 mg/kg/2nd day. The analysis shows that FTY720 completely rescues spine deficits in dendrites distant from amyloid plaques, and significantly ameliorates spine loss in dendritic segments near amyloid plaques in AD mice, compared to vehicle-treated AD and WT littermates. Spine densities are not changed in WT animals upon treatment with FTY720 at a dose of 1 mg/kg/2nd day, compared to untreated WT mice. Data are represented as mean ± SEM; n = 30 dendrites from 3 animals per group. Statistical analysis was performed with two-way ANOVA, followed by Tukey’s post hoc test, and statistical significance was defined as P < 0.05. ** = P < 0.01, *** = P < 0.001. Detailed information on two-way ANOVA (genotype x treatment interaction): F(2, 174) = 21.51, P < 0.0001. Modified figure from Kartalou et al., submitted; preprint available on bioRxiv (Kartalou et al. 2019).

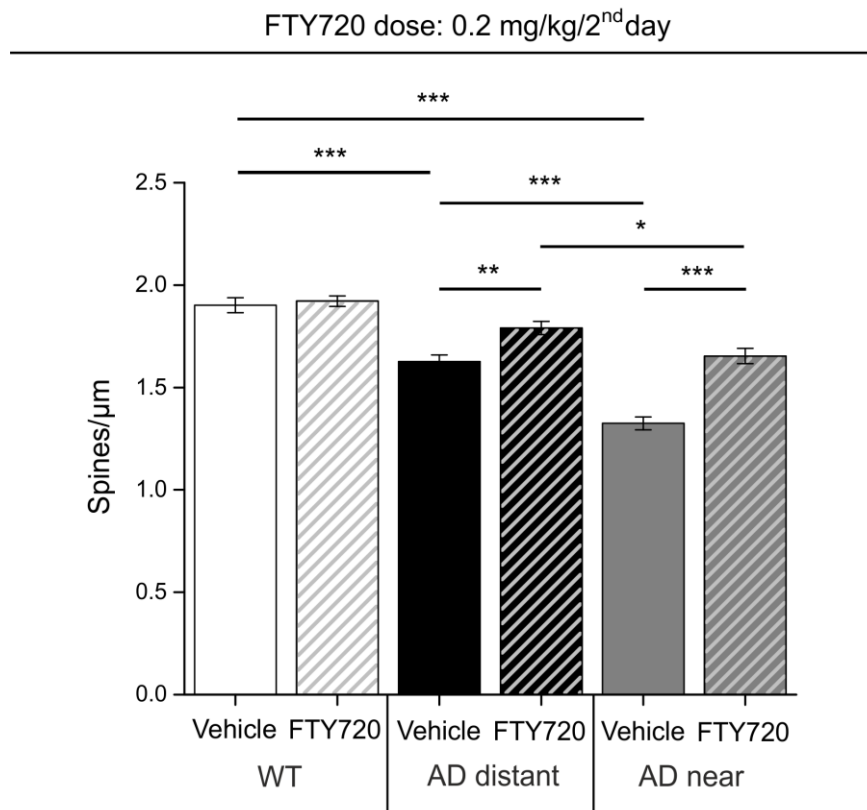


Figure 23: Spine density analysis in apical secondary dendrites after vehicle and FTY720 treatment at a dose of 0.2 mg/kg/2nd day in 6- to 7-month-old male WT and APP/PS1 (AD) mice. The quantification shows that FTY720 results in a total rescue of spine deficits in dendrites distant from amyloid plaques, and significantly improves spine loss in dendritic segments near the plaques in AD mice, compared to vehicle-treated AD and WT littermates. FTY720 treatment, at a dose of 0.2 mg/kg/2nd day, does not change spine density in WT mice, compared to untreated WT animals. Data are represented as mean ± SEM; n = 30 dendrites from 3 animals per WT-vehicle, WT-FTY720, AD-FTY720, AD-FTY720 near groups and n = 26 from 3 animals for AD-vehicle distant and AD-vehicle near groups. Statistical analysis was performed with two-way ANOVA, followed by Tukey's post hoc test, and statistical significance was defined as P < 0.05. * = P < 0.05, ** = P < 0.01, *** = P < 0.001. Detailed information on two-way ANOVA (genotype x treatment interaction): F(2, 166) = 11.05, P < 0.0001.

3.4.2 Chronic treatment with FTY720 reduced microgliosis in the hippocampus and neocortex of APP/PS1 mice

In order to begin addressing the cellular mechanisms of FTY720 action, the state of microglia activation was studied in the hippocampus and neocortex. Immunostaining for Iba1 was used to define the level of microgliosis in the CA1 area of the hippocampus and in neocortex of 6- to 7-month-old untreated (vehicle) or treated with 1 mg/kg/2nd day of FTY720 male APP/PS1 or WT mice (Fig. 24 A, B).

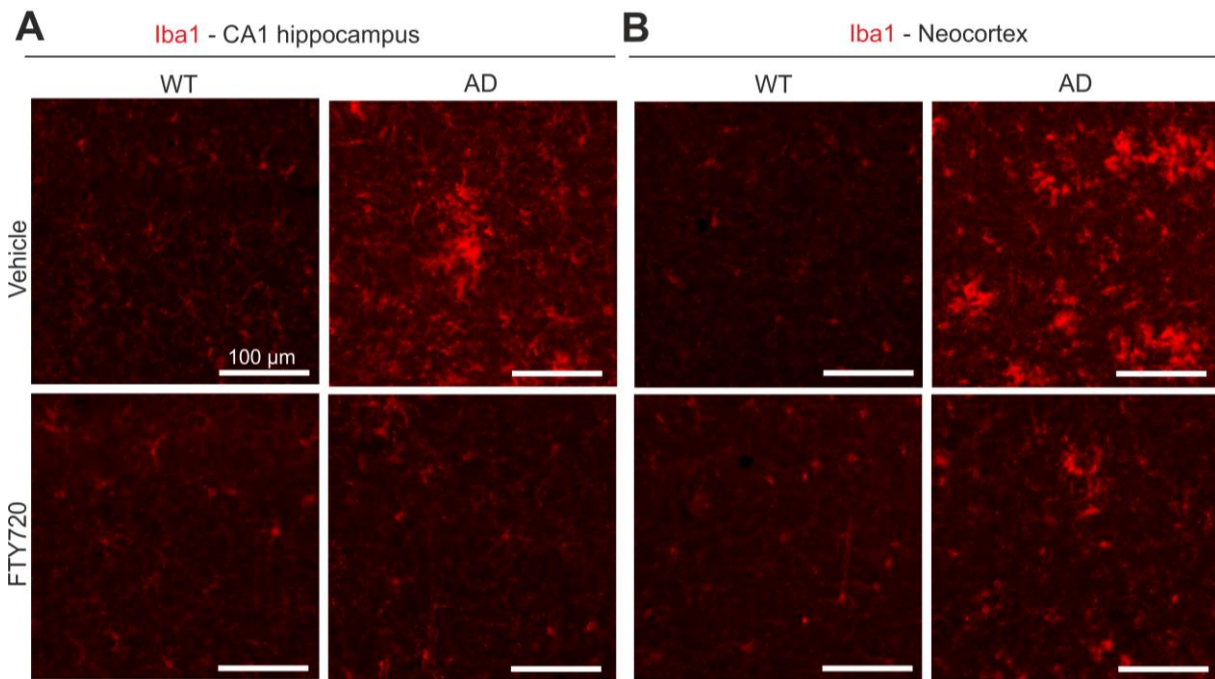


Figure 24: Immunofluorescent detection of Iba1-positive microglia in the CA1 area of the hippocampus (A) and neocortex (B) in coronal brain sections of 6- to 7-month-old untreated or treated (1 mg/kg/2ndday of FTY720) male WT and APP/PS1 (AD) mice. Magnification: 10x. Modified figure from Kartalou et al., submitted; preprint available on bioRxiv (Kartalou et al. 2019).

Quantification of the percent area of Iba1-positive microglia in the CA1 region of the hippocampus indicated an increased level of microgliosis in untreated APP/PS1 mice (APP/PS1-vehicle: 4.73 ± 0.73 , WT-vehicle: 1.48 ± 0.17) which was significantly reduced upon treatment with FTY720 back to WT level (APP/PS1-FTY720: 1.97 ± 0.14 , WT-FTY720: 1.69 ± 0.22), indicating a complete rescue of microgliosis by FTY720. Densitometric analysis showed that the integrated intensity of Iba1 staining divided by the analyzed CA1 area in FTY720-treated APP/PS1 mice was also significantly decreased to the level of the controls (WT-vehicle: 0.50 ± 0.07 , WT-FTY720: 0.46 ± 0.08 , APP/PS1-vehicle: 1.30 ± 0.25 , APP/PS1-FTY720: 0.48 ± 0.05) (Fig. 25 A).

Analysis of the Iba1-positive percent area and integrated intensity in the neocortex of untreated APP/PS1 mice indicated also a robust microgliosis which was significantly reduced after FTY720 treatment [(‘% Iba-positive area’: WT-vehicle: 1.20 ± 0.06 , WT-FTY720: 1.17 ± 0.08 , APP/PS1-vehicle: 8.84 ± 0.88 , APP/PS1-FTY720: 4.12 ± 0.56) & (‘Iba1 integrated intensity’: WT-vehicle: 0.06 ± 0.01 , WT-FTY720: 0.05 ± 0.01 , APP/PS1-vehicle: 0.42 ± 0.04 , APP/PS1-FTY720: 0.18 ± 0.03)] (Fig. 25 B).

These results suggest that, FTY720 drastically reduces microgliosis in APP/PS1 mice.

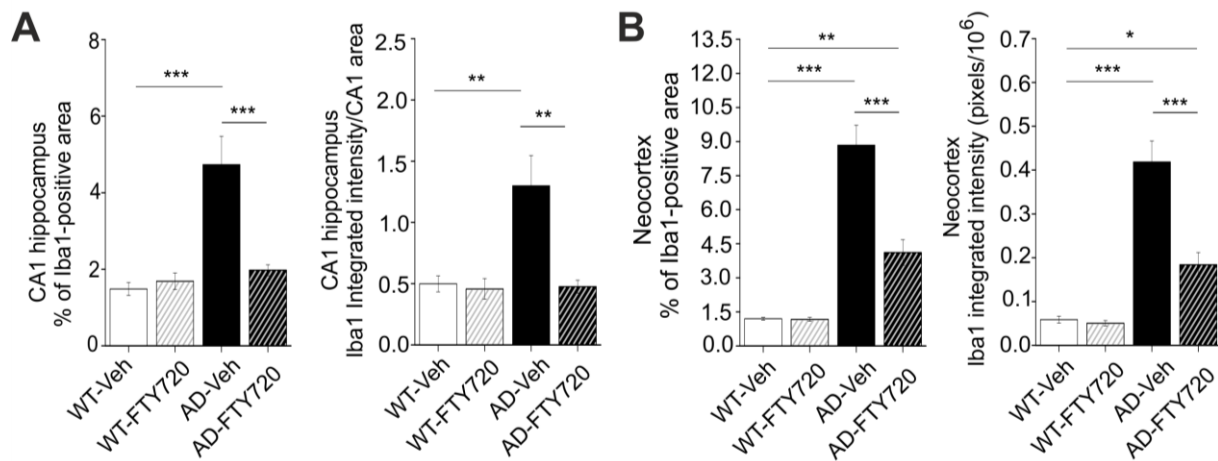


Figure 25: Quantitative analysis of the Iba1-positive microglia in the CA1 area of the hippocampus (A) and neocortex (B) in 6- to 7-month-old male WT and APP/PS1 (AD) mice after vehicle or FTY720 treatment at a dose of 1 mg/kg/2nd day. Quantification of microglial area and integrated intensity normalized to the analyzed area of the section shows a strong increase in the CA1 area of the hippocampus in AD-vehicle mice, which is completely rescued upon chronic FTY720 administration. In the neocortex, the percent area of cortical sections covered by Iba1-positive microglia and the integrated fluorescent pixel intensity are also strongly increased in AD-vehicle mice and dramatically reduced after treatment with FTY720. Data are shown as mean \pm SEM; $n = 6$ mice per WT-vehicle, AD-vehicle and AD-FTY720 groups and 7 mice in the WT-FTY720 group. Statistical analysis was performed with two-way ANOVA, followed by Tukey's post hoc test, and statistical significance was set to $P < 0.05$. * = $P < 0.05$, ** = $P < 0.01$, *** = $P < 0.001$. Detailed information on two-way ANOVA (genotype x treatment interaction): (A) Iba1 covered area: $F(1, 21) = 14.46$, $P = 0.001$, normalized Iba1 intensity: $F(1, 21) = 8.565$, $P = 0.0081$, (B) Iba1 covered area: $F(1, 21) = 21.75$, $P = 0.0001$, Iba1 intensity: $F(1, 21) = 17.42$, $P = 0.0004$. Modified figure from Kartalou et al., submitted; preprint available on bioRxiv (Kartalou et al. 2019).

3.4.3 Chronic treatment with FTY720 reduced astrogliosis in the hippocampus and neocortex of APP/PS1 mice

Immunofluorescence detection for GFAP was used to determine the extent of astrogliosis in the CA1 area of the hippocampus and neocortex of 6- to 7-month-old untreated (vehicle) or treated with 1 mg/kg/2nd day of FTY720 male APP/PS1 or WT mice (Fig. 26 A, B).

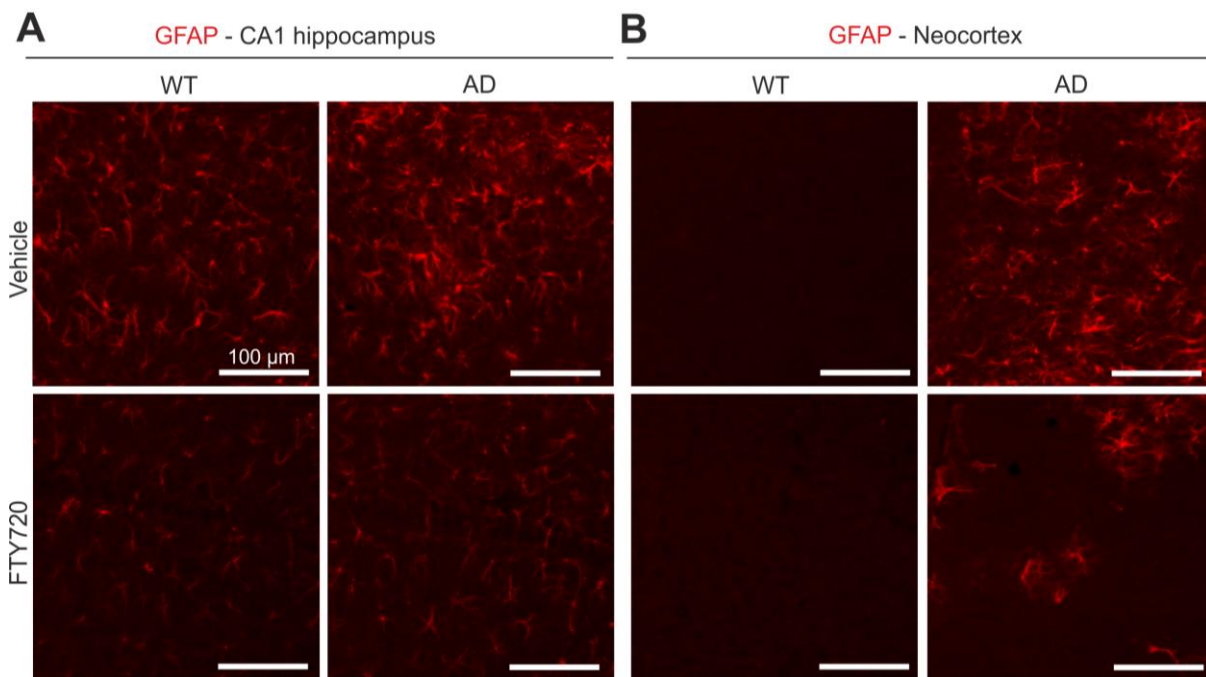


Figure 26: Immunohistological staining for the astrocytic marker GFAP in the CA1 area of the hippocampus (A) and neocortex (B) in coronal brain sections of 6- to 7-month-old untreated or treated (1 mg/kg/2nd day of FTY720) male WT and APP/PS1 (AD) mice. Magnification: 10x. Modified figure from Kartalou et al., submitted; preprint available on bioRxiv (Kartalou et al. 2019).

Analysis of the percentage of hippocampal CA1 area, covered by GFAP-positive activated astrocytes, exhibited an increase in untreated APP/PS1 mice, which was significantly reduced after FTY720 treatment, reaching back to WT levels (WT-vehicle: 4.63 ± 0.33 , WT-FTY720: 2.73 ± 0.28 , APP/PS1-vehicle: 8.01 ± 1.32 , APP/PS1-FTY720: 2.71 ± 0.37). Likewise, the integrated intensity of GFAP staining divided by the analyzed CA1 area in FTY720-treated APP/PS1 mice was significantly reduced to the control levels upon treatment with FTY720. (WT-vehicle: 1.51 ± 0.13 , WT-FTY720: 0.86 ± 0.16 , APP/PS1-vehicle: 2.86 ± 0.47 , APP/PS1-FTY720: 0.91 ± 0.15) (Fig. 27 A).

Quantification of the GFAP-positive percent area and integrated intensity in the neocortex of untreated APP/PS1 mice indicated increased astrogliosis, which was also significantly lowered after treatment with FTY720 [(% GFAP-positive area': WT-vehicle: 0.09 ± 0.01 , WT-FTY720: 0.04 ± 0.01 , APP/PS1-vehicle: 10.22 ± 0.53 , APP/PS-FTY720: 3.73 ± 0.71 and 'GFAP integrated intensity': WT-vehicle: 0.01 ± 0.00 , WT-FTY720: 0.00 ± 0.00 , APP/PS1-vehicle: 0.54 ± 0.06 , APP/PS1-FTY720: 0.21 ± 0.05)] (Fig. 27 B).

These results suggest that FTY720 treatment strongly reduced astrogliosis in APP/PS1 mice, and together with the reduced microgliosis, these cellular actions of the drug are potential mechanisms for the rescue of spine density deficits in this mouse model of AD.

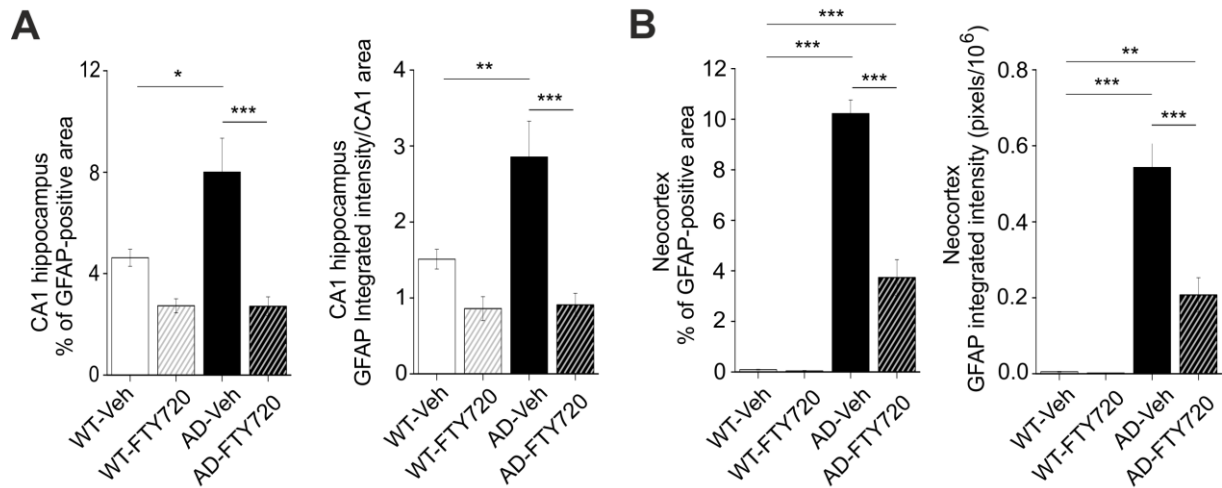


Figure 27: Quantification of the GFAP-positive activated astrocytes in the CA1 area of the hippocampus (A) and neocortex (B) in 6- to 7-month-old male WT and APP/PS1 (AD) mice after vehicle or FTY720 treatment at a dose of 1 mg/kg/2nd. Analysis of astrocytic area and integrated intensity normalized to the analyzed area of the section shows a strong increase in the GFAP-positive area of the CA1 hippocampus in AD-vehicle mice, which is completely rescued after chronic FTY720 administration. In the neocortex, the percent area of cortical sections covered by GFAP-positive reactive astrocytes and the integrated fluorescent pixel intensity indicate a robust activation of astrocytes in AD-vehicle mice that is drastically reduced after treatment with FTY720. Data are shown as mean \pm SEM; n = 6 mice per WT-vehicle, AD-vehicle and AD-FTY720 groups and 7 mice in the WT-FTY720 group. Statistical analysis was performed with two-way ANOVA, followed by Tukey's post hoc test, and statistical significance was set to $P < 0.05$. * = $P < 0.05$, ** = $P < 0.01$, *** = $P < 0.001$. Detailed information on two-way ANOVA (genotype x treatment interaction): (A) GFAP covered area: $F(1, 21) = 5.999$, $P = 0.0232$, normalized GFAP intensity: $F(1, 21) = 6.184$, $P = 0.0214$, (B) GFAP covered area: $F(1, 21) = 56.75$, $P < 0.0001$, GFAP intensity: $F(1, 21) = 20.12$, $P = 0.0002$. Modified figure from Kartalou et al., submitted; preprint available on bioRxiv (Kartalou et al. 2019).

3.4.4 Chronic treatment with FTY720 reduced amyloid plaque load in the hippocampus and neocortex of APP/PS1 mice

In order to study the effects of FTY720 treatment on the presence of amyloid deposits, fluorescence stainings of fibrillar A β aggregates were performed. Thioflavine S fluorescent staining was used to investigate the effects of FTY720 treatment, at a dose of 1 mg/kg/2nd day, on the formation of amyloid plaques in the hippocampus and neocortex of 6- to 7-month-old treated and untreated (vehicle) male APP/PS1 mice (Fig. 28).

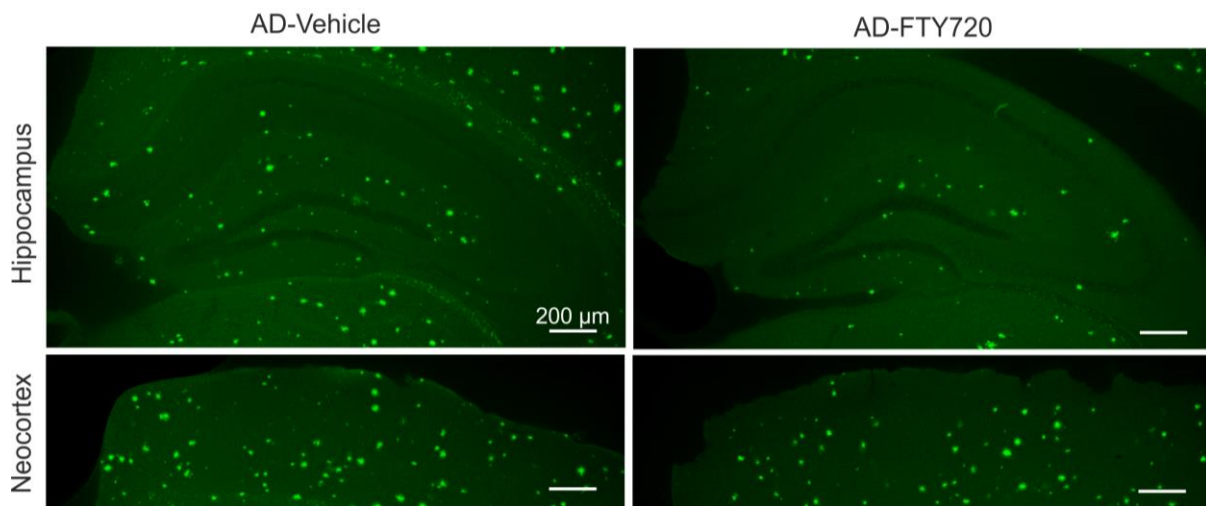


Figure 28: Thioflavine S fluorescent staining of amyloid plaques in the hippocampus (A) and neocortex (B) in coronal brain sections of 6- to 7-month-old untreated or treated (1 mg/kg/2nd day of FTY720) male APP/PS1 (AD) mice. Magnification: 5x. Modified figure from Kartalou et al., submitted; preprint available on bioRxiv (Kartalou et al. 2019).

Quantification of the load, size and number of amyloid plaques in the total hippocampus after FTY720 treatment showed a reduction in APP/PS1 mice, although the changes did not reach statistical significance. Specifically, the load of amyloid plaques displayed a twofold reduction (APP/PS1-vehicle: $0.30 \pm 0.11\%$, APP/PS1-FTY720: $0.14 \pm 0.03\%$). Smaller reductions of the number of amyloid plaques per unit area and of the average size of the plaques were also observed in the hippocampus of FTY720-treated APP/PS1 mice compared to untreated APP/PS1 littermates (Fig. 29 A).

Analysis of amyloid plaques in the neocortex upon FTY720 treatment in APP/PS1 mice revealed a significant reduction of the plaque load (APP/PS1-vehicle: $3.34 \pm 0.57\%$, APP/PS1-FTY720: $1.63 \pm 0.18\%$) and plaque size (APP/PS1-vehicle: 133 ± 7.73 , APP/PS1-FTY720: 100 ± 6.33). Also the number of plaques slightly dropped, without reaching significance (Fig. 29 B).

These results indicated a trend towards reduction of amyloid plaque burden upon chronic FTY720 treatment in this mouse model of AD.

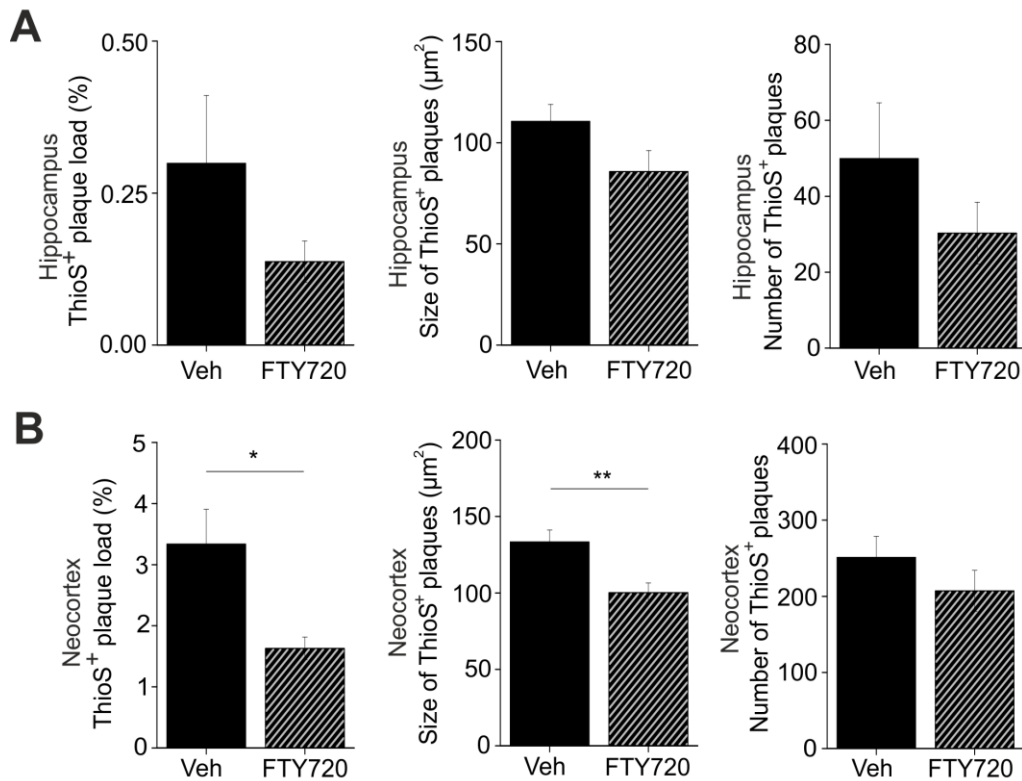


Figure 29: Quantification of Thioflavine S staining in the hippocampus (A) and neocortex (B) of 6- to 7-month-old untreated or treated (1 mg/kg/2ndday of FTY720) male APP/PS1 (AD) mice. Quantitative analysis of the amyloid plaque load (percentage area of positive staining), size and number of plaques shows a trend of reduction in the hippocampus of AD mice upon FTY720 treatment compared to AD-vehicle treated mice. In the neocortex, the analysis reveals significant reductions of the plaque load and the size of the plaques, but only a slight decrease of the number of plaques in AD mice after FTY720 treatment, compared to AD-vehicle treated littermates. Data are represented as mean \pm SEM; n = 6 mice per group. Statistical analysis was performed with unpaired Student's t-test, and statistical significance was defined as $P < 0.05$. * = $P < 0.05$, ** = $P < 0.01$. Modified figure from Kartalou et al., submitted; preprint available on bioRxiv (Kartalou et al. 2019).

3.4.5 Chronic treatment with FTY720 reduced the accumulation of A β in the hippocampus and neocortex of APP/PS1 mice

Immunostaining for A β was performed to evaluate the levels of A β protein (including A β on plaques, oligomers and fibrils) in the hippocampus and neocortex of untreated or with 1 mg/kg/2ndday FTY720 treated male APP/PS1 mice at 6 to 7-months (Fig. 30).

A β (IC16 antibody)

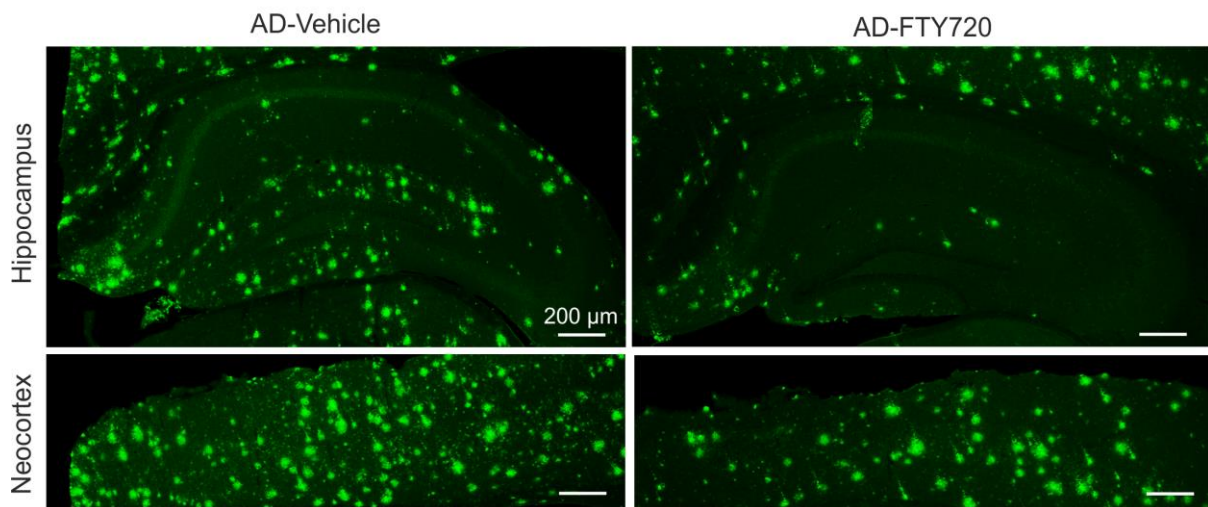


Figure 30: Representative images showing immunohistological staining for the detection of A β (IC16 antibody) in the hippocampus (A) and neocortex (B) in coronal brain sections of 6- to 7-month-old untreated or treated (1 mg/kg/2ndday of FTY720) male APP/PS1 (AD) mice. Magnification: 5x. Modified figure from Kartalou et al., submitted; preprint available on bioRxiv (Kartalou et al. 2019).

Quantitative analysis showed that FTY720 treatment in APP/PS1 mice resulted in significant decreases of A β load in the hippocampus (APP/PS1-vehicle: $2.69 \pm 0.40\%$, APP/PS1-FTY720: $0.97 \pm 0.24\%$) and neocortex (APP/PS1-vehicle: $24.6 \pm 5.0\%$, APP/PS1-FTY720: $12.3 \pm 2.0\%$), compared to vehicle-treated mice (Fig. 31 A, B).

These results indicate that FTY720 treatment reduced A β protein accumulation in APP/PS1 mice. Together with the reduction of neuroinflammation markers and the rescue of spine deficits by the drug, it might represent a potent modulator of AD pathology after the onset of the symptoms.

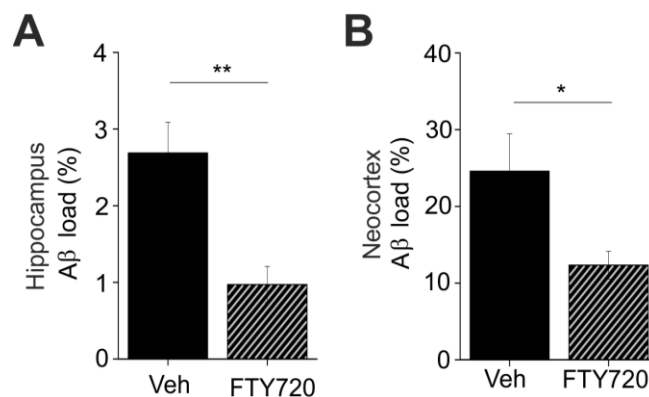


Figure 31: Quantification of A β immunoreactivity in the hippocampus (A) and neocortex (B) reveals a significant reduction upon FTY720 treatment at a dose of 1 mg/kg/2ndday in male APP/PS1 (AD) mice, compared to vehicle treated mice. Data are represented as mean \pm SEM; n = 6 mice per group. Statistical analysis was performed with unpaired Student's t-test, and statistical significance was defined as P < 0.05. * = P

< 0.05, ** = $P < 0.01$. Modified figure from Kartalou et al., submitted; preprint available on bioRxiv (Kartalou et al. 2019).

3.5 Expression of C-terminal fragment 1 (CTF1) of N-cadherin (Ncad), neuroligin 1 (NLG1) and neurexin (NRX) in sporadic AD

AD has been proposed to include a dysfunction of the γ -secretase; a proteolytic protein complex that is involved in the degradation of type I transmembrane proteins, such as the amyloid precursor protein (APP) (De Strooper, 2007; De Strooper et al., 2012). Due to the fact that several synaptic adhesion proteins (Ncad, NLG1, NRX) are also substrates of γ -secretase, a dysfunction of γ -secretase might lead to altered proteolytic processing of synaptic adhesion proteins, accumulation of C-terminal fragments (CTFs), and thereby to destabilization of synapses (Kim et al., 2009; Andreyeva et al., 2012; Uemura et al., 2006; Suzuki et al., 2012; Peixoto et al., 2012). In order to address such changes, the expression levels of CTF1 of Ncad, NLG1 and NRX were studied in post-mortem human brains from AD patients in a second project of this PhD work.

3.5.1 Pharmacological inhibition of γ -secretase activity increased Ncad CTF1, NLG1 CTF1 and NRX CTF1 levels in primary neuronal cultures

To identify specific CTFs on Western blots, their degradation by γ -secretase was inhibited by γ -secretase inhibitors, leading to an enhanced expression of the respective CTFs. In order to inhibit the cleavage of the Ncad CTF1, NLG1 CTF1 and NRX CTF1 domains by γ -secretase, cultures of primary hippocampal neurons from pups at postnatal day 1 (P1) were treated with the γ -secretase inhibitor L-685,458 (5 mM) at 8 days *in vitro*. Western blot analysis revealed a strong increase in the specific CTF1 levels of each protein (Ncad, NLG1 and NRX proteins) at 12 days *in vitro* (Fig. 32 A, B, C). These Western results identified the specific CTFs, and formed the basis for the analysis of CTF expression in the brains of AD patients.

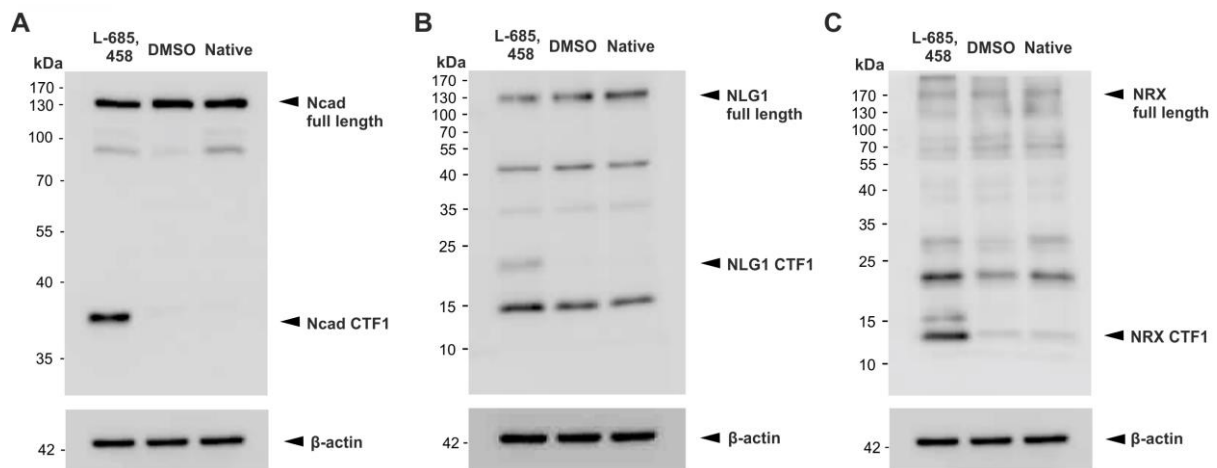


Figure 32: Western blot characterization of Ncad CTF1, NLG1 CTF1 and NRX CTF1 after pharmacological inhibition of γ -secretase in primary cultured hippocampal neural cells from mouse pups at postnatal day 1 (P1). Inhibition of γ -secretase activity by L-685,458 increases the presence of Ncad CTF1 (A, ~ 37 kDa), NLG1 CTF1 (B, ~ 20-22 kDa) and NRX CTF1 (C, ~ 15 kDa) after 4 days of incubation. β -actin was used as loading control (A, B, C, 42 kDa).

3.5.2 Ncad CTF1, NLG1 CTF1 and NRX CTF1 expression levels in post-mortem brains from patients with sporadic AD

Western blot analysis was used to investigate the presence of Ncad CTF1, NLG1 CTF1 and NRX CTF1 in post-mortem brain homogenates from patients with late onset AD. Specifically, post-mortem cortical brain tissue samples from 6 female patients with sporadic AD (age range: 80-87 years) and 5 female non-demented controls (age range: 83-87 years) were used for quantitative analysis (Figs. 33 A, 34 A & 35 A).

Densitometric analysis of the presence of Ncad CTF1, NLG1 CTF1 and NRX CTF1 normalized to the corresponding actin signals (loading control) revealed significantly increased levels of Ncad CTF1 in the post-mortem brains of the patients with AD, compared to the non-demented controls (AD: 1.05 ± 0.09 ; control: 0.67 ± 0.08) (Fig. 33 B). Interestingly, the NLG1 CTF1 levels were significantly lower in post-mortem brain tissue from AD patients, compared to non-demented controls (AD: 0.22 ± 0.04 ; control: 0.49 ± 0.08) (Fig. 34 B), while the NRX CTF1 levels were similar for both groups (Fig. 35 B). These results indicate that the presence of Ncad CTF1 is increased in patients with AD, whereas for the same patients the presence of NLG1 CTF1 is reduced; this suggests that γ -secretase functional impairments in sporadic AD may lead to specific changes in proteolytic cleavage for different substrates.

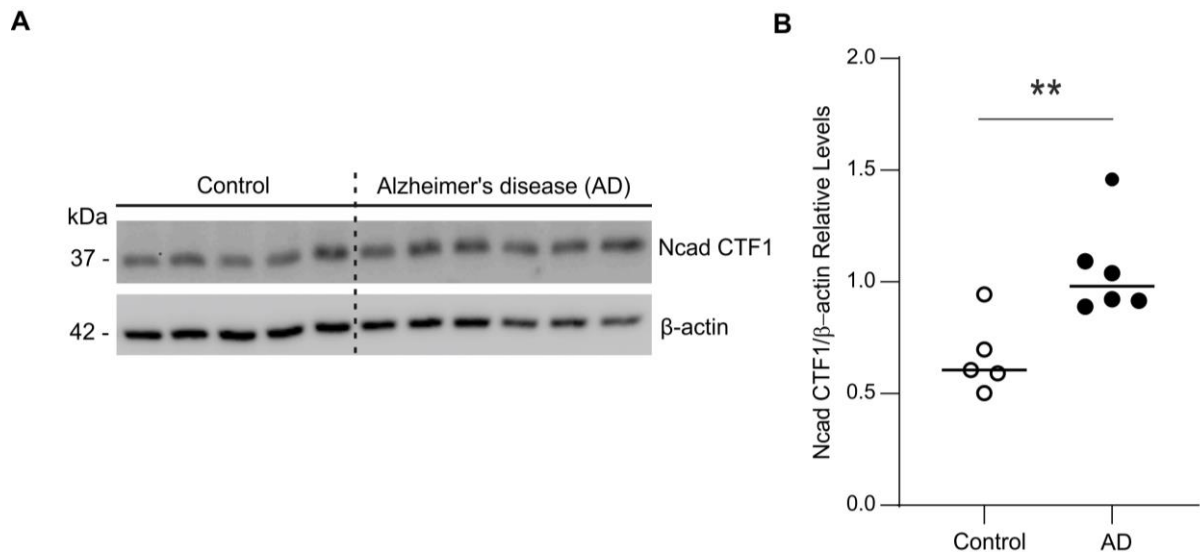


Figure 33: (A) Western blot of post-mortem brain homogenates from patients with sporadic AD and non-demented controls. Ncad CTF1 is detected at 37 kDa. β -actin was used as loading control (42 kDa). (B) Densitometric analysis relative to actin loading control of the Ncad CTF1 presence shows significantly increased levels in patients with AD, compared to non-demented controls. Data are represented as median; $n = 6$ individuals with sporadic AD and 5 non-demented controls. Statistical analysis was performed with unpaired Student's t-test, and statistical significance was defined as $P < 0.05$. ** = $P < 0.01$.

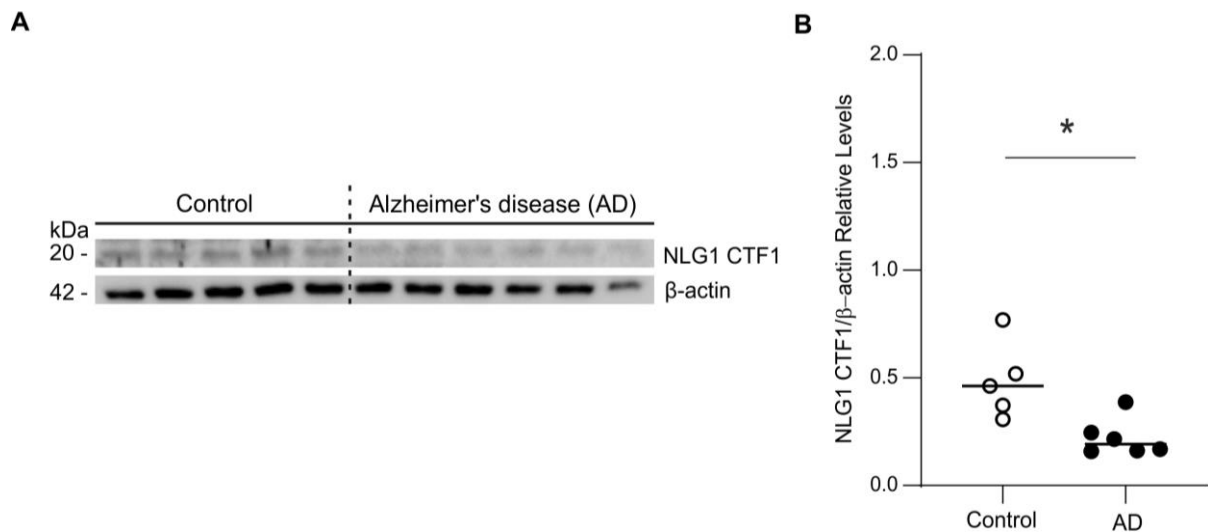


Figure 34: (A) Western blot of post-mortem brain homogenates from patients with sporadic AD and non-demented controls. NLG1 CTF1 is detected at 20 kDa. β -actin was used as loading control (42 kDa). (B) Densitometric analysis relative to actin loading control of the NLG1 CTF1 levels shows a significant reduction in patients with AD, compared to non-demented controls. Data are represented as median; $n = 6$ individuals with sporadic AD and 5 non-demented controls. Statistical analysis was performed with unpaired Student's t-test, and statistical significance was defined as $P < 0.05$. * = $P < 0.05$.

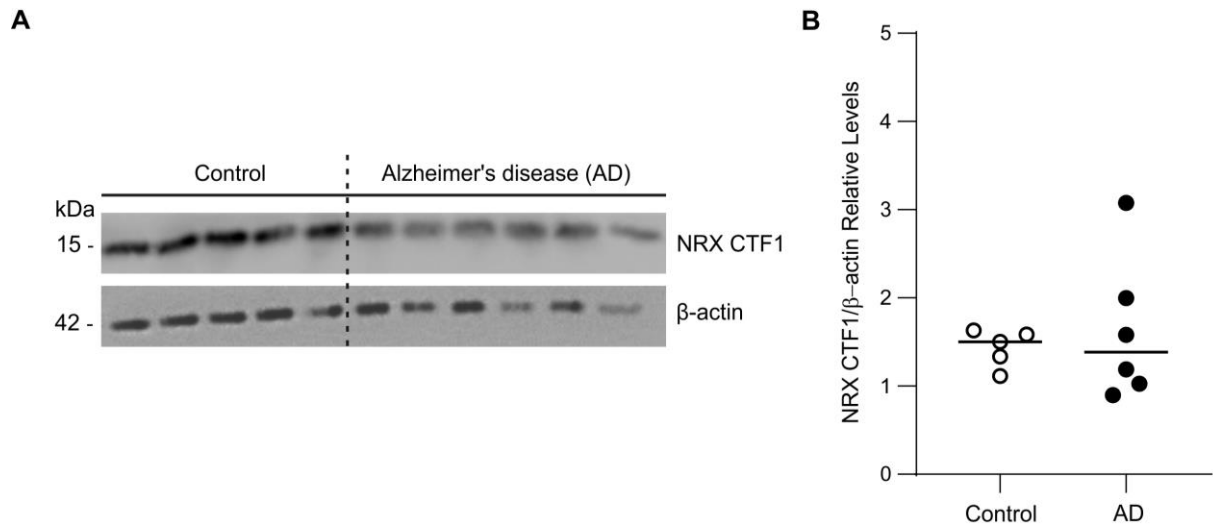


Figure 35: (A) Western blot of post-mortem brain homogenates from patients with sporadic AD and non-demented controls. NRX1 CTF1 is detected at 15 kDa. β -actin was used as loading control (42 kDa). (B) Densitometric analysis relative to actin loading control of the NRX CTF1 presence indicates similar levels in patients with AD, compared to non-demented controls. Data are represented as median; $n = 6$ individuals with sporadic AD and 5 non-demented controls. Statistical analysis was performed with unpaired Student's t-test, and statistical significance was defined as $P < 0.05$.

4. Discussion

Alzheimer's disease (AD) is the most common type of dementia in elderly population (Schachter and Davis, 2000). It is a neurodegenerative disorder characterized by severe and irreversible cognitive impairments (Schachter and Davis, 2000). Although amyloid beta ($A\beta$) aggregation is the most prominent pathological hallmark, which is widely thought to initiate the progression of the disease, substantial evidence supports the involvement of the immediate activation of microglia and astrocytes around amyloid plaques leading to an extreme level of neuroinflammation in the brain of AD patients (Haass and Selkoe, 2007; Heneka et al., 2015). Synaptic failure occurs at an early clinical stage of the disease, and it has been correlated with cognitive deficits in patients with AD. Dendritic spines, small protrusions emerging from neuronal dendrites, are the main postsynaptic compartments for excitatory input in the brain. Substantial dysfunction and decrease in the number of dendritic spines has been shown in AD brains, and mounting evidence suggests that it is caused by several nearby pathophysiological events; such as diffusible oligomeric $A\beta$, fibrillar amyloid plaques, or inflammatory mediators secreted by activated glial cells (Dorostkar et al., 2015). Potential therapies of AD would optimally start after the onset of the disease symptoms (Briggs et al., 2016). Over the recent years, several therapeutic approaches have been proposed, but there is still no effective treatment or cure of AD (Weinstein, 2018; Chen et al., 2017; Rogers and Friedhoff, 1996; Bryson and Benfield, 1997; Woodruff-Pak et al., 2007; Riepe et al., 2006).

The main aim of the current study is to determine the extent of the amyloid plaque-associated spine deficits in APP/PS1 mice, and to investigate novel therapeutic strategies to rescue spine pathology after the onset of the symptomatic phase of the disease in this animal model of AD.

4.1 Reduced spine density in the CA1 area of the hippocampus in a mouse model of AD

4.1.1 Dendritic spine loss in the hippocampus of 13-month-old APP/PS1 mice and in 6 to 7-month-old APP/PS1/BDNF^{+/-} animals

Using Golgi-Cox brain tissue impregnations, I detected significant spine deficits in apical secondary dendrites of hippocampal CA1 pyramidal neurons in APP/PS1 at the age of 13 months. This animal model, which carries the familial 'Swedish' double mutation in the

amyloid precursor protein (APP; KM670/671NL) and Leu166Pro mutation in the Presenilin-1 (PS1) genes, has been previously described to exhibit a strong amyloid pathology in aged animals (Radde et al., 2006). It is known that high levels of A β load and plaque deposition into the brain cause neurotoxicity and severe neuronal damage (Dorostkar et al., 2015). The observed spine pathology in these mice could be probably associated with such impairments.

I also used Golgi-Cox staining to analyze dendritic spine density in pyramidal neurons in the CA1 area of the hippocampus in young animals, at the age of 6 to 7 months. This analysis revealed a slight, non-significant, reduction of the number of spines in APP/PS1 at this age. Recent studies support that spine deficits mostly occur in a proximity to amyloid plaques in young mice of AD (Tsai et al., 2004; Bittner et al., 2012; Liebscher et al., 2014). This fact could explain the difficulty in detecting spine impairments in a non-associated to amyloid plaques spine analysis in young APP/PS1 mice. Moreover, the role of brain-derived neurotrophic factor (BDNF) is known to be essential in synaptic and structural plasticity; however, pathological changes in BDNF availability have also been reported in AD (Psotta et al., 2015; Kellner et al., 2014). My findings showed that reduced levels of endogenous BDNF production significantly decrease spine density in 6- to 7-months-old BDNF^{+/-} animals, and burden spine pathology in this AD mouse model. The results are supported by the detection of spine deficits in a non-local plaque focused spine density analysis in APP/PS1/BDNF^{+/-} mice at the same age.

4.1.2 Dendritic spine deficits near amyloid plaques in the hippocampus of 6- to 7-month-old APP/PS1 mice

Keeping my focus on dendritic spine pathology in AD, I established an innovative combination of the Golgi-Cox staining of neurons with the fluorescent labeling of amyloid plaques by methoxy-X04 (4,4'-[(2-methoxy-1,4-phenylene)di-(1E)-2,1-ethenediyl]bisphenol; C₂₃H₂₀O₃) dye. The fluorescent dye was dissolved in dimethyl sulfoxide (DMSO) and intraperitoneally administrated to all mice twice following a 24-hour interval. Two hours after the last injections the mouse brains were removed and prepared for the Golgi-Cox impregnation. Methoxy-X04 is an organic fluorescent probe that can cross the blood-brain barrier (BBB) and specifically bind to fibrillary β -sheet deposits; it is well established for staining and detecting amyloid plaques (Klunk et al., 2002; Bolmont et al., 2008; Bittner et al., 2012; Liebscher et al., 2014). Methoxy-X04 is widely known to be administrated in living

animals for labeling the amyloid plaques in the intact brains (Klunk et al., 2002; Jährling et al., 2015); a fact which enables to proceed with the classical Golgi-Cox impregnation.

The use of this novel technique of the combined methoxy-X04 with Golgi-Cox stainings allowed the visualization of neuronal dendrites close to amyloid plaques, and specifically the quantitative analysis of dendritic spines in the vicinity of these plaques in 6- to 7-month-old APP/PS1 mice. The number of spines was counted in secondary dendritic branches of hippocampal CA1 pyramidal neurons which were located at a distance $<50\ \mu\text{m}$ to the closest amyloid plaque (near plaques) and at a distance $>50\ \mu\text{m}$ from the plaque's border (distant to plaques). My analysis resulted in the detection of strong spine loss in APP/PS1 mice at the age of 6 to 7 months. Specifically, I found significant reduction in the number of spines in the vicinity of amyloid plaques, both in male and female APP/PS1 mice at this age. My quantitative spine analysis revealed also significant spine deficits in dendritic segments distant to amyloid plaques selectively in male mice; a fact that may indicate gender-specific differences in spine pathology in this mouse model of AD at this age. A possible factor that could explain and be responsible for such gender differences could be the role of estrogen (female anabolic hormone) in female APP/PS1 mice. It has been proposed that estrogens have a protective role in neurodegenerative diseases by acting on neuronal cells (Deshpande, 2000; Miranda et al., 1994). Specifically, it is thought that estrogen can modulate growth factors and neurotrophins related to synaptic and structural plasticity (Deshpande, 2000; Miranda et al., 1994).

In recent years, several other ways of microscopic visualization of dendritic spines close to amyloid plaques have been also used, such as the expression of the enhanced green fluorescent protein (EGFP) in living neuronal cells *in vivo* in transgenic AD mice (Bittner et al., 2012; Dorostkar et al., 2015; Liebscher et al., 2014). Although a detailed analysis of EGFP expressing neurons and spines using high resolution imaging is possible, such approaches are usually accompanied by photobleaching problems and a time-consuming process of data acquisition and analysis; drawbacks that can be overcome by the optimized Golgi-Cox combined with methoxy-X04 staining. By using this new technique, large neuronal data sets from the whole brain can be rapidly analyzed, providing also data repeatability.

4.2 Potential therapeutic innervations for rescuing spine pathology in APP/PS1 mice

It is crucial to highlight that treatments for AD should be tested at relatively early stages of the disease, immediately after the onset of symptoms, in order to better evaluate their

potential to prevent and eventually slowdown the progression of the disease before irreversible damages occur. In this study, I tested two different potential AD treatments in young APP/PS1 mice, such as voluntary running (VR) or chronic administration of fingolimod (FTY720). Both treatments are considered to have neuroprotective effects in several brain impairments and disorders (Aytan et al., 2016; Carreras et al., 2019; Tapia-Rojas et al., 2016).

4.2.1 Voluntary running (VR) rescues spine deficits in APP/PS1 mice

Using my novel, and well established method, which allowed me to visualize Golgi-Cox impregnated neurons close to fluorescent labeled amyloid plaques, I performed spine density analysis in secondary dendrites of hippocampal CA1 pyramidal neurons in 6- to 7-month-old male APP/PS1 mice after two months of voluntary running (VR). All animals had all-time access to running wheels from the age of 4-5 months until the age of 6-7 months. As controls, I used male APP/PS1 littermates kept in cages with blocked running wheels (enriched environment; EE), and male APP/PS1 mice held in cages with the standard nesting material (standard housing; SH). WT littermates kept in the corresponding housing conditions were also used as controls. I conducted dendritic spine quantitative analysis associated to amyloid plaques, and I observed strong spine deficits in APP/PS1-SH mice. I found that VR rescued spine densities in dendritic segments distant from plaques and significantly increased spine densities in dendrites near amyloid plaques in APP/PS1 mice. On the other hand, EE resulted in only improving spine densities in dendritic stretches near amyloid plaques.

Numerous studies support that physical exercise contributes to neuronal cell tolerance against oxidative stress and increases vascularization along with neurotrophin synthesis which are all of great importance in neurogenesis, memory improvement as well as in synaptic and structural plasticity in AD (Tapia-Rojas et al., 2016; Choi et al., 2018; Radak et al., 2010). There is also evidence that VR attenuates several AD-like impairments, such as neuronal cell death, memory loss and neuroinflammation (Tapia-Rojas et al., 2016). Specifically, it has been shown that VR reduces amyloid plaques and A β oligomers as well as the levels of tau phosphorylation and of the reactive astrocytes in the brain of an AD mouse model (APP^{swe}/PSEN1 Δ E9) (Tapia-Rojas et al., 2016). Moreover, VR it is thought to increase cell proliferation and neurogenesis, in combination with BDNF elevated levels in the hippocampus of AD animal models (Tapia-Rojas et al., 2016; Choi et al., 2018; Wrann et al., 2013). Recent evidence revealed that exercise ameliorates cognitive impairments in 5xFAD

mice (a different mouse model of AD) via enhanced hippocampal neurogenesis and BDNF levels in adult animals (Choi et al., 2018). Moreover, other proteins such as postsynaptic density protein 95 (PSD95) and synaptophysin, which play an important role in synaptic plasticity and it is known that they are reduced in AD patients, were found to be elevated in 5xFAD mice after exercise (Choi et al., 2018; Proctor et al., 2010). Interleukin-6 (IL-6) levels which are increased in the hippocampus after physical exercise, were also elevated in 5xFAD mice after exercise (Choi et al., 2018); an important evidence, since IL-6 has been shown to have a positive contribution in cognitive function and neurogenesis (Choi et al., 2018; Bowen et al., 2011). Interestingly, the fibronectin type III domain-containing protein-5 (FNDC5) which regulates the BDNF expression in the mouse hippocampus has been also shown to be enhanced in 5xFAD animals (Choi et al., 2018; Wrann et al., 2013). All these beneficial effects of VR might be in line with my findings which suggest that, VR, starting after the onset of symptoms, dramatically attenuates spine loss in this mouse model of AD.

4.2.2 FTY720 rescues spine deficits and reduces neuroinflammation along with amyloid pathology in APP/PS1 mice

FTY720, a Food and Drug Administration (FDA)-approved drug for multiple sclerosis (MS), is a structural analog of sphingosine and a modulator of sphingosine-1-phosphate (S1P) receptors (Angelopoulou and Piperi, 2019). This drug can cross BBB and accumulate in the central nervous system (CNS), where it is converted to its active phosphorylated form, fingolimod-phosphate (FTY720-P) (Angelopoulou and Piperi, 2019; Rothhammer et al., 2017). The main cells of the CNS, such as neurons, oligodendrocytes, microglia and astrocytes, express S1P receptors on their surfaces and their functional role can be modulated by the drug (Healy and Antel, 2016). It has been shown that FTY720 action in the CNS is associated with a reduction of the production of pro-inflammatory cytokines by microglia through S1P receptors (Noda et al., 2013).

In this study, I was interested in investigating the effects of FTY720 treatment on dendritic spine pathology in AD using young APP/PS1 mice. The animals were treated with FTY720, at a dose of 1 mg/kg/2ndday or with a lower dose of 0.2 mg/kg/2ndday at the age of 5-6 months for one month until the age of 6-7 months. APP/PS1 and WT littermates were treated with vehicle solution and used as controls. I performed dendritic spine quantitative analysis associated to amyloid plaques, in secondary dendrites of hippocampal CA1 pyramidal neurons. Specifically, the analysis was conducted in double stained brain sections,

using my above mentioned novel technique of Golgi-Cox impregnation combined with amyloid plaque fluorescent staining, in treated and untreated animals. My analysis revealed a strong dependence of spine deficits on amyloid plaque proximity in untreated APP/PS1 mice. I found that both high and low FTY720 doses (1 mg/kg/2ndday and 0.2 mg/kg/2ndday respectively) completely rescued spine deficits in dendrites distant from amyloid plaques and significantly ameliorated spine loss near plaques. A more detailed data overview revealed that spine deficits were stronger near amyloid plaques than distant from plaques in untreated APP/PS1 mice. Although both concentrations of FTY720 improved spine pathology in dendrites which were located distant and close to amyloid plaques, only the high dose of FTY720 treatment (1 mg/kg/2ndday) increased spine density at the same level in both distant and close to plaques groups in this mouse model of AD. These results suggest that a potential treatment with FTY720 for slowdown the spine pathology in AD could be more beneficial in a higher than in a lower concentration.

Local spine deficits of amyloid plaques might be related also with neuroinflammatory responses of activated glial cells, such as reactive microglia or reactive astrocytes that surround amyloid plaques (Heneka et al., 2015). The exact mechanisms, which are underlying the glia-mediated synaptic elimination, are still not completely understood. However, there is strong evidence that glial cells are associated with synaptic dysfunction that leads to neuronal injury and degeneration (Kano and Hashimoto, 2009; Wilton et al., 2019). In my study, I observed a robust microgliosis and astrogliosis in the hippocampus and neocortex of untreated APP/PS1 mice. Treatment with FTY720 at a dose 1 mg/kg/2ndday drastically reduced microgliosis and activated astrocytes back to control levels in the hippocampus of treated APP/PS1 mice. Likewise, FTY720 treatment significantly reduced microglia and the astrocytic marker in the neocortex.

Furthermore, I performed a detailed analysis of amyloid pathology in untreated and treated with FTY720 (1 mg/kg/2ndday) APP/PS1 mice. Specifically, I conducted a quantitative analysis of amyloid plaque load, plaque size and plaque number of the total thioflavine S-stained plaques in the hippocampus and neocortex of these animals. My findings resulted in a twofold slight reduction, without reaching significant levels, of amyloid plaque load in the hippocampus and significant decreases of plaque load and size in the neocortex after FTY720 treatment. Interestingly, treatment with FTY720 significantly reduced also the A β protein load in the hippocampus and neocortex of treated APP/PS1 mice. My findings regarding the effects of the drug on astrogliosis and microgliosis as well as on amyloid pathology are consistent with the results of recent studies in a different mouse model of AD (5xFAD

animals), where FTY720 treatment was administrated already from the age of 4 weeks in female mice (Aytan et al., 2016; Carreras et al., 2019).

Recent evidence supports that treatment with FTY720 is associated with neuroprotection correlated with the reduction of several pro-inflammatory cytokines that are secreted by reactive glia and with increased BDNF levels in the brain; effects that might be related to the results in this study (Doi et al., 2013). Specifically, many studies have shown that FTY720 increases the mRNA and protein levels of BDNF in mouse models of several neurodegenerative diseases (Deogracias et al., 2012; Fukumoto et al., 2014; Miguez et al., 2015). It is thought that the BDNF/tropomyosin-related kinase B (TrkB) signaling is involved in AD (Zhang et al., 2012). Deficits in BDNF signaling via TrkB receptor are associated with amyloid and cognitive dysfunction in AD (Zhang et al., 2012; Amoureux et al., 1997; Phillips et al., 1991; Murray et al., 1994), while there is strong evidence that enhanced BDNF/ TrkB signaling improves cognitive dysfunctions in AD mice. In this study, I hypothesized that FTY720 chronic administration can be beneficial on BDNF/TrkB signaling and improve the AD symptoms in these APP/PS1 treated mice (Kartalou et al., 2019). Of note, although my investigation revealed that FTY720 treatment improves the AD-like symptoms in these mice, immediate effects of the drug on BDNF protein levels or on the TrkB signaling efficacy were not observed in AD and WT treated animals (Kartalou et al., 2019). It has been also recently shown that FTY720 modulates microglia activation via S1P receptor signaling, resulting in the inhibition of the production of neuronal A β and the reduction of the levels of A β 42 and A β 40 species in AD mouse models (McManus et al., 2017; Takasugi et al., 2013; Aytan et al., 2016). Moreover, this drug when accesses the CNS can act through the sphingosine-1-phosphate receptors (S1PRs) of microglia to regulate the transition from its pro-inflammatory M1 to the anti-inflammatory M2 phenotype (Qin et al., 2017). There is also evidence that FTY720 has the ability to induce A β phagocytosis by astrocytes as well as to reduce the astrocyte reaction along with the production of inflammatory cytokines which are secreted by these cells (McManus et al., 2017). In this study, the dramatic reduction of the reactive glia upon FTY720 treatment suggests a beneficial role of the elimination of the mediated by these cells neuroinflammation in the rescue of the hippocampal spine deficits in FTY720 treated animals (Kartalou et al., 2019). The complete rescue of the reduced spine densities was mainly observed in neuronal dendrites which were located distant from amyloid plaques than in dendrites close to plaques; an effect that can be associated with the reduction of A β levels in combination with potential alterations in the secreted microglia mediators, such as the pro-inflammatory interleukin-1 (IL-1), interleukin-6 (IL-6) and tumor necrosis factor- α (TNF- α).

Recent studies have shown that adapter protein apoptosis-associated speck-like protein containing a caspase recruitment domain (ASC) specks released by microglia can bind A β and burden amyloid pathology in AD mice (Venegas et al., 2017). The reduction of these microglia-derived ASC specks could be another potential effect of FTY720 that may contribute to the attenuation of the amyloid and spine pathology in these treated APP/PS1 mice.

Overall, my findings demonstrate that FTY720 treatment, starting after the onset of AD symptoms, strongly reduces neuroinflammation, and, together with the reduced amyloid pathology, it might lead to a rescue of spine deficits by the drug. Therefore, FTY720 could be proposed as critical modulator of AD pathology providing neuroprotective effects.

4.3 Analysis of the expression of selected γ -secretase substrates in sporadic AD

Over the years, studies in post-mortem brains have been shown that cognitive impairments in AD are correlated to a higher extent with the loss of post- and presynaptic structures than with the amyloid plaques and neurofibrillary tangles (NFTs) AD characteristics (Terry et al., 1991). Furthermore, deficits in synaptic and structural plasticity, which are intimately linked with impairments in learning and memory, have enhanced the hypothesis of synaptic dysfunction in AD (Walsh and Selkoe, 2007). Unfortunately, the molecular mechanisms behind synaptic elimination is not yet very well known. Mounted evidence has reported that A β , the proteolytic product of APP after sequential cleavage by β - and γ -secretase, is associated with synapse destabilization leading to synaptic failure (Walsh and Selkoe, 2007; Koffie et al., 2009). It has been also shown that different forms of A β protein are localized with presynaptic buttons and postsynaptic spine resulting in their loss (Walsh and Selkoe, 2007; Koffie et al., 2009; Buttini et al., 2005; Hsieh et al., 2006; Shankar et al., 2007; Evans et al., 2008). The exact mechanisms that underlie the long-term stability of synapsis are still not very well understood; however, studies have shown that trans-synaptic interactions between cell adhesion molecules (CAMs) which are expressed in the pre- and postsynaptic sites are required for their physiological stabilization (Li and Sheng, 2003). N-cadherin (Ncad), neuroligin-1 (NLG1) and neurexin (NRX) are thought to be implicated in several synaptic processes, such as synaptic differentiation, synaptic plasticity and stability. Moreover, it has been shown that these synaptic CAMs are important substrates of γ -secretase since they are proteolytically processed similarly to the APP protein; therefore, they may also be implicated in AD (Andreyeva et al., 2012; Peixoto et al., 2012; Borcel et al., 2016).

Specifically, Ncad, NLG1 and NRX are all initially cleaved by α -secretase (A Disintegrin And Metalloproteinase 10; ADAM 10) activity to generate a C-terminal fragment 1 (CTF1) (Ncad CTF1, NLG1 CTF1 and NRX CTF1 respectively) which is further cut by γ -secretase to produce and liberate a C-terminal fragment 2 (CTF2) (Ncad CTF2, NLG1 CTF2 and NRX CTF2 respectively) into the cytoplasm (Andreyeva et al., 2012; Borcel et al., 2016; Peixoto et al., 2012).

There is strong evidence that in early-onset familial Alzheimer's Disease, (EOFAD) γ -secretase dysfunction, due to loss-of-function mutation of the presenilin-1 (PS1) gene, leads to misprocessing or alternative processing of APP protein, resulting in an increase in the generation of A β 42 relative to A β 40 (De Strooper, 2007; Suzuki et al., 1994). Recent studies have reported that alternative APP processing by γ -secretase without curing any mutations in PS1 gene, results in an increase of the A β 42/A β 40 ratio in sporadic AD. This evidence indicates that γ -secretase dysfunction might also occur in sporadic AD; however, the exact pathological mechanisms which underlie this process are still not completely understood (Hata et al., 2011; Kim et al., 2009; Hata et al., 2009).

In this study, in order to investigate the potential γ -secretase dysfunction in sporadic AD, I first looked over the consequence of inhibiting the function of γ -secretase by characterizing the CTF1 levels of the synaptic adhesion molecules Ncad, NLG1 and NRX that are all proteolytically processed by γ -secretase activity in cultured primary hippocampal neurons from mouse pups in postnatal day 1 (P1). I observed by Western blot analysis that pharmacological inhibition of γ -secretase increased the levels of Ncad CTF1, NLG1 CTF1 and NRX CTF1 because their degradation was blocked.

In addition, there is evidence that the CTF1 levels of Ncad are enhanced in AD patients with sporadic AD (Andreyeva et al., 2012). Specifically, it is thought that the increased Ncad CTF1 levels in post-mortem brains of AD patients is possible to enhance A β oligomer-induced synapse impairment, and therefore, to play an important role in AD progression (Andreyeva et al., 2012). I then continued this study evaluating the levels of CTF1 of Ncad, NLG1 and NRX, in post-mortem brains from patients with sporadic AD. Post-mortem brains from non-demented individuals were used as control for my investigation as well. After quantitative analysis, I observed that the Ncad CTF1 levels were significantly elevated in patients with sporadic AD, while the NLG1 CTF1 levels were significantly reduced in the same patients. Of note, I did not observe level alterations of NRX CTF1 between AD patients and non-demented controls. Over the last years, the role of NLG1 in amyloid-associated memory impairments in AD has been extensively investigated (Suzuki et al., 2012;

Dinamarca et al., 2011; Saura et al., 2011; Bie et al., 2014). It is thought that NLG1 is a potential target of A β oligomers related to synaptic damage in AD (Dinamarca et al., 2011; Dinamarca et al., 2012). Moreover experiments in rats have shown that amyloid-induced neuroinflammatory reaction by microglia is related to epigenetic suppression of NLG1 in hippocampal CA1 pyramidal neurons (Bie et al., 2014). According to this evidence, a potential reduction of NLG1 protein in AD could be associated with the observed reduction of the NLG1 CTF1 levels in post-mortem brains from AD patients in this present study.

Overall, my findings indicate that potential γ -secretase activity impairments in sporadic AD may lead to altered proteolytic cleavage of specific substrates by the enzyme. The previous evidence of the increased vulnerability of synaptic damage by A β action, which is accompanied by the enhanced levels of Ncad CTF in AD patients, could be of highly importance for the development of future potential therapeutic strategies targeting γ -secretase and the reduction of the toxic A β without affecting the production of Ncad CTF1 (Andreyeva et al., 2012). However, whether the increase of the Ncad CTF1 presence, which was investigated in this study, is a direct consequence of γ -secretase dysfunction in sporadic AD, is an issue which needs to be further investigated. There is mounting evidence that ADAM10 enzyme (known for its involvement in the APP metabolism) is implicated in AD pathology via mechanisms which underlie synaptic function in the brain, including interactions with its post- and presynaptic Ncad, NLG1 and NRX protein substrates (Yuan et al., 2017). Over the last years, several mutations in ADAM 10 gene as well as changes in its protein levels have been proposed by numerous studies in AD (Yuan et al., 2017; Niemitz, 2013). Moreover, there is also evidence of enhanced ADAM10 expressed protein levels correlated with increased Ncad CTF1 levels in a different neurodegenerative disease [Huntington's disease (HD)] (Vezzoli et al., 2019). Potential changes in ADAM10 activity could be an alternative explanation of the observed alterations of the Ncad CTF1 and NLG1 CTF1 levels in post-mortem brains from patients with sporadic AD, compared to post-mortem brains from non-demented individuals in this current study.

5. References

- Adachi, K., and K. Chiba. 2007. "FTY720 Story. Its Discovery and the Following Accelerated Development of Sphingosine 1-Phosphate Receptor Agonists as Immunomodulators Based on Reverse Pharmacology." *Perspectives in Medicinal Chemistry* 1 (September): 11–23.
- Alvarez, V. A., and B. L. Sabatini. 2007. "Anatomical and Physiological Plasticity of Dendritic Spines." *Annual Review of Neuroscience* 30 (1): 79–97.
- Alzheimer, A., R. A. Stelzmann, N. H. Schnitzlein, and R. F. Murtagh. 1995. "An English Translation of Alzheimer's 1907 Paper, 'Über Eine Eigenartige Erkankung Der Hirnrinde'." *Clinical Anatomy* 8 (6): 429–31.
- Amoureux, M.C., D. Van Gool, M.T. Herrero, R. Dom, F. C. Colpaert and P. J. Pauwels. 1997. "Regulation of metallothionein-III (GIF) mRNA in the brain of patients with Alzheimer disease is not impaired." *Molecular and Chemical Neuropathology* 32:(1-3) 101-21.
- Andersen, P., ed. 2007. *The Hippocampus Book*. Oxford; New York: Oxford University Press.
- Andreyeva, A., K. Nieweg, K. Horstmann, S. Klapper, A. Müller-Schiffmann, C. Korth, and K. Gottmann. 2012. "C-Terminal Fragment of N-Cadherin Accelerates Synapse Destabilization by Amyloid- β ." *Brain* 135 (7): 2140–54.
- Angelopoulou, E., and C. Piperi. 2019. "Beneficial Effects of Fingolimod in Alzheimer's Disease: Molecular Mechanisms and Therapeutic Potential." *Neuromolecular Medicine* 21 (3): 227–38.
- Ardura-Fabregat, A., E. Boddeke, A. Boza-Serrano, S. Brioschi, S. Castro-Gomez, K. Ceyzeriat, C. Dansokho, T. Dierkes, G. Gelders, M. Heneka, L. Hoeijmakers, A. Hoffmann, L. Iaccarino, S. Jahnert, K. Kuhbandner, G. Landreth, N. Lonnemann, P. Löschmann, R. McManus, A. Paulus, K. Reemst, J. Sanchez-Caro, A. Tiberi, A. Perren, A. Vautheny, C. Venegas, A. Webers, P. Weydt, T. Wijasa, X. Xiang, Y. Yang. 2017. "Targeting Neuroinflammation to Treat Alzheimer's Disease." *CNS Drugs* 31 (12): 1057–82.
- Aytan, N., J.K. Choi, I. Carreras, V. Brinkmann, N.W. Kowall, B. G. Jenkins, and A. Dedeoglu. 2016. "Fingolimod Modulates Multiple Neuroinflammatory Markers in a Mouse Model of Alzheimer's Disease." *Scientific Reports* 6 (March): 1–9.

- Bamberger, M. E., M.E. Harris, D.R. McDonald, J.Husemann, and G.E. Landreth. 2003. "A Cell Surface Receptor Complex for Fibrillar Beta-Amyloid Mediates Microglial Activation." *The Journal of Neuroscience: The Official Journal of the Society for Neuroscience* 23 (7): 2665–74.
- Barao, S., D. Moechars, S. F. Lichtenthaler, and B. De Strooper. 2016. "BACE1 Physiological Functions May Limit Its Use as Therapeutic Target for Alzheimer's Disease." *Trends in Neurosciences* 39 (3): 158–69.
- Bayram-Weston, Z., E. Olsen, D. J. Harrison, S. B. Dunnett, and S. P. Brooks 2016. "Optimising Golgi-Cox Staining for Use with Perfusion-Fixed Brain Tissue Validated in the ZQ175 Mouse Model of Huntington's Disease." *Journal of Neuroscience Methods* 265: 81–8.
- Berg, D. A., A. M. Bond, G.L. Ming, and H. Song. 2018. "Radial Glial Cells in the Adult Dentate Gyrus: What Are They and Where Do They Come From?" *F1000Research* 7: 277.
- Bie, B., J. Wu, H. Yang, J. J Xu, D. L. Brown, and M. Naguib. 2014. "Epigenetic Suppression of Neuroligin 1 Underlies Amyloid-Induced Memory Deficiency." *Nature Neuroscience* 17 (2): 223–31.
- Bird, C. M., and N. Burgess. 2008. "The Hippocampus and Memory: Insights from Spatial Processing." *Nature Reviews. Neuroscience* 9 (3): 182–94.
- Bittner, T., S. Burgold, M. M. Dorostkar, M. Fuhrmann, B. M. Wegenast-Braun, B. Schmidt, H. Kretzschmar, and J. Herms. 2012. "Amyloid Plaque Formation Precedes Dendritic Spine Loss." *Acta Neuropathologica* 124 (6): 797–807.
- Blennow, K., M. J de Leon, and H. Zetterberg. 2006. "Alzheimer's Disease." *Lancet* 368 (9533): 387–403.
- Blessed, G., B. E. Tomlinson, and M. Roth. 1968. "The Association between Quantitative Measures of Dementia and of Senile Change in the Cerebral Grey Matter of Elderly Subjects." *The British Journal of Psychiatry: The Journal of Mental Science* 114 (512): 797–811.
- Bolmont, T., F. Haiss, D. Eicke, R. Radde, C. A. Mathis, W. E. Klunk, S. Kohsaka, M. Jucker, and M. E. Calhoun. 2008. "Dynamics of the Microglial/Amyloid Interaction Indicate a Role in Plaque Maintenance." *The Journal of Neuroscience: The Official Journal of the Society for Neuroscience* 28 (16): 4283–92.
- Borcel, E., M. Palczynska, M. Krzisch, M. Dimitrov, G. Ulrich, N. Toni, and P. C. Fraering. 2016. "Shedding of Neurexin 3 β Ectodomain by ADAM10 Releases a Soluble Fragment

- That Affects the Development of Newborn Neurons.” *Scientific Reports* 6 (December): 39310.
- Bot, N., C. Schweizer, S. Ben Halima, and P. C. Fraering. 2011. “Processing of the Synaptic Cell Adhesion Molecule Neurexin-3 β by Alzheimer Disease α - and γ -Secretases.” *Journal of Biological Chemistry* 286 (4): 2762–73.
- Bowen, K. K., R. J. Dempsey, and R. Vemuganti. 2011. “Adult Interleukin-6 Knockout Mice Show Compromised Neurogenesis.” *Neuroreport* 22 (3): 126–30.
- Braak, H., and E. Braak. 1991. “Neuropathological Stageing of Alzheimer-Related Changes.” *Acta Neuropathologica* 82 (4): 239–59.
- Braak, H., and K. Del Tredici. 2011. “The Pathological Process Underlying Alzheimer’s Disease in Individuals under Thirty.” *Acta Neuropathologica* 121 (2): 171–81.
- Briggs, R., S. P Kennelly, and D. O’Neill. 2016. “Drug Treatments in Alzheimer’s Disease.” *Clinical Medicine* 16 (3): 247–53.
- Brummer, T., S. A. Muller, F. Pan-Montojo, F. Yoshida, A. Fellgiebel, T. Tomita, K. Endres, and S. F., Lichtenthaler. 2019. “NrCAM Is a Marker for Substrate-Selective Activation of ADAM10 in Alzheimer’s Disease.” *EMBO Molecular Medicine* 11 (4).
- Bryson, H. M., and P. Benfield. 1997. “Donepezil.” *Drugs & Aging* 10 (3): 231–34.
- Bukalo, O., and A. Dityatev. 2012. “Synaptic Cell Adhesion Molecules.” In *Synaptic Plasticity: Dynamics, Development and Disease*, edited by M. Kreutz, and Sala C., 97–128. Advances in Experimental Medicine and Biology, vol 970. Vienna: Springer.
- Buttini, M., E. Masliah, R. Barbour, H. Grajeda, R. Motter, K. Johnson-Wood, K. Khan, P. Seubert, S. Freedman, D. Schenk, D. Games. 2005. “Beta-Amyloid Immunotherapy Prevents Synaptic Degeneration in a Mouse Model of Alzheimer’s Disease.” *The Journal of Neuroscience : The Official Journal of the Society for Neuroscience* 25 (40): 9096–101.
- Cappellano, G., M. Carecchio, T. Fleetwood, L. Magistrelli, R. Cantello, U. Dianzani, and C. Comi. 2013. “Immunity and Inflammation in Neurodegenerative Diseases.” *American Journal of Neurodegenerative Disease* 2 (2): 89–107.
- Carreras, I., N. Aytan, J.K. Choi, C. M. Tognoni, N. W. Kowall, B. G. Jenkins, and A. Dedeoglu. 2019. “Dual Dose-Dependent Effects of Fingolimod in a Mouse Model of Alzheimer’s Disease.” *Scientific Reports* 9 (1): 1-11.
- Chapman, M. R., L. S. Robinson, J. S. Pinkner, R. Roth, J. Heuser, M. Hammar, S. Normark, and S. J. Hultgren. 2002. “Role of Escherichia Coli Curli Operons in Directing Amyloid Fiber Formation.” *Science* 295 (5556): 851–55.

- Chen, G.F., T.H. Xu, Y. Yan, Y. R. Zhou, Y. Jiang, K. Melcher, and H. E. Xu. 2017. “Amyloid Beta: Structure, Biology and Structure-Based Therapeutic Development.” *Acta Pharmacologica Sinica* 38 (9): 1205–35.
- Chen, X.Q., and W. C. Mobley. 2019. “Alzheimer Disease Pathogenesis: Insights From Molecular and Cellular Biology Studies of Oligomeric A β and Tau Species.” *Frontiers in Neuroscience* 13: 659.
- Chi, H. 2011. “Sphingosine-1-Phosphate and Immune Regulation: Trafficking and Beyond.” *Trends in Pharmacological Sciences* 32 (1): 16–24.
- Chicurel, M. E., and K. M. Harris. 1992. “Three-Dimensional Analysis of the Structure and Composition of CA3 Branched Dendritic Spines and Their Synaptic Relationships with Mossy Fiber Boutons in the Rat Hippocampus.” *The Journal of Comparative Neurology* 325 (2): 169–82.
- Choi, S. H., E. Bylykbashi, Z. K. Chatila, S. W. Lee, B. Pulli, G. D. Clemenson, E. Kim, A. Rompala, M.K. Oram, C. Asselin, J. Aronson, C. Zhang, S.J. Miller, A. Lesinski, J.W. Chen, Kim D.Y.1, H. van Praag, B. M. Spiegelman, F.H. Gage, R.E. Tanzi. 2018. “Combined Adult Neurogenesis and BDNF Mimic Exercise Effects on Cognition in an Alzheimer’s Mouse Model.” *Science* 361 (6406): eaan8821.
- Chun, J., and V. Brinkmann. 2011. “A Mechanistically Novel, First Oral Therapy for Multiple Sclerosis: The Development of Fingolimod (FTY720, Gilenya).” *Discovery Medicine* 12 (64): 213–28.
- Chun, W., and G. V. W. Johnson. 2007. “The Role of Tau Phosphorylation and Cleavage in Neuronal Cell Death.” *Frontiers in Bioscience: A Journal and Virtual Library* 12 (January): 733–56.
- Cruickshanks, N., J. L. Roberts, M. D. Bareford, M. Tavallai, A. Poklepovic, L. Booth, S. Spiegel, and P. Dent. 2015. “Differential Regulation of Autophagy and Cell Viability by Ceramide Species.” *Cancer Biology & Therapy* 16 (5): 733–42.
- Cummings, J. L., G. Tong, and C. Ballard. 2019. “Treatment Combinations for Alzheimer’s Disease: Current and Future Pharmacotherapy Options.” *Journal of Alzheimer’s Disease: JAD* 67 (3): 779–94.
- Danysz, W., and C. G. Parsons. 2012. “Alzheimer’s Disease, β -Amyloid, Glutamate, NMDA Receptors and Memantine--Searching for the Connections.” *British Journal of Pharmacology* 167 (2): 324–52.
- Das, G., K. Reuhl, and R. Zhou. 2013. “The Golgi–Cox Method.” In *Neural Development*, edited by R. Zhou, and L. Mei, 313–21. *Methods in Molecular Biology (Methods and*

- Protocols), vol 1018. Totowa, NJ: Humana Press.
- De Strooper, B. 2007. "Loss-of-Function Presenilin Mutations in Alzheimer Disease. Talking Point on the Role of Presenilin Mutations in Alzheimer Disease." *EMBO Reports* 8 (2): 141–46.
- De Strooper, B., T. Iwatsubo, and M. S. Wolfe. 2012. "Presenilins and γ -Secretase: Structure, Function, and Role in Alzheimer Disease." *Cold Spring Harbor Perspectives in Medicine* 2 (1): a006304.
- Deogracias, R., M. Yazdani, M. P. J. Dekkers, J. Guy, M. C. S. Ionescu, K. E. Vogt, and Y.-A. Barde. 2012. "Fingolimod, a Sphingosine-1 Phosphate Receptor Modulator, Increases BDNF Levels and Improves Symptoms of a Mouse Model of Rett Syndrome." *Proceedings of the National Academy of Sciences* 109 (35): 14230–35.
- Deshpande, S. B. 2000. "Protective Role of Estrogen in the Neurodegenerative Disorders." *Indian Journal of Physiology and Pharmacology* 44 (1): 43–9.
- Dinamarca, M. C., J. A. Rios, and N. C. Inestrosa. 2012. "Postsynaptic Receptors for Amyloid-Beta Oligomers as Mediators of Neuronal Damage in Alzheimer's Disease." *Frontiers in Physiology* 3: 464.
- Dinamarca, M. C., D. Weinstein, O. Monasterio, and N. C. Inestrosa. 2011. "The Synaptic Protein Neuroligin-1 Interacts with the Amyloid Beta-Peptide. Is There a Role in Alzheimer's Disease?" *Biochemistry* 50 (38): 8127–37.
- Docampo-Seara, A., G. N. Santos-Duran, E. Candal, and M. A. Rodriguez Diaz. 2019. "Expression of Radial Glial Markers (GFAP, BLBP and GS) during Telencephalic Development in the Catshark (*Scyliorhinus Canicula*)." *Brain Structure & Function* 224 (1): 33–56.
- Doi, Y., H. Takeuchi, H. Horiuchi, T. Hanyu, J. Kawanokuchi, S. Jin, B. Parajuli, Y. Sonobe, T. Mizuno, and A. Suzumura. 2013. "Fingolimod Phosphate Attenuates Oligomeric Amyloid β -Induced Neurotoxicity via Increased Brain-Derived Neurotrophic Factor Expression in Neurons." *PLoS ONE* 8 (4): 1–10.
- Dorostkar, M. M., C. Zou, L. Blazquez-Llorca, and J. Herms. 2015. "Analyzing Dendritic Spine Pathology in Alzheimer's Disease: Problems and Opportunities." *Acta Neuropathologica* 130 (1): 1–19.
- Evans, N. A., L. Facci, D. E. Owen, P. E. Soden, S. A. Burbidge, R. K. Prinjha, J. C. Richardson, and S. D. Skaper. 2008. "A β (1-42) Reduces Synapse Number and Inhibits Neurite Outgrowth in Primary Cortical and Hippocampal Neurons: A Quantitative Analysis." *Journal of Neuroscience Methods* 175 (1): 96–103.

- Fakhoury, M. 2018. "Microglia and Astrocytes in Alzheimer's Disease: Implications for Therapy." *Current Neuropharmacology* 16 (5): 508–18.
- Ferreira-Vieira, T. H., I. M. Guimaraes, F. R. Silva, and F. M. Ribeiro. 2016. "Alzheimer's Disease: Targeting the Cholinergic System." *Current Neuropharmacology* 14 (1): 101–15.
- Forloni, G., V. Artuso, P. La Vitola, and C. Balducci. 2016. "Oligomeropathies and Pathogenesis of Alzheimer and Parkinson's Diseases." *Movement Disorders: Official Journal of the Movement Disorder Society* 31 (6): 771–81.
- Francis, P. T., A. M. Palmer, M. Snape, and G. K. Wilcock. 1999. "The Cholinergic Hypothesis of Alzheimer's Disease: A Review of Progress." *Journal of Neurology, Neurosurgery, and Psychiatry* 66 (2): 137–47.
- Fukumoto, K., H. Mizoguchi, H. Takeuchi, H. Horiuchi, J. Kawanokuchi, S. Jin, T. Mizuno, and A. Suzumura. 2014. "Fingolimod Increases Brain-Derived Neurotrophic Factor Levels and Ameliorates Amyloid Beta-Induced Memory Impairment." *Behavioural Brain Research* 268 (July): 88–93.
- Glenner, G. G., and C. W. Wong. 1984. "Alzheimer's Disease: Initial Report of the Purification and Characterization of a Novel Cerebrovascular Amyloid Protein." *Biochemical and Biophysical Research Communications* 120 (3): 885–90.
- Goate, A., M. C. Chartier-Harlin, M. Mullan, J. Brown, F. Crawford, L. Fidani, L. Giuffra, A. Haynes, N. Irving, and L. James. 1991. "Segregation of a Missense Mutation in the Amyloid Precursor Protein Gene with Familial Alzheimer's Disease." *Nature* 349 (6311): 704–6.
- Goedert, M., M. G. Spillantini, and R. A. Crowther. 1991. "Tau Proteins and Neurofibrillary Degeneration." *Brain Pathology* 1 (4): 279–86.
- Golgi, C., M. Bentivoglio, and L. Swanson. 2001. "On the Fine Structure of the Pes Hippocampi Major (with Plates XIII-XXIII). 1886." *Brain Research Bulletin* 54 (5): 461–83.
- Gomes, C., R. Ferreira, J. George, R. Sanches, D. I. Rodrigues, N. Gonçalves, and R. A. Cunha. 2013. "Activation of Microglial Cells Triggers a Release of Brain-Derived Neurotrophic Factor (BDNF) Inducing Their Proliferation in an Adenosine A2A Receptor-Dependent Manner: A2A Receptor Blockade Prevents BDNF Release and Proliferation of Microglia." *Journal of Neuroinflammation* 10: 1–13.
- Gottmann, K. 2008. "Transsynaptic Modulation of the Synaptic Vesicle Cycle by Cell-Adhesion Molecules." *Journal of Neuroscience Research* 86 (2): 223–32.

- Gottmann, K., T. Mittmann, and V. Lessmann. 2009. "BDNF Signaling in the Formation, Maturation and Plasticity of Glutamatergic and GABAergic Synapses." *Experimental Brain Research* 199 (3–4): 203–34.
- Haass, C., and D. J. Selkoe. 2007. "Soluble Protein Oligomers in Neurodegeneration: Lessons from the Alzheimer's Amyloid β -Peptide" 8 (February).
- Hampel, H., R. Vassar, B. De Strooper, J. Hardy, M. Willem, N. Singh, J. Zhou, R. Yan, E. Vanmechelen, A. De Vos, R. Nisticò, M. Corbo, B. P. Imbimbo, J. Streffer, I. Voytyuk, M. Timmers, A. A. Tahami Monfared, M. Irizarry, B. Albala, A. Koyama, N. Watanabe, T. Kimura, L. Yarenis, S. Lista, L. Kramer, A. Vergallo. 2020. "The Beta-Secretase BACE1 in Alzheimer's Disease." *Biological Psychiatry* S0006-3223 (20): 30063–69
- Hardy, J. A., and G. A. Higgins. 1992. "Alzheimer's Disease: The Amyloid Cascade Hypothesis." *Science* 256 (5054): 184–85.
- Hardy, J., and D. J. Selkoe. 2002. "The Amyloid Hypothesis of Alzheimer's Disease: Progress and Problems on the Road to Therapeutics." *Science* 297 (5580): 353–56.
- Harris, K. M. 1999. "Structure, Development, and Plasticity of Dendritic Spines." *Current Opinion in Neurobiology* 9 (3): 343–48.
- Harris, K. M., and S. B. Kater. 1994. "Dendritic Spines: Cellular Specializations Imparting Both Stability and Flexibility to Synaptic Function." *Annual Review of Neuroscience* 17: 341–71.
- Hasselmo, M. E. 2006. "The Role of Acetylcholine in Learning and Memory." *Current Opinion in Neurobiology* 16 (6): 710–15.
- Hata, S., S. Fujishige, Y. Araki, N. Kato, M. Araseki, M. Nishimura, D. Hartmann, P. Saftig, F. Fahrenholz, M. Taniguchi, K. Urakami, H. Akatsu, R. N. Martins, K. Yamamoto, M. Maeda, T. Yamamoto, T. Nakaya, S. Gandy, T. Suzuki. 2009. "Alcadein Cleavages by Amyloid Beta-Precursor Protein (APP) Alpha- and Gamma-Secretases Generate Small Peptides, P3-Alcs, Indicating Alzheimer Disease-Related Gamma-Secretase Dysfunction." *The Journal of Biological Chemistry* 284 (52): 36024–33.
- Hata, S., S. Fujishige, Y. Araki, M. Taniguchi, K. Urakami, E. Peskind, H. Akatsu, M. Araseki, K. Yamamoto, R. N. Martins, M. Maeda, M. Nishimura, A. Levey, K.A. Chung, T. Montine, J. Leverenz, A. Fagan, A. Goate, R. Bateman, D. M. Holtzman, T. Yamamoto, T. Nakaya, S. Gandy, T. Suzuki. 2011. "Alternative Processing of Gamma-Secretase Substrates in Common Forms of Mild Cognitive Impairment and Alzheimer's Disease: Evidence for Gamma-Secretase Dysfunction." *Annals of Neurology* 69 (6): 1026–31.

- Healy, L. M., and J. P. Antel. 2016. "Sphingosine-1-Phosphate Receptors in the Central Nervous and Immune Systems." *Current Drug Targets* 17 (16): 1841–50.
- Hebert, L. E., J. Weuve, P. A. Scherr, and D. A. Evans. 2013. "Alzheimer Disease in the United States (2010-2050) Estimated Using the 2010 Census." *Neurology* 80 (19): 1778–83.
- Heneka, M. T., M. J. Carson, J. El Khoury, G. E. Landreth, F. Brosseron, D. L. Feinstein, A. H. Jacobs, T. Wyss-Coray, J. Vitorica, R. M. Ransohoff, K. Herrup, S. A. Frautschy, B. Finsen, G. C. Brown, A. Verkhratsky, K. Yamanaka, J. Koistinaho, E. Latz, A. Halle, G. C. Petzold, T. Town, D. Morgan, M. L. Shinohara, V. H. Perry, C. Holmes, N. G. Bazan, D. J. Brooks, S. Hunot, B. Joseph, N. Deigendesch, O. Garaschuk, E. Boddeke, C. A. Dinarello, J. C. Breitner, G. M. Cole, D. T. Golenbock, M. P. Kummer. 2015. "Neuroinflammation in Alzheimer's Disease." *The Lancet. Neurology* 14 (4): 388–405.
- Heneka, M. T., M. P. Kummer, A. Stutz, A. Delekate, S. Schwartz, A. Vieira-Saecker, A. Griep, D. Axt, A. Remus, T. C. Tzeng, E. Gelpi, A. Halle, M. Korte, E. Latz, D. T. Golenbock. 2013. "NLRP3 Is Activated in Alzheimer's Disease and Contributes to Pathology in APP/PS1 Mice." *Nature* 493 (7434): 674–78.
- Heneka, M. T., R. M. McManus, and E. Latz. 2019. "Author Correction: Inflammasome Signalling in Brain Function and Neurodegenerative Disease." *Nature Reviews. Neuroscience*. 20 (3): 187.
- Heneka, M. T., and M. K. O'Banion. 2007. "Inflammatory Processes in Alzheimer's Disease." *Journal of Neuroimmunology* 184 (1–2): 69–91.
- Hering, H., and Morgan S.. 2001. "Dendritic Spines: Structure, Dynamics and Regulation." *Nature Reviews Neuroscience* 2 (12): 880–88.
- Herms, J., and M. M. Dorostkar. 2016. "Dendritic Spine Pathology in Neurodegenerative Diseases." *Annual Review of Pathology* 11 (1): 221–50.
- Hsieh, H., J. Boehm, C. Sato, T. Iwatsubo, T. Tomita, S. Sisodia, and R. Malinow. 2006. "AMPA Removal Underlies Abeta-Induced Synaptic Depression and Dendritic Spine Loss." *Neuron* 52 (5): 831–43.
- Ingelsson, M., H. Fukumoto, K. L. Newell, J. H. Growdon, E. T. Hedley-Whyte, M. P. Frosch, M. S. Albert, B. T. Hyman, and M. C. Irizarry. 2004. "Early Abeta Accumulation and Progressive Synaptic Loss, Gliosis, and Tangle Formation in AD Brain." *Neurology* 62 (6): 925–31.
- Iqbal, K., C. Alonso Adel, S. Chen, M. O. Chohan, E. El-Akkad, C. X. Gong, S. Khatoon, B. Li, F. Liu, A. Rahman, H. Tanimukai, I. Grundke-Iqbal. 2005. "Tau Pathology in

- Alzheimer Disease and Other Tauopathies.” *Biochimica et Biophysica Acta* 1739 (2–3): 198–210.
- Ishiura, S., M. Asai, C. Hattori, N. Hotoda, B. Szabo, N. Sasagawa, and S. Tanuma. 2000. “APP α -Secretase, a Novel Target for Alzheimer Drug Therapy.” *Madame Curie Bioscience Database [Internet]* 9: 7–11.
- Ishizuka, N., W. M. Cowan, and D. G. Amaral. 1995. “A Quantitative Analysis of the Dendritic Organization of Pyramidal Cells in the Rat Hippocampus.” *The Journal of Comparative Neurology* 362 (1): 17–45.
- Isik, A. T. 2010. “Late Onset Alzheimer’s Disease in Older People.” *Clinical Interventions in Aging* 5 (October): 307–11.
- Jährling, N., K. Becker, B. M. Wegenast-Braun, S. A. Grathwohl, M. Jucker, and H. Ulrich Dodt. 2015. “Cerebral β -Amyloidosis in Mice Investigated by Ultramicroscopy.” *PLoS ONE* 10 (5): 1–13.
- Jesko, H., A. Stepien, W. J. Lukiw, and R. P. Strosznajder. 2019. “The Cross-Talk Between Sphingolipids and Insulin-Like Growth Factor Signaling: Significance for Aging and Neurodegeneration.” *Molecular Neurobiology* 56 (5): 3501–21.
- Jesko, H., P. L. Wencel, W. J. Lukiw, and R. P. Strosznajder. 2019. “Modulatory Effects of Fingolimod (FTY720) on the Expression of Sphingolipid Metabolism-Related Genes in an Animal Model of Alzheimer’s Disease.” *Molecular Neurobiology* 56 (1): 174–85.
- Jevtic, S., A. S. Sengar, M. W. Salter, and J. McLaurin. 2017. “The Role of the Immune System in Alzheimer Disease: Etiology and Treatment.” *Ageing Research Reviews* 40 (November): 84–94.
- Ji, Y., Y. Lu, F. Yang, W. Shen, T. Tze-Tsang Tang, L. Feng, S. Duan, and B. Lu. 2010. “Acute and Gradual Increases in BDNF Concentration Elicit Distinct Signaling and Functions in Neurons.” *Nature Neuroscience* 13 (3): 302–9.
- Jin, M., N. Shepardson, T. Yang, G. Chen, D. Walsh, and D. J. Selkoe. 2011. “Soluble Amyloid Beta-Protein Dimers Isolated from Alzheimer Cortex Directly Induce Tau Hyperphosphorylation and Neuritic Degeneration.” *Proceedings of the National Academy of Sciences of the United States of America* 108 (14): 5819–24.
- Jonsson, T., H. Stefansson, S. Steinberg, I. Jonsdottir, P. V. Jonsson, J. Snaedal, S. Bjornsson, et al. 2013. “Variant of TREM2 Associated with the Risk of Alzheimer’s Disease.” *The New England Journal of Medicine* 368 (2): 107–16.
- Kang, H., and E. M. Schuman. 1995. “Long-Lasting Neurotrophin-Induced Enhancement of Synaptic Transmission in the Adult Hippocampus.” *Science* 267 (5204): 1658–62.

- Kano, M., and K. Hashimoto. 2009. "Synapse Elimination in the Central Nervous System." *Current Opinion in Neurobiology* 19 (2): 154–61.
- Karch, C. M., and A. M. Goate. 2015. "Alzheimer's Disease Risk Genes and Mechanisms of Disease Pathogenesis." *Biological Psychiatry* 77 (1): 43–51.
- Kartalou, G.I., A. R. S. Pereira, T. Endres, A. Lesnikova, P. Casarotto, P. Pousinha, K. Delanoe, E. Edelmann, E. Castrén, K. Gottmann, H. Marie, and V. Lessmann. 2019. "Anti-Inflammatory Treatment with FTY720 Starting after Onset of Symptoms Reverses Synaptic and Memory Deficits in an AD Mouse Model." *BioRxiv*, January, 2019.12.15.868026.
- Kellner, Y., N. Gödecke, T. Dierkes, N. Thieme, M. Zagrebelsky, and M. Korte. 2014. "The BDNF Effects on Dendritic Spines of Mature Hippocampal Neurons Depend on Neuronal Activity." *Frontiers in Synaptic Neuroscience* 6: 5.
- Kim, M., J. Suh, D. Romano, M. H. Truong, K. Mullin, B. Hooli, D. Norton, G. Tesco, K. Elliott, S. L. Wagner, R. D. Moir, K. D. Becker, R. E. Tanzi. 2009. "Potential Late-Onset Alzheimer's Disease-Associated Mutations in the ADAM10 Gene Attenuate {alpha}-Secretase Activity." *Human Molecular Genetics* 18 (20): 3987–96.
- Kinney, J. W., S. M. Bemiller, A. S. Murtishaw, A. M. Leisgang, A. M. Salazar, and B. T. Lamb. 2018. "Inflammation as a Central Mechanism in Alzheimer's Disease." *Alzheimer's & Dementia* 4: 575–90.
- Klunk, W. E., B. J. Bacsikai, C. A. Mathis, S. T. Kajdasz, M. E. McLellan, M. P. Frosch, M. L. Debnath, D. P. Holt, Y. Wang, and B. T. Hyman. 2002. "Imaging Abeta Plaques in Living Transgenic Mice with Multiphoton Microscopy and Methoxy-X04, a Systemically Administered Congo Red Derivative." *Journal of Neuropathology and Experimental Neurology* 61 (9): 797–805.
- Koffie, R. M., M. Meyer-Luehmann, T. Hashimoto, K. W. Adams, M. L. Mielke, M. Garcia-Alloza, K. D. Micheva, S. J. Smithc, M. L. Kimd, V. M. Leed, B. T. Hymana, and T. L. Spires-Jones. 2009. "Oligomeric Amyloid Beta Associates with Postsynaptic Densities and Correlates with Excitatory Synapse Loss near Senile Plaques." *Proceedings of the National Academy of Sciences of the United States of America* 106 (10): 4012–17.
- Korte, M., P. Carroll, E. Wolf, G. Brem, H. Thoenen, and T. Bonhoeffer. 1995. "Hippocampal Long-Term Potentiation Is Impaired in Mice Lacking Brain-Derived Neurotrophic Factor." *Proceedings of the National Academy of Sciences of the United States of America* 92 (19): 8856–60.
- Kraft, M. L. 2016. "Sphingolipid Organization in the Plasma Membrane and the Mechanisms

- That Influence It.” *Frontiers in Cell and Developmental Biology* 4: 154.
- Kuhn, P.H., A. V. Colombo, B. Schusser, D. Dreymueller, S. Wetzel, U. Schepers, J. Herber, A. Ludwig, E. Kremmer, D. Montag, U. Müller, M. Schweizer, P. Saftig, S. Bräse, S. F. Lichtenthaler. 2016. “Systematic Substrate Identification Indicates a Central Role for the Metalloprotease ADAM10 in Axon Targeting and Synapse Function.” *ELife* 5 (January).
- Lambert, J. C., C. A. Ibrahim-Verbaas, D. Harold, A. C. Naj, R. Sims, C. Bellenguez, A. L. DeStafano, et al. 2013. “Meta-Analysis of 74,046 Individuals Identifies 11 New Susceptibility Loci for Alzheimer’s Disease.” *Nature Genetics* 45 (12): 1452–58.
- Lane, C. A., J. Hardy, and J. M. Schott. 2018. “Alzheimer’s Disease.” *European Journal of Neurology* 25 (1): 59–70.
- Lavenex, P., and D. G. Amaral. 2000. “Hippocampal-Neocortical Interaction: A Hierarchy of Associativity.” *Hippocampus* 10 (4): 420–30.
- Lee, C. Y. Daniel, and G. E. Landreth. 2010. “The Role of Microglia in Amyloid Clearance from the AD Brain.” *Journal of Neural Transmission* 117 (8): 949–60.
- Lessmann, V. 1998. “Neurotrophin-Dependent Modulation of Glutamatergic Synaptic Transmission in the Mammalian CNS.” *General Pharmacology* 31 (5): 667–74.
- Lessmann, V., K. Gottmann, and R. Heumann. 1994. “BDNF and NT-4/5 Enhance Glutamatergic Synaptic Transmission in Cultured Hippocampal Neurons.” *Neuroreport* 6 (1): 21–5.
- Li, Y., S. Li, X. Qin, W. Hou, H. Dong, L. Yao, and L. Xiong. 2014. “The Pleiotropic Roles of Sphingolipid Signaling in Autophagy.” *Cell Death & Disease* 5 (May): e1245.
- Li, Z., and M. Sheng. 2003. “Some Assembly Required: The Development of Neuronal Synapses.” *Nature Reviews Molecular Cell Biology* 4 (11): 833–41.
- Liebscher, S., R. M. Page, K. Kafer, E. Winkler, K. Quinn, E. Goldbach, E. F. Brigham, D. Quincy, G. S. Basi, D. B. Schenk, H. Steiner, T. Bonhoeffer, C. Haass, M. Meyer-Luehmann, and M. Hübener. 2014. “Chronic γ -secretase Inhibition Reduces Amyloid Plaque-Associated Instability of Pre- and Postsynaptic Structures.” *Molecular Psychiatry* 19 (8): 937–46.
- Liu, Y., S. Walter, M. Stagi, D. Cherny, M. Letiembre, W. Schulz-Schaeffer, H. Heine, B. Penke, H. Neumann, and K. Fassbender. 2005. “LPS Receptor (CD14): A Receptor for Phagocytosis of Alzheimer’s Amyloid Peptide.” *Brain: A Journal of Neurology* 128 (Pt 8): 1778–89.
- Lott, I. T., and E. Head. 2005. “Alzheimer Disease and Down Syndrome: Factors in Pathogenesis.” *Neurobiology of Aging* 26 (3): 383–89.

- Love, S., K. Chalmers, P. Ince, M. Esiri, J. Attems, K. Jellinger, M. Yamada, M. McCarron, T. Minett, F. Matthews, S. Greenberg, D. Mann, P. G. Kehoe. 2014. "Development, Appraisal, Validation and Implementation of a Consensus Protocol for the Assessment of Cerebral Amyloid Angiopathy in Post-Mortem Brain Tissue." *American Journal of Neurodegenerative Disease* 3 (1): 19–32.
- Lu, A., V. G. Magupalli, J. Ruan, Q. Yin, M. K. Atianand, M. R. Vos, G. F. Schroder, K. A. Fitzgerald, H. Wu, and E. H. Egelman. 2014. "Unified Polymerization Mechanism for the Assembly of ASC-Dependent Inflammasomes." *Cell* 156 (6): 1193–206.
- Marambaud, P., J. Shioi, G. Serban, A. Georgakopoulos, S. Sarner, V. Nagy, L. Baki, P. Wen, S. Efthimiopoulos, Z. Shao, T. Wisniewski, and N. K. Robakis. 2002. "A Presenilin-1/Gamma-Secretase Cleavage Releases the E-Cadherin Intracellular Domain and Regulates Disassembly of Adherens Junctions." *The EMBO Journal* 21 (8): 1948–56.
- Marambaud, P., P. H. Wen, A. Dutt, J. Shioi, A. Takashima, R. Siman, and N. K. Robakis. 2003. "A CBP Binding Transcriptional Repressor Produced by the PS1/Epsilon-Cleavage of N-Cadherin Is Inhibited by PS1 FAD Mutations." *Cell* 114 (5): 635–45.
- Masters, C. L., R. Bateman, K. Blennow, C. C. Rowe, R. A. Sperling, and J. L. Cummings. 2015. "Alzheimer's Disease." *Nature Reviews Disease Primers* 1 (1): 15056.
- Maurer, K., S. Volk, and H. Gerbaldo. 1997. "Auguste D and Alzheimer's Disease." *Lancet* 349 (9064): 1546–49.
- Mayeux, R., and Y. Stern. 2012. "Epidemiology of Alzheimer Disease." *Cold Spring Harbor Perspectives in Medicine* 2 (8).
- McCloskey, K. "Alzheimer's Disease 2.0: State of Diagnosis." Clinical Correlations: The NYU Langone Health Online Journal of Medicine, October 4, 2017, <https://www.clinicalcorrelations.org>.
- McGeer, P. L., and E. G. McGeer. 2015. "Targeting Microglia for the Treatment of Alzheimer's Disease." *Expert Opinion on Therapeutic Targets* 19 (4): 497–506.
- McManus, R. M., O. M. Finucane, M. M. Wilk, K. H. G. Mills, and M. A. Lynch. 2017. "FTY720 Attenuates Infection-Induced Enhancement of Abeta Accumulation in APP/PS1 Mice by Modulating Astrocytic Activation." *Journal of Neuroimmune Pharmacology: The Official Journal of the Society on NeuroImmune Pharmacology* 12 (4): 670–81.
- Miguez, A., G. Garcia-Diaz Barriga, V. Brito, M. Straccia, A. Giralt, S. Gines, J. M. Canals, and J. Alberch. 2015. "Fingolimod (FTY720) Enhances Hippocampal Synaptic Plasticity and Memory in Huntington's Disease by Preventing P75NTR up-Regulation and

- Astrocyte-Mediated Inflammation.” *Human Molecular Genetics* 24 (17): 4958–70.
- Miranda, R. C., F. Sohrabji, and D. Toran-Allerand. 1994. “Interactions of Estrogen with the Neurotrophins and Their Receptors during Neural Development.” *Hormones and Behavior* 28 (4): 367–75.
- Möller, H.J., and M. B. Graeber. 1998. “The Case Described by Alois Alzheimer in 1911.” *European Archives of Psychiatry and Clinical Neuroscience* 248 (3): 111–22.
- Murray, K. D., C. M. Gall, E. G. Jones, and P. J. Isackson. 1994. “Differential regulation of brain-derived neurotrophic factor and type II calcium/calmodulin-dependent protein kinase messenger RNA expression in Alzheimer's disease.” *Neuroscience* 60 (1): 37-48.
- Neves, G., S. F. Cooke, and T. V. P. Bliss. 2008. “Synaptic Plasticity, Memory and the Hippocampus: A Neural Network Approach to Causality.” *Nature Reviews. Neuroscience* 9 (1): 65–75.
- Niemitz, E. 2013. “ADAM10 and Alzheimer’s Disease.” *Nature Genetics* 45 (11): 1273.
- Noda, H., H. Takeuchi, T. Mizuno, and A. Suzumura. 2013. “Fingolimod Phosphate Promotes the Neuroprotective Effects of Microglia.” *Journal of Neuroimmunology* 256 (1–2): 13–8.
- Ohno-Shosaku, T., and M. Kano. 2014. “Endocannabinoid-Mediated Retrograde Modulation of Synaptic Transmission.” *Current Opinion in Neurobiology* 29 (December): 1–8.
- Olabarria, M., H. N. Noristani, A. Verkhratsky, and J. J. Rodriguez. 2010. “Concomitant Astroglial Atrophy and Astrogliosis in a Triple Transgenic Animal Model of Alzheimer’s Disease.” *Glia* 58 (7): 831–38.
- Olabarria, M., H. N. Noristani, A. Verkhratsky, and J. J. Rodriguez. 2011. “Age-Dependent Decrease in Glutamine Synthetase Expression in the Hippocampal Astroglia of the Triple Transgenic Alzheimer’s Disease Mouse Model: Mechanism for Deficient Glutamatergic Transmission?” *Molecular Neurodegeneration* 6 (July): 55.
- Olsen, A. S. B., and N. J. Faergeman. 2017. “Sphingolipids: Membrane Microdomains in Brain Development, Function and Neurological Diseases.” *Open Biology* 7 (5).
- Paresce, D. M., R. N. Ghosh, and F. R. Maxfield. 1996. “Microglial Cells Internalize Aggregates of the Alzheimer’s Disease Amyloid Beta-Protein via a Scavenger Receptor.” *Neuron* 17 (3): 553–65.
- Peixoto, R. T., P. A. Kunz, H. Kwon, A. M. Mabb, B. L. Sabatini, B. D. Philpot, and M. D. Ehlers. 2012. “Transsynaptic Signaling by Activity-Dependent Cleavage of Neuroligin-1.” *Neuron* 76 (2): 396–409.
- Phillips, H. S., J. M. Hains, M. Armanini, G. R. Laramée, S. A. Johnson, and J. W. Winslow.

1991. "BDNF mRNA is decreased in the hippocampus of individuals with Alzheimer's disease." *Neuron* 7 (5): 695–702.
- Prince, M., E. Albanese, M. Guerchet, and M. Prina. "Dementia and Risk Reduction an Analysis of Protective and Modifiable Factors." Alzheimer's Disease International, September 2014. <https://www.alz.co.uk/research/world-report-2014>.
- Proctor, D. T., E. J. Coulson, and P. R. Dodd. 2010. "Reduction in Post-Synaptic Scaffolding PSD-95 and SAP-102 Protein Levels in the Alzheimer Inferior Temporal Cortex Is Correlated with Disease Pathology." *Journal of Alzheimer's Disease* 21: 795–811.
- Pruett, S. T., A. Bushnev, K. Hagedorn, M. Adiga, C. A. Haynes, M. C. Sullards, D. C Liotta, and A. H. Jr. Merrill. 2008. "Biodiversity of Sphingoid Bases ('sphingosines') and Related Amino Alcohols." *Journal of Lipid Research* 49 (8): 1621–39.
- Psotta, L., C. Rockahr, M. Gruss, E. Kirches, K. Braun, V. Lessmann, J. Bock, and T. Endres. 2015. "Impact of an Additional Chronic BDNF Reduction on Learning Performance in an Alzheimer Mouse Model." *Frontiers in Behavioral Neuroscience* 9 (March): 58.
- Pyapali, G. K., A. Sik, M. Penttonen, G. Buzsaki, and D. A. Turner. 1998. "Dendritic Properties of Hippocampal CA1 Pyramidal Neurons in the Rat: Intracellular Staining in Vivo and in Vitro." *The Journal of Comparative Neurology* 391 (3): 335–52.
- Qi, X.M., and J.F. Ma. 2017. "The Role of Amyloid Beta Clearance in Cerebral Amyloid Angiopathy: More Potential Therapeutic Targets." *Translational Neurodegeneration* 6: 22.
- Qin, C., W.H. Fan, Q. Liu, K. Shang, M. Murugan, L.J. Wu, W. Wang, and D.S. Tian. 2017. "Fingolimod Protects Against Ischemic White Matter Damage by Modulating Microglia Toward M2 Polarization via STAT3 Pathway." *Stroke* 48 (12): 3336–46.
- Qiu, C., M. Kivipelto, and E. von Strauss. 2009. "Epidemiology of Alzheimer's Disease: Occurrence, Determinants, and Strategies toward Intervention." *Dialogues in Clinical Neuroscience* 11 (2): 111–28.
- Qizilbash, N., J. Gregson, M. E. Johnson, N. Pearce, I. Douglas, K. Wing, S. J. W. Evans, and S. J. Pocock. 2015. "BMI and Risk of Dementia in Two Million People over Two Decades: A Retrospective Cohort Study." *The Lancet. Diabetes & Endocrinology* 3 (6): 431–36.
- Radak, Z., N. Hart, L. Sarga, E. Koltai, M. Atalay, H. Ohno, and I. Boldogh. 2010. "Exercise Plays a Preventive Role Against Alzheimer's Disease." *Journal of Alzheimer's Disease* 20: 777–83.
- Radde, R., T. Bolmont, S. A. Kaeser, J. Coomaraswamy, D. Lindau, L. Stoltze, M. E.

- Calhoun, F. Jäggi, H. Wolburg, S. Gengler, C. Haass, B. Ghetti, C. Czech, C. Hölscher, P. M. Mathews, and M. Jucker. 2006. "Abeta42-Driven Cerebral Amyloidosis in Transgenic Mice Reveals Early and Robust Pathology." *EMBO Reports* 7 (9): 940–46.
- Rajan, K. B., R. S. Wilson, J. Weuve, L. L. Barnes, and D. A. Evans. 2015. "Cognitive Impairment 18 Years before Clinical Diagnosis of Alzheimer Disease Dementia." *Neurology* 85 (10): 898–904.
- Reiman E. M., Y. T. Quiroz, A. S. Fleisher, K. Chen, C. Velez-Pardo, M. Jimenez-Del-Rio, A. M. Fagan, A. R. Shah, S. Alvarez, A. Arbelaez, M. Giraldo, N. Acosta-Baena, R. A. Sperling, B. Dickerson, C. E. Stern, V. Tirado, C. Munoz, R. A. Reiman, M. J. Huentelman, G. E. Alexander, J. B. Langbaum, K. S. Kosik, P. N. Tariot, F. Lopera. 2012. "Brain Imaging and Fluid Biomarker Analysis in Young Adults at Genetic Risk for Autosomal Dominant Alzheimer's Disease in the Presenilin 1 E280A Kindred: A Case-Control Study." *The Lancet. Neurology* 11 (12): 1048–56.
- Riepe, M. W., G. Adler, B. Ibach, B. Weinkauff, I. Gunay, and F. Tracik. 2006. "Adding Memantine to Rivastigmine Therapy in Patients with Mild-to-Moderate Alzheimer's Disease: Results of a 12-Week, Open-Label Pilot Study." *Primary Care Companion to the Journal of Clinical Psychiatry* 8 (5): 258–63.
- Rizzi, L., I. Rosset, and M. Roriz-Cruz. 2014. "Global Epidemiology of Dementia: Alzheimer's and Vascular Types." *BioMed Research International* 2014: 908915.
- Rogers, S. L., and L. T. Friedhoff. 1996. "The Efficacy and Safety of Donepezil in Patients with Alzheimer's Disease: Results of a US Multicentre, Randomized, Double-Blind, Placebo-Controlled Trial. The Donepezil Study Group." *Dementia* 7 (6): 293–303.
- Rose, C. R., L. Felix, A. Zeug, D. Dietrich, A. Reiner, and C. Henneberger. 2017. "Astroglial Glutamate Signaling and Uptake in the Hippocampus." *Frontiers in Molecular Neuroscience* 10: 451.
- Rothhammer, V., J. E. Kenison, E. Tjon, M. C. Takenaka, K. A. de Lima, D. M. Borucki, C.C. Chao, A. Wilz, M. Blain, L. Healy, J. Antel, F. J. Quintana. 2017. "Sphingosine 1-Phosphate Receptor Modulation Suppresses Pathogenic Astrocyte Activation and Chronic Progressive CNS Inflammation." *Proceedings of the National Academy of Sciences of the United States of America* 114 (8): 2012–17.
- Rubio-Perez, J. M., and J. M. Morillas-Ruiz. 2012. "A Review: Inflammatory Process in Alzheimer's Disease, Role of Cytokines." *The Scientific World Journal* 2012: 756357.
- Salter, M. W., and B. Stevens. 2017. "Microglia Emerge as Central Players in Brain Disease." *Nature Medicine* 23 (9): 1018–27.

- Saura, C. A., E. Servian-Morilla, and F. G. Scholl. 2011. "Presenilin/Gamma-Secretase Regulates Neurexin Processing at Synapses." *PloS One* 6 (4): e19430.
- Schachter, A. S., and K. L. Davis. 2000. "Alzheimer's Disease." *Dialogues in Clinical Neuroscience* 2 (2): 91–100.
- Schafer, D. P., and B. Stevens. 2015. "Microglia Function in Central Nervous System Development and Plasticity." *Cold Spring Harbor Perspectives in Biology* 7 (10): a020545.
- Schlepckow, K., G. Kleinberger, A. Fukumori, R. Feederle, S. F. Lichtenthaler, H. Steiner, and C. Haass. 2017. "An Alzheimer-Associated TREM2 Variant Occurs at the ADAM Cleavage Site and Affects Shedding and Phagocytic Function." *EMBO Molecular Medicine* 9 (10): 1356–65.
- Schneider, J. A., Z. Arvanitakis, S. E. Leurgans, and D. A. Bennett. 2009. "The Neuropathology of Probable Alzheimer Disease and Mild Cognitive Impairment." *Annals of Neurology* 66 (2): 200–8.
- Scoville, W. B., and B. Milner. 1957. "Loss of Recent Memory after Bilateral Hippocampal Lesions." *Journal of Neurology, Neurosurgery, and Psychiatry* 20 (1): 11–21.
- Selkoe, D. J. 2001. "Alzheimer's Disease: Genes, Proteins, and Therapy." *Physiological Reviews* 81 (2): 741–66.
- Selkoe, D. J. 2011. "Alzheimer's Disease." *Cold Spring Harbor Perspectives in Biology* 3 (7).
- Selkoe, D. J., and J. Hardy. 2016. "The Amyloid Hypothesis of Alzheimer's Disease at 25 Years." *EMBO Molecular Medicine* 8 (6): 595–608.
- Selkoe, D., E. Mandelkow, and D. Holtzman. 2012. "Deciphering Alzheimer Disease." *Cold Spring Harbor Perspectives in Medicine* 2 (1): a011460.
- Serrano-Pozo, A., M. P. Frosch, E. Masliah, and B. T. Hyman. 2011. "Neuropathological Alterations in Alzheimer Disease." *Cold Spring Harbor Perspectives in Medicine* 1 (1): a006189.
- Shankar, G. M., B. L. Bloodgood, M. Townsend, D. M. Walsh, D. J. Selkoe, and B. L. Sabatini. 2007. "Natural Oligomers of the Alzheimer Amyloid- **Beta** Protein Induce Reversible Synapse Loss by Modulating an NMDA- Type Glutamate Receptor-Dependent Signaling Pathway" 27 (11): 2866–75.
- Shapiro, L. A., M. J. Korn, Z. Shan, and C. E. Ribak. 2005. "GFAP-Expressing Radial Glia-like Cell Bodies Are Involved in a One-to-One Relationship with Doublecortin-Immunolabeled Newborn Neurons in the Adult Dentate Gyrus." *Brain Research* 1040

(1–2): 81–91.

- Sierra-Filardi, E., A. Puig-Kroger, F. J. Blanco, C. Nieto, R. Bragado, M. I. Palomero, C. Bernabeu, M. A. Vega, and A. L. Corbi. 2011. “Activin A Skews Macrophage Polarization by Promoting a Proinflammatory Phenotype and Inhibiting the Acquisition of Anti-Inflammatory Macrophage Markers.” *Blood* 117 (19): 5092–101.
- Sofroniew, M. V., and H. V. Vinters. 2010. “Astrocytes: Biology and Pathology.” *Acta Neuropathologica* 119 (1): 7–35.
- Sorra, K. E., and K. M. Harris. 2000. “Overview on the Structure, Composition, Function, Development, and Plasticity of Hippocampal Dendritic Spines.” *Hippocampus* 10 (5): 501–11.
- Spires-Jones, T., and S. Knafo. 2012. “Spines, Plasticity, and Cognition in Alzheimer’s Model Mice.” *Neural Plasticity* 2012: 319836.
- Spires-Jones, T. L., M. Meyer-Luehmann, J. D. Osetek, P. B. Jones, E. A. Stern, B. J. Bacskai, and B. T. Hyman. 2007. “Impaired Spine Stability Underlies Plaque-Related Spine Loss in an Alzheimer’s Disease Mouse Model.” *The American Journal of Pathology* 171 (4): 1304–11.
- Spruston, N. 2008. “Pyramidal Neurons: Dendritic Structure and Synaptic Integration.” *Nature Reviews. Neuroscience* 9 (3): 206–21.
- Stewart, C. R., L. M. Stuart, K. Wilkinson, J. M. van Gils, J. Deng, A. Halle, K. J. Rayner, L. Boyer, R. Zhong, W. A. Frazier, A. Lacy-Hulbert, J. El Khoury, D. T. Golenbock, K. J. Moore. 2010. “CD36 Ligands Promote Sterile Inflammation through Assembly of a Toll-like Receptor 4 and 6 Heterodimer.” *Nature Immunology* 11 (2): 155–61.
- Strader, C. R., C. J. Pearce, and N. H. Oberlies. 2011. “Fingolimod (FTY720): A Recently Approved Multiple Sclerosis Drug Based on a Fungal Secondary Metabolite.” *Journal of Natural Products* 74 (4): 900–7.
- Suh, J., S. H. Choi, D. M. Romano, M. A. Gannon, A. N. Lesinski, D. Y. Kim, and R. E. Tanzi. 2013. “ADAM10 Missense Mutations Potentiate Beta-Amyloid Accumulation by Impairing Prodomain Chaperone Function.” *Neuron* 80 (2): 385–401.
- Suzuki, K., Y. Hayashi, S. Nakahara, H. Kumazaki, J. Prox, K. Horiuchi, M. Zeng, S. Tanimura, Y. Nishiyama, S. Osawa, A. Sehara-Fujisawa, P. Saftig, S. Yokoshima, T. Fukuyama, N. Matsuki, R. Koyama, T. Tomita, T. Iwatsubo. 2012. “Activity-Dependent Proteolytic Cleavage of Neuroligin-1.” *Neuron* 76 (2): 410–22.
- Suzuki, N., T. T. Cheung, X. D. Cai, A. Odaka, L. Jr. Otvos, C. Eckman, T. E. Golde, and S. G. Younkin. 1994. “An Increased Percentage of Long Amyloid Beta Protein Secreted by

- Familial Amyloid Beta Protein Precursor (Beta APP717) Mutants.” *Science* 264 (5163): 1336–40.
- Takasugi, N., T. Sasaki, I. Ebinuma, S. Osawa, H. Isshiki, K. Takeo, T. Tomita, and T. Iwatsubo. 2013. “FTY720/Fingolimod, a Sphingosine Analogue, Reduces Amyloid- β Production in Neurons.” *PLoS ONE* 8 (5): 1–8.
- Tanzi, R. E., J. F. Gusella, P. C. Watkins, G. A. Bruns, P. St George-Hyslop, M. L. Van Keuren, D. Patterson, S. Pagan, D. M. Kurnit, and R. L. Neve. 1987. “Amyloid Beta Protein Gene: CDNA, MRNA Distribution, and Genetic Linkage near the Alzheimer Locus.” *Science* 235 (4791): 880–84.
- Tanzi, R. E. 2012. “The Genetics of Alzheimer Disease.” *Cold Spring Harbor Perspectives in Medicine* 2 (10).
- Tapia-Rojas, C., F. Aranguiz, L. Varela-Nallar, and N. C. Inestrosa. 2016. “Voluntary Running Attenuates Memory Loss, Decreases Neuropathological Changes and Induces Neurogenesis in a Mouse Model of Alzheimer’s Disease.” *Brain Pathology* 26 (1): 62–74.
- Terry, R. D., E. Masliah, D. P. Salmon, N. Butters, R. DeTeresa, R. Hill, L. A. Hansen, and R. Katzman. 1991. “Physical Basis of Cognitive Alterations in Alzheimer’s Disease: Synapse Loss Is the Major Correlate of Cognitive Impairment.” *Annals of Neurology* 30 (4): 572–80.
- Tsai, J., J. Grutzendler, K. Duff, and W.B. Gan. 2004. “Fibrillar Amyloid Deposition Leads to Local Synaptic Abnormalities and Breakage of Neuronal Branches.” *Nature Neuroscience* 7 (11): 1181–83.
- Tuppo, E. E., and H. R. Arias. 2005. “The Role of Inflammation in Alzheimer’s Disease.” *The International Journal of Biochemistry & Cell Biology* 37 (2): 289–305.
- Tyler, W. J., and L. Pozzo-Miller. 2003. “Miniature Synaptic Transmission and BDNF Modulate Dendritic Spine Growth and Form in Rat CA1 Neurons.” *The Journal of Physiology* 553 (Pt 2): 497–509.
- Uemura, K., T. Kihara, A. Kuzuya, K. Okawa, T. Nishimoto, H. Ninomiya, H. Sugimoto, A. Kinoshita, and S. Shimohama. 2006. “Characterization of Sequential N-Cadherin Cleavage by ADAM10 and PS1.” *Neuroscience Letters* 402 (3): 278–83.
- Vassar, R. 2013. “ADAM10 Prodomain Mutations Cause Late-Onset Alzheimer’s Disease: Not Just the Latest FAD.” *Neuron* 80 (2): 250–53.
- Venegas, C., S. Kumar, B. Franklin, T. Dierkes, R. Brinkschulte, D. Tejera, A. Vieira-Saecker, S. Schwartz, F. Santarelli, M. P. Kummer, A. Griep, E. Gelpi, M. Beilharz, D.

- Riedel, D. T. Golenbock, M. Geyer, J. Walter, E. Latz & M. T. Heneka. “Microglia-Derived ASC Specks Cross-Seed Amyloid-Beta in Alzheimer’s Disease.” *Nature* 552 (7685): 355–61.
- Verghese, P. B., J. M. Castellano, and D. M. Holtzman. 2011. “Apolipoprotein E in Alzheimer’s Disease and Other Neurological Disorders.” *The Lancet. Neurology* 10 (3): 241–52.
- Veugelen, S., T. Saito, T. C. Saido, L. Chavez-Gutierrez, and B. De Strooper. 2016. “Familial Alzheimer’s Disease Mutations in Presenilin Generate Amyloidogenic Abeta Peptide Seeds.” *Neuron* 90 (2): 410–16.
- Vezzoli, E., I. Caron, F. Talpo, D. Besusso, P. Conforti, E. Battaglia, E. Sogne, A. Falqui, L. Petricca, M. Verani, P. Martufi, A. Caricasole, A. Bresciani, O. Cecchetti, P. Rivetti di Val Cervo, G. Sancini, O. Riess, H. Nguyen, L. Seipold, P. Saftig, G. Biella, E. Cattaneo, C. Zuccato. 2019. “Inhibiting Pathologically Active ADAM10 Rescues Synaptic and Cognitive Decline in Huntington’s Disease.” *The Journal of Clinical Investigation* 129 (6): 2390–2403.
- von Bohlen und Halbach, O., and V. von Bohlen und Halbach. 2018. “BDNF Effects on Dendritic Spine Morphology and Hippocampal Function.” *Cell and Tissue Research* 373 (3): 729–41.
- Walsh, D. M., and D. J. Selkoe. 2007. “A Beta Oligomers - a Decade of Discovery.” *Journal of Neurochemistry* 101 (5): 1172–84.
- Wei, W., L. N. Nguyen, H. W. Kessels, H. Hagiwara, S. Sisodia, and R. Malinow. 2009. “Amyloid Beta from Axons and Dendrites Reduces Local Spine Number and Plasticity.” *Nature Neuroscience* 13 (2): 190–96.
- Weinstein, J. D. 2018. “A New Direction for Alzheimer’s Research.” *Neural Regeneration Research* 13 (2): 190–93.
- Willem, M., S. Tahirovic, M. A. Busche, S. V. Ovsepian, M. Chafai, S. Kootar, D. Hornburg, L. D. Evans, S. Moore, A. Daria, H. Hampel, V. Müller, C. Giudici, B. Nuscher, A. Wenninger-Weinzierl, E. Kremmer, M. T. Heneka, D. R. Thal, V. Giedraitis, L. Lannfelt, U. Müller, F. J. Livesey, F. Meissner, J. Herms, A. Konnerth, H. Marie, C. Haass. “ η -Secretase Processing of APP Inhibits Neuronal Activity in the Hippocampus.” *Nature* 526 (7573): 443–47.
- Wilton, D. K., L. Dissing-Olesen, and B. Stevens. 2019. “Neuron-Glia Signaling in Synapse Elimination.” *Annual Review of Neuroscience* 42 (July): 107–27.
- Witter, M. P. 1993. “Organization of the Entorhinal-Hippocampal System: A Review of

- Current Anatomical Data.” *Hippocampus* 3 Spec No: 33–44.
- Witter, M. P., A. W. Griffioen, B. Jorritsma-Byham, and J. L. Krijnen. 1988. “Entorhinal Projections to the Hippocampal CA1 Region in the Rat: An Underestimated Pathway.” *Neuroscience Letters* 85 (2): 193–98.
- Woodruff-Pak, D. S., M. J. Tobia, X. Jiao, K. D. Beck, and R. J. Servatius. 2007. “Preclinical Investigation of the Functional Effects of Memantine and Memantine Combined with Galantamine or Donepezil.” *Neuropsychopharmacology: Official Publication of the American College of Neuropsychopharmacology* 32 (6): 1284–94.
- Wrann, C. D., J. P. White, J. Salogiannis, D. Laznik-Bogoslavski, J. Wu, D. Ma, J. D. Lin, M. E. Greenberg, and B. M. Spiegelman. 2013. “Exercise Induces Hippocampal BDNF through a PGC-1alpha/FNDC5 Pathway.” *Cell Metabolism* 18 (5): 649–59.
- Wyss-Coray, T., and J. Rogers. 2012. “Inflammation in Alzheimer Disease—a Brief Review of the Basic Science and Clinical Literature.” *Cold Spring Harbor Perspectives in Medicine* 2 (1): a006346.
- Xu, W., L. Tan, H.F. Wang, T. Jiang, M.S. Tan, L. Tan, Q.F. Zhao, J.Q. Li, J. Wang, and J.T. Yu. 2015. “Meta-Analysis of Modifiable Risk Factors for Alzheimer’s Disease.” *Journal of Neurology, Neurosurgery, and Psychiatry* 86 (12): 1299–306.
- Yamanaka, M., T. Ishikawa, A. Griep, D. Axt, M. P. Kummer, and M. T. Heneka. 2012. “PPAR/RXR-Induced and CD36-Mediated Microglial Amyloid- Phagocytosis Results in Cognitive Improvement in Amyloid Precursor Protein/Presenilin 1 Mice.” *Journal of Neuroscience* 32 (48): 17321–31.
- Yiannopoulou, K. G., and S. G. Papageorgiou. 2013. “Current and Future Treatments for Alzheimer’s Disease.” *Therapeutic Advances in Neurological Disorders* 6 (1): 19–33.
- Yuan, X.Z., S. Sun, C.C. Tan, J.T. Yu, and L. Tan. 2017. “The Role of ADAM10 in Alzheimer’s Disease.” *Journal of Alzheimer’s Disease: JAD* 58 (2): 303–22.
- Zhang, F., Zhilong K., W. Li, Z. Xiao, and X. Zhou. 2012. “Roles of Brain-Derived Neurotrophic Factor/Tropomyosin-Related Kinase B (BDNF/TrkB) Signalling in Alzheimer’s Disease.” *Journal of Clinical Neuroscience: Official Journal of the Neurosurgical Society of Australasia* 19 (7): 946–49.

Acknowledgements

This research study would not have been possible without the guidance, corporation and support of all those who stood by my side during my journey as a PhD student in Germany.

I would like to express my sincere gratitude to my supervisor, Prof. Dr. Kurt Gottmann, for giving me the opportunity to carry out my PhD study in his research group at the Heinrich Heine University Düsseldorf as well as for his continuous guidance, support and encouragement during the past four years. His immense knowledge, inexhaustible patience and motivation, along with his meticulous suggestions helped me in perusing diligent research and writing of this dissertation.

My sincerest thanks to my advisor, Prof. Dr. Volkmar Lessmann, who provided me a chance to join his team, and conduct the experimental part of my doctoral thesis in his laboratory at the Institute of Physiology in Magdeburg. I am truly grateful for his decisive contribution in my project's coordination, his wise and valuable scientific advice and guidance during my research study. His enthusiasm and genuine love for science have always inspired me to work hard and keep myself motivated overcoming unexpected frustrations.

I cordially thank Prof. Dr. Christine Rose for her co-supervision of my PhD study and for her time to read and evaluate this thesis.

Moreover, I am thankful to the EU Joint Program - Neurodegenerative Disease Research (JPND) project CircProt and Deutsche Forschungsgemeinschaft (DFG) for financially supporting my PhD research. I am also truly grateful for the scientific discussions with all the JPND-CircProt partners during the annual CircProt meetings.

I would like to thank Dr. Thomas Enders for his scientific support, our constructive collaboration and fruitful discussions as well as Dr. Thomas Munsch for providing me with valuable insights in fluorescent and confocal microscopy. I also thank Dr. Elke Edelmann and Dr. Susanne Meis for their interesting comments on my research.

Furthermore, special thanks go to Sabine Eichler, Anja Reupsch, Margit Schmidt, Regina Ziegler, Kathrin Friese and Evelyn Friedl for their excellent technical support. My deep appreciation goes out to my labmates for our stimulating discussions, and for sharing with me their positive thoughts: Machhindra Garad, Efraín Augusto Cepeda-Prado, Monique Klausch, Xiaoyun Ma, Babak Khodaie, Gloria Quiceno, Wenxi Xing, Jeimmy Marcela Ceron Gonzalez and Jana Köhler.

My warmest thanks to those friends I met in Germany, who offered me their sincere friendship that I needed during various stages of my life in Magdeburg. In particular, to Lilianna Papaioannou, Nikos Davaris and Maria Raptaki.

I am indebted to my companions on my scientific and personal path since 2013 for their encouragement and long discussions: Olga Gkountidi, Paraskevi Kogionou, Sofia Zenalak and my dear long time supporter Arthur Antonopoulos. Very special thanks to my sweet friend Evi Paouri and to the one and only Øystein Rød Brekk, for listening patiently to all my research ideas, queries and frustrations, no matter the time zone difference separating us. I thank kindly Rania Tzara for being always next to me when I needed her the most.

My life would not be so bright without my precious friends with whom our friendship already counts 20 years and it keeps getting stronger. I deeply thank Stela Theodoropoulou for keeping me sane, and for making my life easier in Germany in all respects, from the very first day I arrived in Düsseldorf. I thank her for making the local language not to stand as a barrier for my daily activities and for our sleepless nights that we spent sharing the same uncertainties. I am also thankful to her assistance in translating the summary of this dissertation in German. Moreover, I thank Afrodite Kofopoulou and Nancy Kantzouki for being supportive throughout my lifetime and persisting tirelessly in listening to my concerns.

I am grateful to Alexis, for our beautiful journeys and conversations that offered me strength to complete my research and the writing of this dissertation.

I would like to express my immense thankfulness to my beloved sister Nikolia, for always being there for me as my greatest pillar of support since we were little. She is a true inspiration for me and motivates me to stay focused on my research with her creative suggestions.

To this end, words are not enough to express my gratitude to my parents Mihalis and Eleni, who are always by my side with their unconditional love. I thank them for their continuous patience, understanding and generosity. I owe them many thanks for teaching me to have courage and be kind; I use these virtues as a guide for every professional and personal step in my life. I deeply thank them for believing in me and for supporting me to make my scientific dream to come true.

Curriculum vitae

Personal information

Last name: Kartalou

Name: Georgia-Ioanna

Date of birth: 05.12.1988

Place of birth: Cholargos, Attica, Greece

Nationality: Greek

Education

Since 2016 **PhD Candidate**

Heinrich Heine University Düsseldorf, Germany

2012 - 2014 **MSc in Clinical Biochemistry - Molecular Diagnostics**

National and Kapodistrian University of Athens, Greece

2006 - 2012 **BSc in Biological Applications & Technology**

University of Ioannina, Greece

Work experience

2016 **Research Assistant**

Hellenic Pasteur Institute, Athens, Greece

Laboratory of Molecular Neurobiology & Immunology

2014 - 2015 **Research Associate**

Biomedical Research Foundation of the Academy of Athens, Greece

Laboratory of Cellular Neurobiology

2011- 2012 **Research Intern**

Biomedical Research Foundation of the Academy of Athens, Greece

Laboratory of Bioinformatics and Computational Biology

List of publications

Kartalou GI, Pereira ARS, Endres T, Lesnikova A, Casarotto P, Pousinha P, Delanoë K, Edelmann E, Castrén E, Gottmann K, Marie H, and Lessmann V. “Anti-inflammatory treatment with FTY720 starting after onset of symptoms reverses synaptic and memory deficits in an AD mouse model.” (Submitted)

Kartalou GI, Endres T, Lessmann V, and Gottmann K. “Golgi-Cox impregnation combined with fluorescence staining of amyloid plaques reveals local spine loss in an Alzheimer mouse model.” (Under review)

Paouri E, Tzara O, **Kartalou GI**, Zenelak S, and Georgopoulos S. “Peripheral tumor necrosis factor-alpha (TNF- α) modulates amyloid pathology by regulating blood-derived immune cells and glial response in the brain of AD/TNF transgenic mice.” *The Journal of Neuroscience* 37, no. 20 (2017): 5155-5171.

Hatzimichael E, Dasoula A, Lagos K, **Kartalou G**, Dranitsaris G, Briasoulis E, and Crook T. “Methylation status of the collagen prolyl-3 hydroxylases (C-P3H) and C-P4H genes in multiple myeloma: P3H2 is selectively methylated.” *Blood* 118, no 21 (2011): 4639.

List of poster presentations in conferences

Kartalou GI, Casarotto P, and Lessmann V. “CircProt: Synaptic circuit protection in Alzheimer’s disease (AD) and Huntington’s disease (HD): BDNF/TrkB and Arc signaling as rescue factors.” Poster presented at the JPND/JPco-fuND symposium, Brussels, BE, November 27-28, 2019.

Kartalou GI, Endres T, Lessmann V, and Gottmann K. “Potential therapeutic approaches to prevent dendritic spine pathology in the hippocampus of APP/PS1 mice.” Poster presented at The Brain Conferences, Understanding and Targeting Alzheimer's Disease, Copenhagen, DK, May 5-8, 2019.

* The abstract was also selected for a spotlight oral presentation

Kartalou GI, Endres T, Lessmann V, and Gottmann K. “Rescue of dendritic spine pathology in the hippocampus of APP/PS1 mice.” Poster presented at the 13th Gottingen Meeting of the German Neuroscience Society, Gottingen, DE, March 20-23, 2019.

Kartalou GI, Endres T, Lessmann V, and Gottmann K. “Rescue of dendritic spine loss in hippocampal CA1 pyramidal neurons in a mouse model of Alzheimer's disease.” Poster presented at the 11th FENS Forum of Neuroscience, Berlin, DE, July 1-11, 2018.

Kartalou GI, Endres T, Hölzl G, Edelmann E, Gottmann K, and Lessmann V. “Fear and fear extinction learning in APP/PS1 mice.” Poster presented at the 12th Gottingen Meeting of the German Neuroscience Society, Gottingen, DE, March 22-25, 2017.

Declaration

I hereby declare that this thesis is an original work and has not been submitted in whole, or in part, for a degree at this or any other university. Nor does it contain, to the best of my knowledge and belief, any material published or written by any other person, except as acknowledged in the text. This thesis is in compliance with the ‘Principles for Ensuring Good Scientific Practice at the Heinrich-Heine-University.’ I have not made any unsuccessful promotions.

Düsseldorf, May 5, 2020

Georgia-Ioanna Kartalou

Eidesstattliche Erklärung

Ich versichere an Eides Statt, dass die vorliegende Dissertation von mir selbständig und ohne unzulässige fremde Hilfe unter Beachtung der „Grundsätze zur Sicherung guter wissenschaftlicher Praxis an der Heinrich-Heine-Universität Düsseldorf“ erstellt worden ist. Diese Dissertation wurde keiner anderen Fakultät vorgelegt und es gab bisher keine erfolglosen Promotionsversuche.

Düsseldorf, den 5. Mai 2020

Georgia-Ioanna Kartalou